Naval Research Laboratory

Washington, DC 20375-5320

NRL/MR/6124--19-9984

Mechanistic Study of Fungi Degradation of Organic Coatings Used in Aircraft Finishing Systems

Jason Lee
Treva Brown

Ocean Sciences Branch
Ocean Sciences Division

James Wynne
Grant Daniels

Materials Chemistry Branch
Chemistry Division

Steve Brown
Dane Hanson

Naval Air Warfare Center Aircraft Division
Patuxent River, MD

Doug Hansen
Ronald Zeszut

University of Dayton Research Institute
Dayton, Ohio

March 6, 2020

REPORT DOCUMENTATION PAGE

Form Approved
OMB No. 0704-0188

1. REPORT DATE *(DD-MM-YYYY)*	**2. REPORT TYPE**	**3. DATES COVERED** *(From - To)*
06-03-2019	NRL Memorandum Report	03/01/18 – 04/30/19

4. TITLE AND SUBTITLE

Mechanistic Study of Fungi Degradation of Organic Coatings Used in Aircraft Finishing Systems

5a. CONTRACT NUMBER

5b. GRANT NUMBER

5c. PROGRAM ELEMENT NUMBER
61-9512-B7-5

6. AUTHOR(S)

Jason Lee, Treva Brown, James Wynne, Grant Daniels, Steve Brown,* Dane Hanson,* Doug Hansen,** and Ronald Zeszut**

5d. PROJECT NUMBER

5e. TASK NUMBER

5f. WORK UNIT NUMBER
9512

7. PERFORMING ORGANIZATION NAME(S) AND ADDRESS(ES)

Naval Research Laboratory
1009 Balch Blvd
Stennis Space Center, MS 39529-5004

Naval Research Laboratory
4555 Overlook Avenue, SW
Washington, DC 20375-5320

8. PERFORMING ORGANIZATION REPORT NUMBER

NRL/MR/6124--19-9984

9. SPONSORING / MONITORING AGENCY NAME(S) AND ADDRESS(ES)

Strategic Environment R&D Program
4800 Mark Center Drive
Suite 16F16
Alexandria, VA 22350-3605

10. SPONSOR / MONITOR'S ACRONYM(S)

SERDP

11. SPONSOR / MONITOR'S REPORT NUMBER(S)
WP-2747

12. DISTRIBUTION / AVAILABILITY STATEMENT

DISTRIBUTION STATEMENT A: Approved for public; release distribution is unlimited.

13. SUPPLEMENTARY NOTES

*NAWCAD, 22347 Cedadr Point Road, Patuxent River, MD 20670
**University of Dayton Research Institute, 300 College Park Ave., Dayton, Ohio, 45469

14. ABSTRACT

Navy and Marine Corps aircraft operate around the world, most often in hot, humid environments where fungi such as mold and mildew spores attach and proliferate in regions of the aircraft without sunlight/ultraviolet light exposure. Chemicals and materials such as hydraulic fluids, corrosion prevention compounds, atmospheric contaminants, and organic coatings act as a feedstock for microbes which leave by-products of organic acids, esterases, and lipases which are destructive to some coatings, corrosive to aluminum alloys, and can lead to human health concerns. This report investigated the role of the following factors: (a) two common topcoats with differing characteristics, (b) the corrosion inhibitor and topography of chromated vs. non-chromated primers, (c) hydraulic fluid contamination, and (d) applied corrosion prevention compounds formulated with and without a fungistat. Multiple analytical techniques were used to characterize species proliferating for each test condition, the degree of attachment to coatings' surfaces before and after cleaning/sanitizing techniques, and incipient coating degradation.

15. SUBJECT TERMS

Coating, Degradation, Polyurethane, Fungi, Mold, Mildew, Chromate, Hydrophobic, Hydraulic fluid

16. SECURITY CLASSIFICATION OF:			**17. LIMITATION OF ABSTRACT**	**18. NUMBER OF PAGES**	**19a. NAME OF RESPONSIBLE PERSON**
a. REPORT	**b. ABSTRACT**	**c. THIS PAGE**			Grant C. Daniels
Unclassified Unlimited	Unclassified Unlimited	Unclassified Unlimited	Unclassified Unlimited	91	**19b. TELEPHONE NUMBER** *(include area code)* (202) 404-6730

Standard Form 298 (Rev. 8-98)
Prescribed by ANSI Std. Z39.18

This page intentionally left blank.

Table of Contents

Figures

Tables

Acronyms

AFM	Atomic Force Microscopy
AFRL	Air Force Research Laboratory
ATCC	American Type Culture Collection
ATR-FTIR	Attenuated Total Reflectance Fourier Transform Infrared
C	Control, Unexposed
CC	Climate Controlled
CPC	Corrosion Preventative Compound
CPD	Contact Potential Difference
dH_2O	Distilled Water
dI	Deionized [water]
EIS	Electrochemical Impedance Spectroscopy
ESEM	Environmental Scanning Electron Microscopy
GC-MS	Gas Chromatograph / Mass Spectroscopy
GPC	Gel Permeation Chromatography
IPA	Isopropyl Alcohol
IR	Infrared
LSM	Laser Scanning Microscope
M	Microbial Exposed
MIC	Microbiologically Induced Corrosion
MIL-STD	Military Standard
MW	Molecular Weight
NAVAIR	Naval Air Systems Command
NAWCAD	Naval Air Warfare Center – Aircraft Division
NRL–DC	Naval Research Laboratory, Washington D.C.
NRL–SSC	Naval Research Laboratory-Stennis Space Center

OCP	Open Circuit Potential
OSP	Optical Surface Profilometer
PDA	Potato Dextrose Agar
RMS	Root-Mean-Square
SCE	Saturated Calomel Electrode
S.D.	Standard Deviation
SEC	Size Exclusion Chromatography
SKP	Scanning Kelvin Probe
UDRI	University of Dayton Research
Institute UV	Ultraviolet

Keywords

Fungi, organic coatings, humidity, CPC, hydraulic fluid, super-hydrophobic

Acknowledgements

This work represents a subset of a recognized Naval Aviation Enterprise Corrosion Prevention Team (NAE CPT) priority area designated “aircraft interiors”, and including structural material condition, presence and condition of protection systems, drainage effects, and micro-biological growth and side effects. Currently, other parallel efforts in the micro-biological growth sub-field - including establishing and monitoring biological growth exposure sites at 8 field level Navy/Marine Corps sites, sampling from aircraft and work spaces at operational sites, and performing on-aircraft demonstrations of promising cleaning materials and protective treatment processes - have already leveraged findings uncovered through this study. Likewise, our hope is that this and future lab studies can leverage findings and developments from these parallel field efforts.

In support of this joint initiative, the authors wish to thank the following parties:

- Dr. Robin Nissan from the SERDP Program Office and Mr. Randy Boatwright from the NAE CPT for financial support;
- The Naval Air Technical Data and Engineering Service Command (NATEC) Corrosion Maintenance Readiness Team (C-MRT) members Mike Mulac (NS Norfolk, VA), Jeremy Clement (MCAS New River, NC), Bryan Canady (MCAS Miramar, CA), Mike Ransom (NAS Whidbey Island, WA), Northrup Okuda (MCAS Kaneohe Bay, HI), and Jeff Smith (MCAS Futenma, Okinawa, Japan);
- The US Naval Reserves In-Service Engineering and Logistics (ISEL) Unit members CDR Sean Neally, CDR Jim McDonnell, CDR Joey Walker, LCDR Matt Kiefer, LT Dan Rolfe, and LT Steven Cox.
- The NAVAIR Fleet Support Team members, Ms. Rosa Cafasso (In-Service Support Center Southeast) and Mr. Larry Learn (In-Service Support Center East).
- And various other parties for technical and administrative support: Mr. Craig Matzdorf, Dr. Victor Rodriguez-Santiago, Mr. Joseph Ullmann, Mr. Jose Perez (Naval Air Warfare Center Aircraft Division), Ms. Louise Nicoloff (In Service Support Center Southeast), and Mr. Braxton Lewis (SERDP Program Office).

Abstract

Navy and Marine Corps aircraft operate around the world most frequently in hot, humid environments. In interior regions of the aircraft where sunlight/ultraviolet light (UV) cannot penetrate and, exacerbated by the heat and humidity, mold and mildew (fungal) spores may attach and proliferate leading to biofouling, biodegradation and ultimately microbiologically influenced corrosion (MIC). This type of growth-influenced corrosion is unsightly, produces objectionable odors, and ultimately can compromise aircraft structural integrity by breakdown of protective finish systems and production of corrosive by-products. In addition to heat, humidity and the lack of natural deterrents (i.e. UV light), the presence of organic materials such as hydraulic fluid, corrosion preventative compounds, and organic coatings act as a feedstock for the microbes. Microbial digestion of the organic content produces metabolites such as organic acids, esterases, and lipases which are corrosive and destructive to protective coatings and structural metals. We proposed a broad comprehensive study of the life cycle of the microbe in operational conditions to determine the factors that most closely influence coating degradation and microbial proliferation. With a greater understanding of the role of these and other environmental factors in degrading coatings, mitigation mechanisms can be devised which thwart the microbe exploitation of these conditions.

Technical Approach

The activities needed to initiate microbe attack on organic coatings are summarized as (1) spore attachment, (2) spore activation, and (3) microbe proliferation. During proliferation, microbes are hypothesized to be metabolizing organic coating constituents; furthermore, we hypothesized that other conditions of the coating including its surface free energy, surface roughness, and anti-microbial additives play roles during these three stages of microbe activity where a greater understanding could contribute to alternative means of mitigation. Thus, we included various components of the operational environment that play a role in these activities. Regions of aircraft susceptible to microbe growth may contain primer or top-coat, environmental organic contaminants, corrosion preventative compounds and known operational fluids such as hydraulic fluid. This goal of the study was to determine the role of each of the following in inhibiting microbial activity: (a) the corrosion inhibitor toxicity (by including chromated and non-chromated primers); (b) the surface roughness and energy of the coating by including four coatings with differing characteristics (two topcoats, two primers); and (c) the role of hydraulic fluid and corrosion preventative compounds in the microbe life cycle in this environment. We exposed five known microbes to temperature and humidity conditions typical in operational growth areas, and subsequently analyzed the compromised coating surfaces using multiple analytical techniques.

Results

Environmental scanning electron microscopy clearly documented microbial growth patterns on the surface of test coupons and the effectiveness of cleaning procedures used to remove microbes to permit the surfaces analyses. Significant amount of fungal growth was observed on the coupons which were not purposely inoculated. As completely sterile conditions were not maintained throughout the 84 day experiment, some growth was expected on control surfaces, but not to the extent observed. Chromated epoxy primer was not as resistant to microbial propagation as expected compared to the non-chromated primer based on observations, however, resistant species will require DNA analysis for positive identification. Laser scanning microscopy documented comparatively smooth surfaces of the non-chrome primer which may be less likely to physically harbor spores from a geometric perspective relative to the chromate primer which had a rougher and more hydrophilic matte finish. Infrared spectral analyses showed that hydraulic fluid was consumed by the microbes. The lack of clear degradation in the coatings indicates the microbes are consuming either leachable material or applied fluids and not the polymer backbone of the coatings. Analysis of the extracts from all samples showed no peaks in the gel permeation chromatography indicating

that molecular weights in the range of 2,500 to 936,000 were not detected for the exposure conditions in this project. The scanning Kelvin probe (SKP) analysis differentiated both qualitatively and quantitatively amongst the fungi-inoculated, the climate controlled, and control coupons, and therefore may provide a unique method to characterize microbiological growth effects on materials and coating systems. Various common cleaning solvents (e.g. isopropyl alcohol, acetone, ethanol and methanol) used on the fungal hyphae/mycelia were shown to be relatively ineffective in removing the attached growths from the coating surfaces. NavClean was the most effective in removing growths from organic coatings surfaces. Combinations of cleaning procedures may be required to remove both fungal growths and organic films of various origin which are acting as additional nutrients for microbiological propagation.

Benefits

Environmental scanning electron microscopy was most useful for defining the extent of coating areas affected by microbial growths, determining completeness of microbial removal after various cleaning/sanitizing procedures, and visually characterizing known species with high certainty; follow-on sampling and DNA analyses are still required for absolute species identification. Gas chromatography and mass spectrometry analysis of coating extracts showed new peaks indicating leaching or possible degradation; the exception where this technique did not detect leaching was for the climate controlled hydrophobic coating. Infrared spectroscopy was capable of detecting evidence of suspected polyurethane degradation based on reduction of peak areas of the Amide I and Amide II bonds after microbiological growth; this technique will be more effective with a smaller spot size. Infrared spectroscopy was also useful in documenting surface residues of contaminant films after ineffective cleaning procedures. Although the study was not able to ascertain completely, SKP may effectively be used to differentiate both qualitatively and quantitatively among various fungi-attacked coating systems as compared to control coating conditions; likewise, it may provide a method to quantify fungal growth on other materials used across the Naval Aviation Enterprise. Further developments in characterizing what component of the fungal contamination results in changes in work function values of materials/coatings would refine this applied technique. Although the limit of the duration of exposure for this study prevented more definite conclusions regarding coating degradation, laser scanning microscopy could be a valuable quantitative tool for analyzing coupons exposed for a longer duration or for more heavily degraded coatings obtained from systems in operational environments. Similarly, gel permeation chromatography is expected to provide more data when sufficiently large molecular degradation products are formed and extracted into analyte solutions. Another potential benefit of GPC is that it could be effective in quantifying non-planar irregular shaped materials which have experienced growths.

Introduction

Navy aircraft operate around the world most frequently in hot, humid environments. In interior regions of the aircraft where ultraviolet light cannot penetrate and exacerbated by the heat and humidity, mold and mildew spores may attach and proliferate. Microbiologically induced corrosion (MIC) is a plague because it is unsightly, produces objectionable odors, and ultimately compromises aircraft structural integrity. In addition to heat, humidity, and the lack of natural deterrents (i.e. UV light), the presence of organic materials such as hydraulic fluid, corrosion preventive compounds, and various organic materials and coatings act as feedstock for the microbes. Digesting the organic content, the microbes leave by-products such as organic acids, esterases, and lipases which are corrosive and destructive to protective coatings. Once the protective coatings have been compromised, the exposed structure is susceptible to attack by the by-products and the corrosive operating environment. The former lacquer-based military coatings were more susceptible to fungal growth than some newer polyester polyurethane formulations (Lavoie et al. 1997). Navy and Marine Corps military aircraft interiors have been recently observed to have problems with objectionable growths, so we proposed a comprehensive study of the life cycle of the microbe in operational conditions – heat, humidity, exposure to common operational fluids - to determine the factors that most closely influence coating degradation and ultimately degradation of the structure.

Coating degradation mechanisms induced by microbes are complex due to the relationship of different microbial organisms in the environment (e.g. symbiotic, antagonistic), the fluctuation of environmental factors (e.g. heat, humidity) which accelerate or impede microbial growth, the effects of other operational materials, and the complex nature of the organic coating under attack. For this limited scope study, we selected a subset of these characteristics, which maintained steady heat and humidity, contained a consortium of known fungal species, several additional operational materials in addition to the organic coatings themselves, and only 2 top-coats and 2 primers for investigation. Thus, coatings not previously exposed to degrading chemical conditions, a single fungal consortium, and a subset of operational materials were used to control scope. Due to the inherent differences of the coating systems under investigation multiple analysis techniques were utilized to characterize the pathways in which the organic coatings may be degraded when in close contact with microbe species. Degradation in the operational environment is dependent on the specific organic coating substrate, the variety of contaminating media which may all be present simultaneously and the nature and duration of the growth environment. With a greater understanding of the role of all factors of the environment in degrading coatings, mitigation mechanisms can be devised which thwart the microbe exploitation of these conditions.

Ray et al. (2010) evaluated fungal growth on aluminum 2024 panels in the presence of fungal inhibiting compounds, corrosion preventative compounds (CPC(s)) and hydraulic fluid for up to 68 days. The most fungal growth was observed on panels with CPC Cor-Ban 35 without any fungal inhibiting chemical addition. The fungicide Omacide 100 was the most effective inhibiting chemical for reducing fungal growth.

Lavoie et al. (1997) surveyed five H-53 aircraft during depot maintenance for fungal growth. They isolated nine genera of fungi from multiple locations and materials aboard the aircraft including Psetolotia, Tricoderma, Epicoccum, Phoma, Stemphylium, Alternaria, Hormoconis, Penicillium and Aureobasidium. In controlled laboratory exposures, lacquer and polyester polyurethane paint coated AA2024 panels were exposed to five of the fungi genera. The lacquer paint was quickly overgrown with blisters formed after the 32-day exposure. Polyester polyurethane paint was more slowly covered by fungi and did not show any degradation. The authors concluded longer exposures were required to determine if the polyester polyurethane paints were ultimately susceptible to fungal degradation. In addition, the authors simulated field cleaning procedures by wiping the infected panels with 75% ethanol (in water) which removed most of the fungal structures; however, the viability of the remaining fungi were not assessed.

Manuscript approved January 14, 2020.

It is unknown whether fungal growths that initiate within surface contaminant films can cause damage to underlying materials even though that material may be categorized as resistant to direct attack—this is referenced in the MIL-STD-810F (updated to version 'G') pertaining to environmental degradation and testing methodology. Hence, this was another focus of the current study.

Success criteria for this project include establishing the following capabilities: (1) Identification and maturation of existing and novel techniques to characterize chemical and physical changes to coatings as a result of microbiological exposure; (2) Characterization of common military aviation contaminant films before and after exposure to microbes in the presence of hydraulic fluid and corrosion preventative compounds; (3) Characterization of the qualitative effect of fungistats, and specifically their effect in reducing microbial propagation on coating surfaces; and (4) Establishment of a preferred microbial sanitization method, which will lead to tangible changes in methods used by the Navy/U.S.M.C. aviation maintenance community.

Methods and Materials

Baseline Controls

As-coated 7075-T6 aluminum panels (2" x 2" x 1/8") served as the baseline controls; six (6) different types of base coating systems were representative of the paint surface that would be exposed to the contaminant fluids and microbiological inoculation. The panels were coated on one side only with the back side left bare. Common organic coatings used by the Navy as well as an experimental hydrophobic coating were investigated in this study:

- Chromated primer, MIL-PRF-85582. Class C
- Non-chromated primer, MIL-PRF-85582, Class N
- Polyurethane topcoat, standard high-solids MIL-PRF-85285 Type I, Class H
- Extended weatherability polyurethane topcoat, MIL-PRF-85285 Type IV, Class H
- Hydrophobic coating, Rust-Oleum NeverWet™ applied over MIL-PRF-85285 Type I
- Hydrophobic coating, Rust-Oleum NeverWet™ applied over MIL-PRF-85285 Type IV

The chromate primer and non-chromate primers were epoxy-based; the chromated primer contained hexavalent chromium as a corrosion inhibitor. Topcoats were polyurethane-based with Type I being the standard Navy topcoat and Type IV an extended weatherability formulation also known as advanced performance topcoat. One super-hydrophobic coating was included within this study and was applied as a supplemental coating over both topcoats. The full test matrix for this study is presented in Appendix A

Fungal Species Selection

Experiments in this study were based, but not limited by, the MIL-STD-810 guidelines for fungal exposures. MIL-STD-810F lists two groups of fungi commonly used in the evaluation of fungal degradation of materials including U.S. and European groups. Paragraph 2.2.2b of the standard specifically allows for adjustment of the fungal group based on prior knowledge of specific material degradation. Therefore, fungi species were selected from three different source materials: 1) MIL-STD-810F, 2) Lavoie et al. (1997) and

3) Ray et al. (2010) to maximize the number of fungal genera used. Lavoie et al. (1997) collected sampled

from an H-53 aircraft. Ray et al. (2010) used a fungal group to evaluate CPCs and fungicides on bare aluminum. Table 1 lists the fungi acquired from American Type Culture Collection (ATCC) and their respective source material. MIL-STD-810 was updated in January 2019 to the 'H' designation and limited the adjustment language in Paragraph 2.2.2 to include addition but not substitution of fungal species. It should be noted that the approved fungal list has changed for the U.S. and Europe groups in each of the last several designations.

Biological Culture Preparation

Potato dextrose agar (PDA) (Mfr. No. BD 213400 by BD Difco) was prepared in the lab by placing 39g of PDA in 1L of deionized (dI) water, as instructed by the manufacturer. The mixture was then heated with slow stirring until the color became clear and boiling was observed. The PDA was then covered with aluminum foil and autoclaved. After slight cooling, PDA was poured into clean petri dishes, covered, and left to harden overnight.

Frozen fungal species samples were purchased from ATCC including *Aspergilus brasiliensis, Hormoconis resinae*, *Trichoderma virens, Aureobasidium pullulans*, and *Talaromyces pinophilus*. The frozen samples were revived according to ATCC instructions. The five fungal species were individually swabbed and streaked onto the prepared PDA plates and left to incubate upside down in a humidity chamber at 30°C at 95% relative humidity for 2 weeks.

Spore Suspension Preparation

The five fungal samples (Table 1) were separately inoculated onto fresh potato dextrose agar (PDA) plates and left in a humidity chamber at 30°C for 2 weeks. To harvest the spores, the plate cultures were flooded with 10 - 20 microliters of 1% TWEEN 80 solution (Polysorbate 80 from ACROS Organics in distilled water) then dislodged from the agar using a rounded sterile glass rod. The solution was then filtered via a sterile 5 ml pipette outfitted with a swab of cotton. The filtrate was obtained in a 15 ml centrifuge tube and washed twice via centrifugation for eight minutes at low speed. The supernatant was discarded, and the pellet was re-suspended in 1 ml of 1% TWEEN 80 solution and refrigerated overnight.

Spore concentration was calculated with the assistance of a C-Chip hematocytometer, and a final dilution of 45 ml was made from each specimen. Individual spore suspensions of 10^6 spores/ml was prepared for each individual culture in sodium chloride mineral salt before mixing the suspensions for spraying. The coupons for testing were sprayed with an atomizer containing the prepared fungal spore suspensions under a fume hood.

Table 1. Fungal species used for biological exposure.

ATCC	Fungus	Source(s)	Morphology
ATCC 9642	*Aspergillus brasiliensis* *(*Aspergillus niger)*	MIL-STD-810F (US, Euro) MIL-STD-810H (US, Euro)	
ATCC 9348	*Aureobasidium pullulans*	Lavoie et. al (1997) Ray et. al (2010)	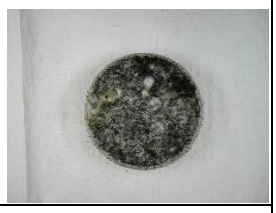
ATCC 22712	*Hormoconis resinae*	Lavoie et. al (1997) Ray et. al (2010)	
ATCC 11797	*Talaromyces pinophilus* *(*Penicillium funiculosum*)	MIL-STD-810F (US, Euro) MIL-STD-810H (Euro) Lavoie et. al (1997)	
ATCC 9645	*Trichoderma virens*	MIL-STD-810F (Euro) MIL-STD-810H (US, Euro) Lavoie et. al (1997) Ray et. al (2010)	

*formerly known as

Additives

The contaminant fluids consisted of a common hydraulic fluid (MIL-PRF-83282, Royco 782) and the CPC Cor-Ban 35 (MIL-PRF-85054). Cor-Ban was formulated with and without an added fungistat, 0.5% Omacide 100. Additives were applied with a foam brush making sure the entire surface was covered by additive.

Experimental Matrix

The full listing of the exposure matrix is shown in Appendix A. Panels were divided into three different sets:

- (C) control - unexposed for baseline analyses

- (CC) climate controlled - exposed in elevated humidity/temperature without intentional fungal inoculation
- (M) microbial - exposed in elevated humidity/temperature without intentional fungal inoculation

The panels were subdivided into Groups 1-12 representing different topcoats (with and without Rust-o-Oleum NeverWet super-hydrophobic coating) and additives (i.e., Cor-Ban 35 CPC with and without 0.5% Omacide; Royco 782 hydraulic fluid). All panels except Group 2 had chromate primer. CC panels were not coated with CPC or hydraulic fluid.

- Group 1 (C1, CC1, M1) – Chromate primer only
- Group 2 (C2, CC2, M2) – Non-chromate primer only
- Group 3 (C3, CC2, M3) – Type I topcoat
- Group 4 (C4, CC4, M4) – Type IV topcoat
- Group 5 (CC5, M5) – Type I topcoat + Cor-Ban 35
- Group 6 (CC6, M6) – Type I topcoat + Cor-Ban 35 with 0.5% Omacide
- Group 7 (C7, CC7, M7) – Type I topcoat + NeverWet super-hydrophobic coating
- Group 8 (CC8, M8) – Type I topcoat + Royco 782 hydraulic fluid
- Group 9 (CC9, M9) – Type IV topcoat + Cor-Ban 35
- Group 10 (CC10, M10) – Type IV topcoat + Cor-Ban 35 with 0.5% Omacide
- Group 11 (C11, CC11, M11) – Type IV topcoat + NeverWet super-hydrophobic coating
- Group 12 (C12, M12) – Type IV topcoat + Royco 782 hydraulic fluid

Elevated Humidity/Temperature Exposure

The prepared suspension of five different fungus species (Table 1) was sprayed onto the panels M1-12. Climate controlled panels CC1-12 were sprayed with the same sodium chloride salt solution used in the spore suspension but without any intentional fungal spore addition. The C panels were placed into plastic containers containing a dish filled with the salt solution and a remote temperature/hygrometer sensor. The salt solution maintained a relative humidity of 95% inside the containers and limited cross-contamination from the intentionally inoculated panels. Control panels with the same additive (e.g. hydraulic fluid) were placed in the same container. Panels C and M were exposed to 84 days of 95% relative humidity and 30±1 °C in a humidity chamber (Mfr. Shel Labs). These testing parameters were based on MIL-STD-810F. The temperature/humidity parameters are the same used in the latest 'H' designation of MIL-STD-810.

Cleaning of Microbiologically Exposed and Control Coupons

The effect of chemicals and processes used to remove and/or neutralize (sanitize) the biological growths and operational chemical residues were examined, with respect to the removal of growths as well as to control for the effect of cleaning procedures on results of the various analytical results on the underlying

coating surfaces. Cleaning processes necessarily differed depending on the doped fluids present on the coupon (e.g., hydraulic fluid). Where the additional information was expected to be useful, coupons were analyzed prior to and after removal of the contaminant films. Analyses performed before and after cleaning are listed in Table 2.

Cleaning Procedure Definitions

For consistency in describing coupon cleaning procedures after biological exposures the designations below are used in the following sections of this report.

- Cleaning #1: Isopropyl Alcohol Wipe. 99.953% anhydrous, zero residue, water free pre- saturated wipes, Catalog No. 824-W by M.G. Chemicals. Wiped in each of four directions on the coupon, using a new section of the wipe for each direction.

- Cleaning #2: Isopropyl Alcohol application by cotton swab or other cloth locally for spot analyses, or a cloth in the directional wiping pattern as defined in Cleaning #1 above.

- Cleaning #3: IPA/Acetone/Ethanol/Methanol sequential solvents wiped over the same area.

- Cleaning #4: NavClean applied by wiping with cloth or cotton swabs.

- Cleaning #5: Leached with acetonitrile for analyses requiring a liquid analyte (i.e. GC-MS and GPC).

NavClean Cleaning Protocol

Deionized water (~9.5 mL) was heated to ~50°C with stirring. All of the components in the NavClean kit were added to the heated water in the order of A (0.034 mL), B (0.034 mL), C (0.14 g), and D (0.024 g) with continuous stirring. The solution is complete once a clear solution is observed. The solution was allowed to cool to room temperature prior to application, cleaning of the area(s) of interest must be completed soon after components are mixed as the solution will settle upon sitting. After cleaning the area with a cotton swab, the area was swabbed immediately after with water to remove excess residue from the NavClean.

Specimens Analyzed and Cleaning Procedures Used

For each analytical method, more than one cleaning method was used to compare surface chemistry and conditions prior to and after microbial exposures, and prior to and after various cleaning procedures. Table 2 outlines which experimental procedures were used for each coupon condition along with information pertaining to cleaning procedures used prior to the analyses.

Table 2. Coupons Analyzed and Cleaning Methods Applied

	Control (C) Unexposed	Non-inoculated (CC) Exposed	Non-inoculate (CC) Exposed After Cleaning	Inoculated (M) Exposed Before	Inoculated (M) Exposed After Cleaning
ESEM	X	X	X	X	X (Note
Optical Microscopy	---	X	---	X	---
Phase Contract Microscopy	---	X	---	X	X (Note 2,3,4)
FTIR	X	X	X	X	X
GPC	X (Note 5)	X (Note	X (Note 5)	X (Note	X (Note 5)
GC-MS	X (Note 5)	X (Note	X (Note 5)	X (Note	X (Note 5)
LSM	X	---	---	X	X (Note 1)
EIS	X	---	---	---	---
SKP	X	X	X (Note 2,4)	X	X (Note 2,4)

Note 1: Cleaning procedure #1 (IPA pre-saturated wipe)
Note 2: Cleaning Procedure #2 IPA applied locally with a cotton swab
Note 3: Cleaning Procedure #3 (IPA/Acetone/EtOH/MeOH sequence, for experimental comparison)
Note Note 4: Cleaning Procedure #4 (NavClean)
Note 5: Coupon leached with acetonitrile to solubilize extractibles for analyses

Gross Imaging

Digital images were acquired with a Nikon Coolpix 12.1 megapixel digital camera. The samples were laid flat on a clean surface and imaged in macro mode under a light source.

Analytical Techniques

Nine analytical techniques were proposed to provide a comprehensive view of the microbial degradation mechanisms of organic coatings used in combinations of aerospace finish systems. The techniques constitute a comprehensive analysis by analyzing both bulk and localized electro-chemical (anodic/cathodic) activity, film barrier properties (capacitive and resistive), surface micro-roughness, functional group analysis, and elemental valence state analysis of constituents, chemical identity of digestion by-products and film degradation by-products, and other information:

1. Light and Fluorescent Microscopy
2. Environmental Scanning Electron Microscopy (ESEM)
3. Laser Scanning Microscopy (LSM)
4. Scanning Kelvin Probe (SKP)
5. Fourier Transform Infrared (FTIR) Spectroscopy
6. Gas Chromatography and Mass Spectrophotometer (GC-MS)
7. Gel Permeation Chromatography (GPC)
8. Electrochemical Impedance Spectroscopy (EIS)
9. Atomic Force Microscopy (AFM)

Light and Fluorescent Microscopy

Optical images were acquired on an Olympus CX41 microscope equipped with a X-Cite® 120Q wide field fluorescence microscope excitation light source. Fungal specimens were collected by contact slides, isolated and identified with optical light and fluorescent microscopy, as well as phase contrast spectroscopy. Lactophenol Cotton Blue Stain was used to stain the fungal specimens before observation under the microscope. Images were taken at 4x and 10x magnifications for light and fluorescent microscopy, and for phase imaging, immersion oil was used atop of the contact slides for 10x, 40x and 100x magnifications.

Environmental Scanning Electron Microscope (ESEM)

Examinations of intact fungal mats were performed at Naval Research Laboratory at Stennis Space Center (NRL-SSC) using low kV SEM at 5 kV accelerating voltage and 1μA beam current. The coupons were mounted atop a stub using carbon tape with no further modifications.

Scanning Kelvin Probe (SKP)

A computer controlled Biologic M470 scanning probe workstation was used for this application. A scanning Kelvin probe (SKP) system was used to examine differences in the work function measured on the surface of the coating systems. The Kelvin probe has been used in ambient atmospheric conditions to measure the difference in work function between a conducting probe and conducting or semiconducting metals, nonmetals, polymers, thin films, organic films, and biological samples (Baikie et al. 1999). The work function, Φ, is defined as the potential that an electron at the Fermi level must overcome to reach the level of zero kinetic energy away from a solid surface to infinity in a vacuum (Bare and Somarjai 2002). When two metals (such as the Kelvin probe and a metal surface) having different work functions are electrically connected, electrons will distribute themselves such that an equilibrium of charge will be established. This redistribution of electrons establishes a contact potential, Ψ, and any contact potential difference (CPD) between the work functions of two metals in contact at thermal equilibrium is defined as:

$$\Delta\psi = \Phi_{\text{probe}} - \Phi_{\text{metal surface}} \quad (1)$$

However, in the present case of ambient atmospheric conditions, a layer of oriented dipoles (such as water, organic polymers or biomolecules) will produce an electric double layer, giving rise to the surface potential, χ (Janata and Josowicz 1997). The work function of a solid material at a solid/liquid interface can therefore be divided into two components, the contact potential (also defined as the Volta potential [Mc-Naught et al.]) and the surface potential, which when added together are defined as the Galvani potential (Bergveld et al. 1998), Φ:

$$\Phi_{\text{surface}} = \Psi + \chi \quad (2)$$

The relationship between work function and the Galvani potential for a liquid/solid interface is well defined (Grunmeier et al. 2000) and providing that the work function of the Kelvin probe is constant, variations in the contact potential difference (CPD) can be attributed to changes in the surface potential on the sample substrate directly below the scanning Kelvin probe tip (Baikie et al. 1999). The measurement of the CPD can provide information about molecular conformation in adsorbed organic layers at the air/solution interface and on solid substrates (Hansen et al. 2003). This capability can be used to determine the presence of fungal biomaterial as well as any effect of cleaning agents used to remove the fungal biomaterial on a coating system in a non-destructive manner.

The technique involves vibrating a probe in close proximity to the surface of the sample being studied, with the probe moved by stepper motors in the X and Y directions over the sample. The sample connection is made using copper tape attached to the uncoated back of the panel. At each scan position, a value for the

CPD is determined as the difference between the potential of the probe tip and the surface of the sample below the probe tip and presented as a two dimensional map. Two probes of different tip diameters were used: 150 µm and 500 µm. The 500 µm diameter probe was used extensively, as this allowed for a larger signal-area ratio as well as a faster and more accurate scan over a larger area. The 150 µm diameter probe allowed for more precision over a smaller area, and was used only when attempting to resolve the small fungal clusters. Across experiments, the probe distance from the surface varied from 60 µm to 100 µm. In a single experiment, the probe distance is maintained by probe movement in the Z direction according to a previously generated topography map. The topography map was generated using an Optical Surface Profilometer (OSP), which is part of the M470 system. Before using the SKP, an optical surface profiler height map is generated, so that constant working distance can be maintained over the entire SKP scan area. Table 3 shows a range of values for each of the parameters used to measure CPD.

Table 3. SKP Scan Parameters and Operating Values

Parameter	Value
Full Scale Sensitivity	1-5 mV
Output Time Constant	0.1 s
Vibration Amplitude	30 µm
Vibration Frequency	80 Hz
Reference Phase	125-190°

For each scan condition, multiple measurement scans were made. Due to charges that may accumulate on the surface, observing how the work function changes over time is important so that a steady state value for work function can be measured; these charges often dissipate after several hours, so by the third scan, the sample is usually at steady state. Surface charging due to outside effects do not reflect the nature of the sample, so their effect must be mitigated. In some cases, humidified air was passed over the sample surface to reduce surface charging.

When comparing separate scans, changes in temperature, humidity, and other factors make direct comparison of results difficult. In many cases, multiple panels were arranged adjacent to each other and scanned at the same time. This method resulted in work function values that are directly comparable, with the resulting area scan maps of the surfaces displaying the CPD values as a work function (millivolts, or mV) were used for analysis.

Data from the OSP and SKP area scans were analyzed and images generated in the M470 software, as well as imported into Microsoft Excel for additional plotting and calculations. Panel and section averages were determined, with corresponding standard deviations.

Laser Scanning Microscopy (LSM)

Coatings which are not inhibiting to fungal or microbiological type growths may be subject to degradation mechanisms which can be characterized by changes in surface roughness and chemistry. Initiation of the degradation is accelerated by the presence of contaminating films of organics and operational chemicals used on aircraft. Dissolution or metabolism of carbon as present in constituents such as organic molecules, corrosion inhibitors, hydraulic fluid residues, pigments, etc. may also be a factor in these surface changes, which were characterized through a Laser Scanning Microscope (LSM) for rapid profilometry which provides three dimensional results. The Keyence LSM is capable of profilometry incorporating both optical and laser methods and will be used for detailed characterization of the coatings' surface roughness parameters prior to and after the mold/mildew growth on the coating surfaces. The LSM was used for these 3-D areal roughness characterization, which is a non-contact computer driven metrology tool which develops detailed parameters for surface texture and profile information on the submicron scale. There are numerous roughness and waviness parameters which were used to characterize surfaces in bulk such as the

root-mean-square and arithmetic or average roughness values, while there are other LSM parameters reflecting height or depth of localized features. Of greatest interest in this study are areas which were expected to be microscopic void or pit type defects with discrete dimensions, although these may exist to a greater extent over the surface. Full, through thickness channels or pores would not be detected by line-of-sight profilometry methods, and would be difficult to detect by other methods. The LSM parameters selected for these analyses were (1) arithmetic roughness (Sa), (2) Root Mean Square (RMS) roughness (Sq), (3) maximum profile valley depth (Sv), (4) developed interfacial area ratio (area deviation compared to a plane), (Sdr), (5) maximum profile peak height (Sp), (6) maximum height, Sz. The tool is also equipped with different void characterization parameters such as Vv(p) which may be used with appropriate cutoff thresholds to characterize changes in voided areas. While any uniform, generalized attack will be best characterized by the roughness parameters listed such as Sa, Sq, Sdr, the Sv parameter was expected to most likely detect any locally pitted areas.

Characterization results from the LSM were exported to Microsoft Excel to calculate differences in before-and-after profile data, and each exposure/test condition was correlated to changes in the various roughness parameters to determine those of greatest significance in describing the breadth of results observed. These geometrical data may be related to known features within the coating that may be subject to attack if they are nutrients for microbiological type activity (this would be on microscopic scale). Post-exposure coupons were initially wiped with the pre- saturated IPA wipes/cloths described in *Cleaning Procedure Definitions*.

Electrochemical Impedance Spectroscopy (EIS)

EIS was used to quantify the differences in impedance and corrosion potential characteristics of the test coating systems. Computer controlled Gamry 3000 Potentiostat/Galvanostat equipment was used to analyze coatings. Coating systems were immersed in sodium chloride solution (3.5%) using cylindrical glass electrochemical cells clamped to the test coupons with an O-ring. Filled electrochemical cells were stored in the laboratory environment after covering the glass tube with Parafilm to control evaporation and concentration of the salt solution in-between tests. A potassium chloride Saturated Calomel Electrode (SCE) was used for the potential measurement. Electrochemical measurements were performed while the electrochemical cell was contained within a Faraday cage over the frequency range of 100 kHz to 0.01 Hz using AC amplitude of ±10mV around the DC open circuit potential (OCP). OCP was determined after a voltage stabilization (+/- 1 mV/min) period of 10 min to 2 hrs. Newly immersed coating systems took two hours to obtain reasonable OCP data, while once immersed for days or months as the case was with these experiments, the program recipes were changed to use a ten-minute dwell time prior to the EIS sweeps. Assemblies were tested after various intervals to monitor for trends in changing film impedance, resistance and capacitance. Data from the Gamry computer was imported into Microsoft Excel for plotting and analysis. Nyquist plots were created to determine impedance values for each coating system at each immersion dwell time used for the control coupons. Bode plots were created for determination of resistance and capacitance values.

Gas Chromatography / Mass Spectrometer (GC-MS) and Gel Permeation Chromatography (GPC) [aka Size Exclusion Chromatography (SEC)]

GC-MS was used to monitor and identify small molecules extracted from controls and exposed coatings. GPC was used to analyze molecular weights of extracted large molecules, greater than 1K molecular weight from the microbial-compromised coatings' surfaces. Solvent extractions utilized acetonitrile as a solvent non-aggressive to the coatings yet able to broadly dissolve organics especially small molecules from digestion process and other byproducts. These were analyzed by molecular weight and bonding energies to discern chemical identities. Extractions for GCMS and GPC were done by soaking samples in 20 mL acetonitrile for 5 minutes. The acetonitrile from the sample extracts was then concentrated to 1.5 mL through rotary evaporation. The concentrated samples were then run on GPC and GCMS. GCMS analyses of sample extracts were performed on an Agilent 7890A gas chromatograph and 5975C mass spectrometer

with an inlet temperature of 250 °C, auxiliary temperature of 280 °C, ion source temperature of 230 °C and quadrupole temperature of 150°C. The GC method run started at 55°C for 3 minutes, then ramped at the rate of 5 °C up to 150°C, then by 10 °C to 300 °C. The GC was equipped with a Restek Rxi-5ms column with helium carrier gas, 1 mL per min, and the Agilent 5975C mass selective detector operated in scan mode, 35-500 amu, with electron ionization. Chromatographic analysis and peak identification was performed with Agilent ChemStation software. GPC analysis was conducted using a Waters Alliance e2695 gel permeation chromatograph with a degasser, Shodek KF-806M and Waters Styragel column, both 7.8 X 300 mm, connected in series at 40 °C, and a 2414 refractive index detector. Acetonitrile was used as the eluent at a flow rate of 0.1 mL/minute. The system was calibrated with poly(methyl methacrylate) standards and the Empower software was used for analysis.

Fourier Transform Infrared (FTIR) Spectroscopy

FTIR was employed to identify changes in the surface composition molecular bonding energies analysis. The appearance of new peaks and changing intensities of existing peaks signifies chemical changes which have occurred in the organic coating surface by the activity of the microbes. For this study, ATR-FTIR spectroscopy was performed on a Nicolet iS50-FT-IR with iS50 ATR attachment equipped and a diamond ATR crystal from Thermo Scientific with 64 scans compiled for each spectrum. Spectra were recorded from 4000 – 500 cm^{-1} with a resolution of 2 cm^{-1}, and were analyzed using the Nicolet OMNIC software suite. ATR-FTIR spectra was conducted on all samples before exposure, after exposure for both climate and microbial, and after both were washed with NavClean. The samples before exposure were used as controls to monitor changes from all the other samples.

Atomic Force Microscopy (AFM)

AFM observations were carried out with intermittent “tapping” mode in ambient on an Agilent 5500 SPM/AFM system equipped with PicoView v1.20 software (Keysight Technologies, Inc., Santa Rosa, CA) at Louisiana State University. The surface was investigated using commercially available silicon nitride (Si_3N_4) AFM tips (SSS- NCH50, resonance frequency of 330 kHz) purchased from NanoSensors (Tempe, AZ). Raw images were collected in situ and processed with Gwyddion[1] software (version 2.47, 64-bit).

Results and Discussion

Light Optical Microscopy, Phase Contrast Microscopy, and ESEM Observations:

Fungal Morphologies

Five species of fungi were selected from various sources as stated previously: *Hormoconis resinae, Aspergillus brasiliensis, Aureobasidium pullulans, Talaromyces pinophilus and Trichoderma virens*. The fungi were cultured separately on potato dextrose agar plates. Figure 1 shows the morphologies of *H. resinae, A. brasiliensis* and *A. pullulans*. All three have a similar 'mace ball' spore morphology. *A. pullans* has segmented hyphae while *H. resinae and* A. *brasiliensis are* not. Figure 2 shows the other two fungi; *T. pinophilus* and *T. virens* have smooth, oblate spores with segmented hyphae. *T. pinophilus* produces hyphae of multiple sizes while *T. virens exhibits* hyphae of one size. Control PDA plates were sprayed by the mixed specie spore suspension at the same time as the coated metal samples were sprayed. Figure 3 shows the resulting fungal mat of the five specie mixed culture.

Hormoconis resinae Aspergillus brasiliensis Aureobasidium pullulans

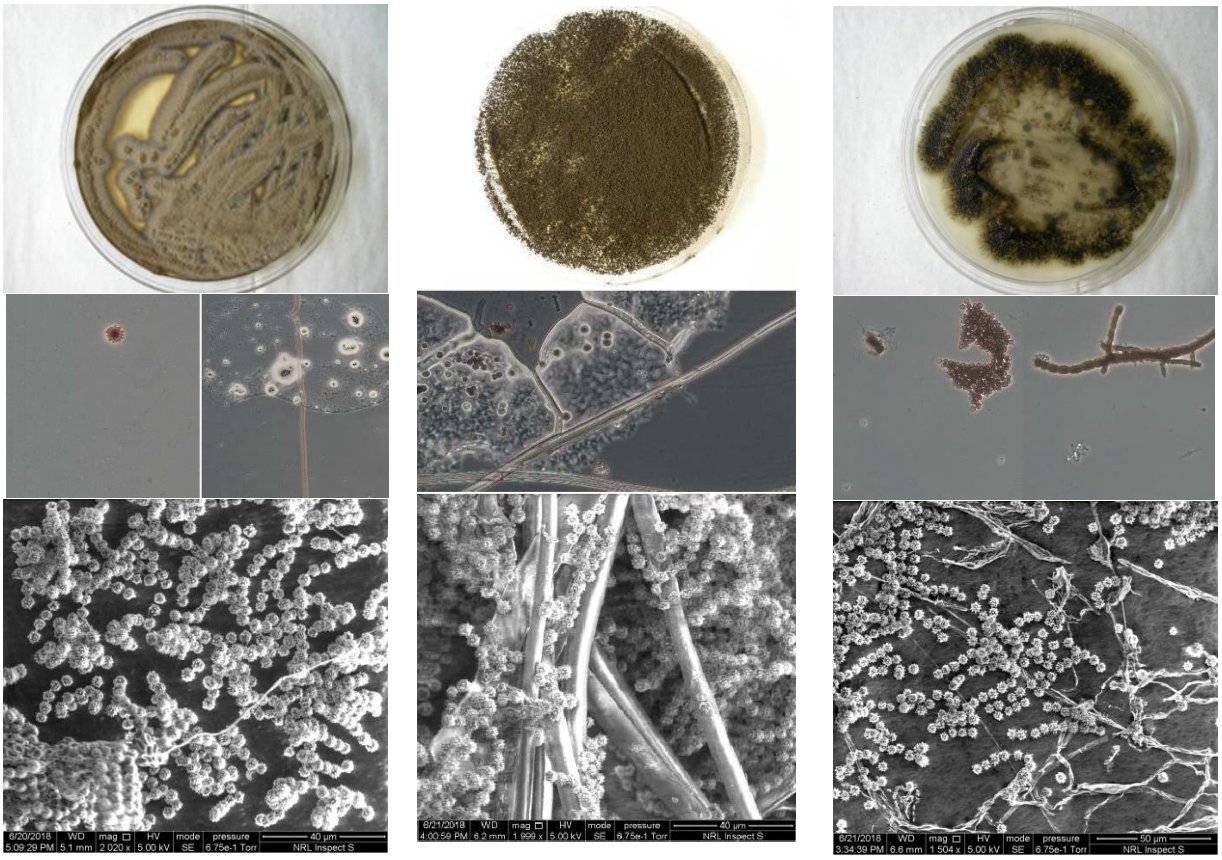

Figure 1. Morphologies of fungal species *Hormoconis resinae*, *Aspergillus brasiliensis* and *Aureobasidium pullulans* as shown by growth on potato dextrose agar (top), phase contrast microscopy (middle) and low vacuum scanning electron microscopy (bottom).

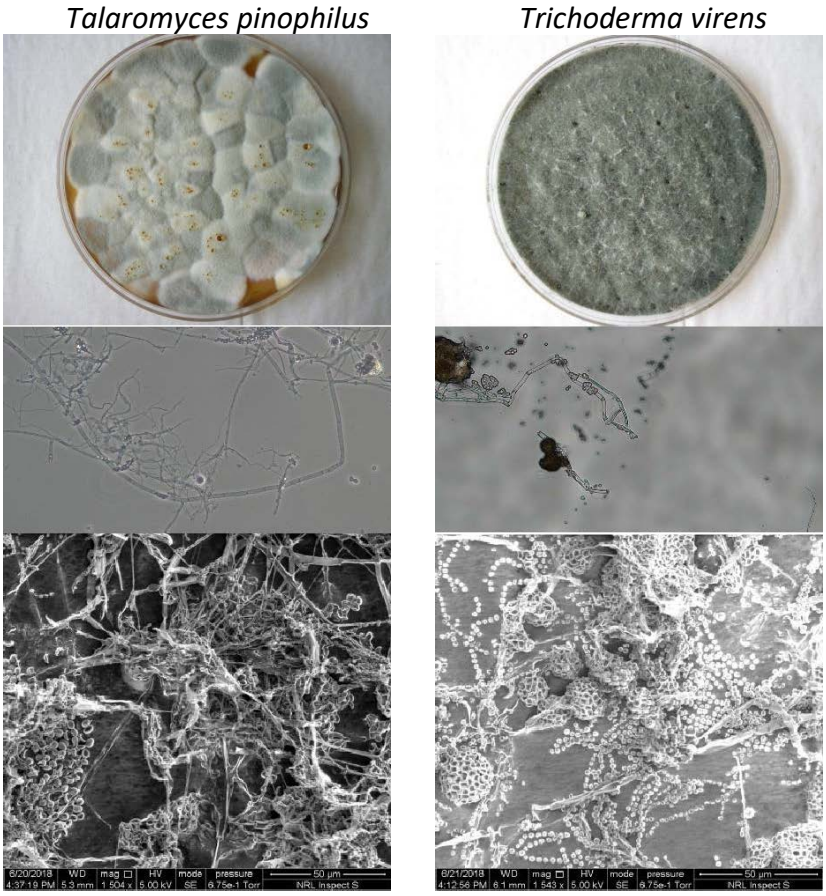

Figure 2. Morphologies of fungal species *Talaromyces pinophilus* and *Trichoderma virens* as shown by growth on potato dextrose agar (top), phase contrast microscopy (middle) and low vacuum scanning electron microscopy (bottom).

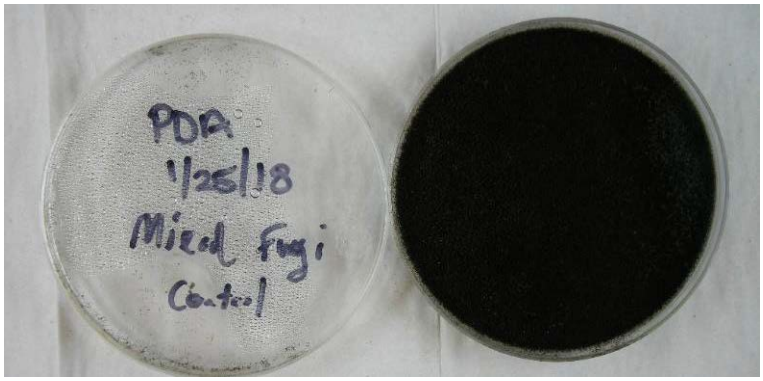

Figure 3. Potato dextrose agar 7 days after inoculation with mixed, five-specie fungal spore suspicion. Growth on PDA confirmed fungal spores were delivered to coupons surfaces.

Environmental Chamber Exposure

The following sections illustrate the effects of 84 days of exposure in a controlled environment of 35°C with 95% relative humidity with (M designation) and without (CC designation) fungal spore inoculation. Each section compares CC vs M exposures and select systems will also compare unexposed samples. Figures are standardized in format with CC images on the left and M images on the right. First, the whole 2-inch x 2-inch coupon was imaged with a digital camera equipped with a macro lens followed by light microscopy with a 4X magnification. The light source was then switched to a fluorescence lamp to view the same region as was imaged at 4X. Finally, each coupon was placed into a scanning electron microscope capable of low vacuum imaging and representative areas were documented between 1000 and 2000X magnification. In addition, biological samples were swabbed off of each coupon after the 84-day exposure and streaked onto PDA plates with the CC on the left and M on the right. Images of the plates after 7-day incubation and 23-day incubation are shown at the top and bottom of each figure, respectively. Fungal growth quantification and identification was not performed due to constraints of this limited scope effort.

Primer Only: Chromate (Group 1) vs. Non-chromate (Group 2)

Primers with and without chromate after exposure are shown in Figures 4 and 5, respectively. Neither primer type supported large amounts of fungal growth; however, small clusters of spores and hyphae were observed on both primers. The chromate primer had a rougher surface morphology compared to the non-chromate primer. Examination of the culture plates showed very similar results where control samples had fewer colonies but the colonies were more diverse in species. Chromate is anecdotally believed to be a biocide towards fungi. These results show that the presence of chromate did not significantly alter fungal growth compared to the non-chromate primer. Different fungal species are known to have different susceptibilities to chromate. Lee et al. (2012a) showed that in a mixed fungal consortium, *Aspergillus sp.* was unaffected by chromate but *Aureobasidium pullulans* was. Both of these fungi were used in the current work but the fungal biofilm was not specie-specifically quantified using molecular techniques. This knowledge gap would be part of continuing work. Lee et al. (2012b) showed that chromate did not prevent fungal growth on aluminum 2024, rather the fungi were able to sequester the chromate and prevent it from inhibiting active corrosion sites (pits). In general, chromate is an excellent corrosion inhibitor but is not an effective biocide.

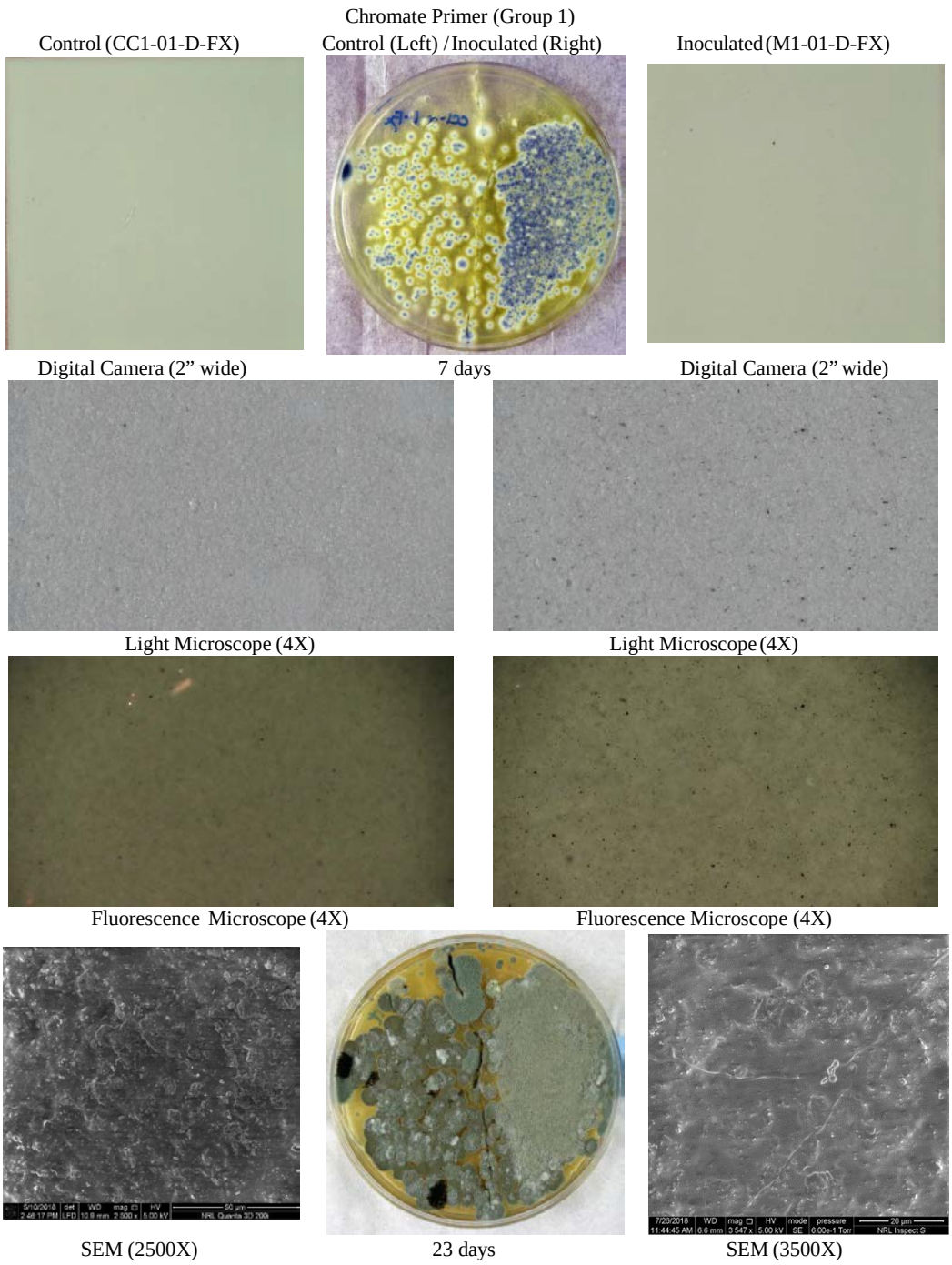

Figure 4. (Group 1): Metal coupons covered with chromate primer exposed to elevated heat and humidity for 86 days without fungi (control, left) and inoculated (right). Potato dextrose agar culture plates were inoculated with swabs taken from the coupons after 86-day exposure; left side of the plate was swabbed from the control coupon, while the right side was swabbed from the inoculated coupon. Culture plates are shown at 7 and 23 days after inoculation.

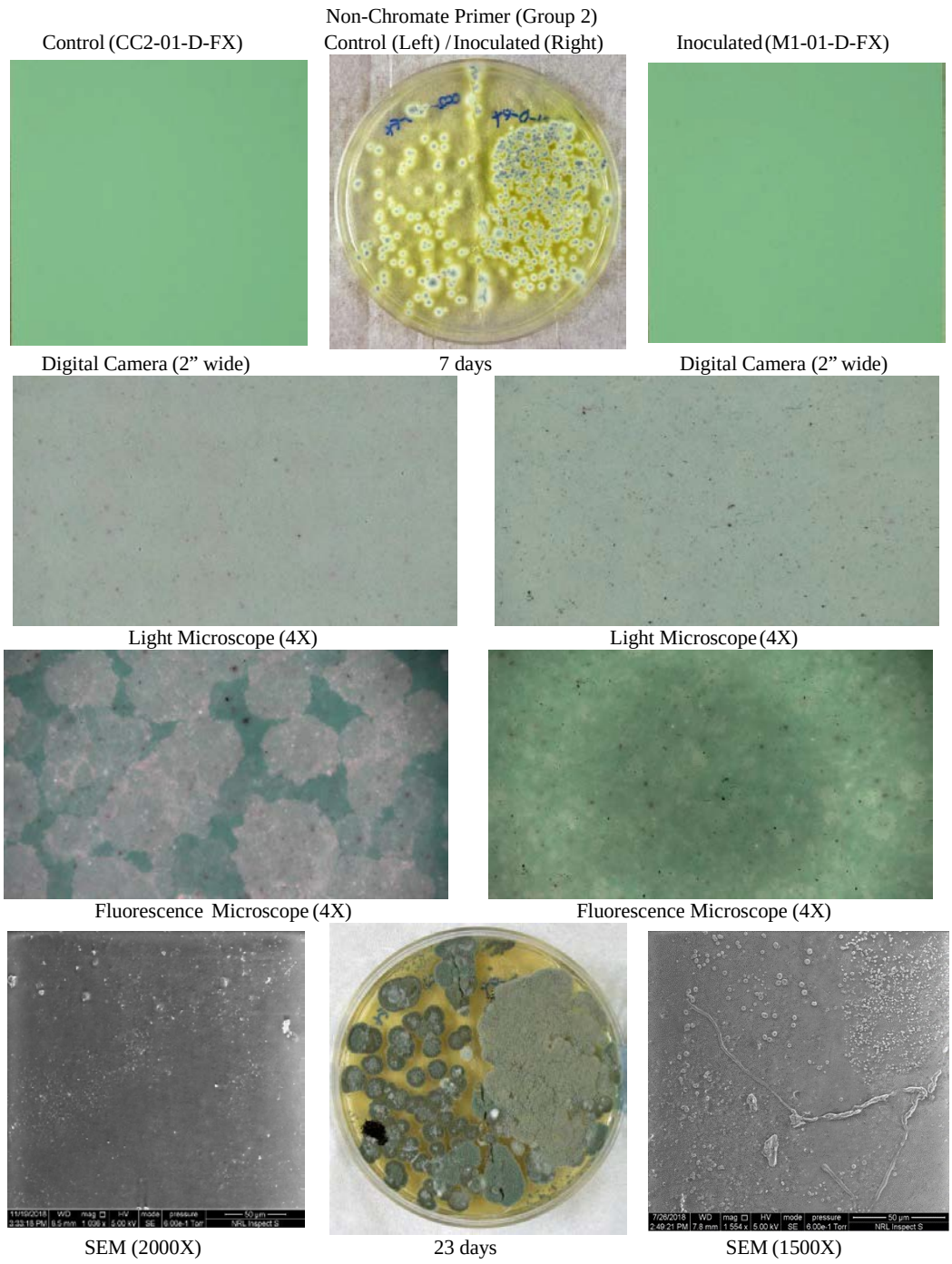

Figure 5. (Group 2): Metal coupons covered with non-chromate primer exposed to elevated heat and humidity for 86 days without fungi (control, left) and inoculated (right). Potato dextrose agar culture plates were inoculated with swabs taken from the coupons after 86-day exposure; left side of the plate was swabbed from the control coupon, while the right side was swabbed from the inoculated coupon. Culture plates are shown at 7 and 23 days after inoculation.

Topcoat: Type I (Group 3) vs. Type IV (Group 4)

Figures 6 and 7 show the results for exposure of metal coupons coated with Type I and Type IV Topcoats, respectively. Type I topcoat exhibited small amounts of fungal growth, mainly isolated patches of fungal spores and hyphae. In comparison, Type IV topcoat had significantly more fungal growth than Type I. Patches of dark spore congregations were visible in the digital and light microscope images. Fluorescent light illuminated the hyphae as bright orange which distinguished them from the spores. Interestingly, the exposed control (CC) coupon that was subjected to elevated temperature and humidity but not fungi, shows what looks like cracks in the topcoat under fluorescent light. These cracks were not seen in the unexposed control sample (C) as shown for comparison in Figure 7. Inspection of the culture plates showed a difference between the Type I and Type IV topcoat fungal mat. Type I growth plate showed more diversity compared to Type IV. Both control culture plates showed fungal growth but to a lesser extent as compared to their inoculated counterparts.

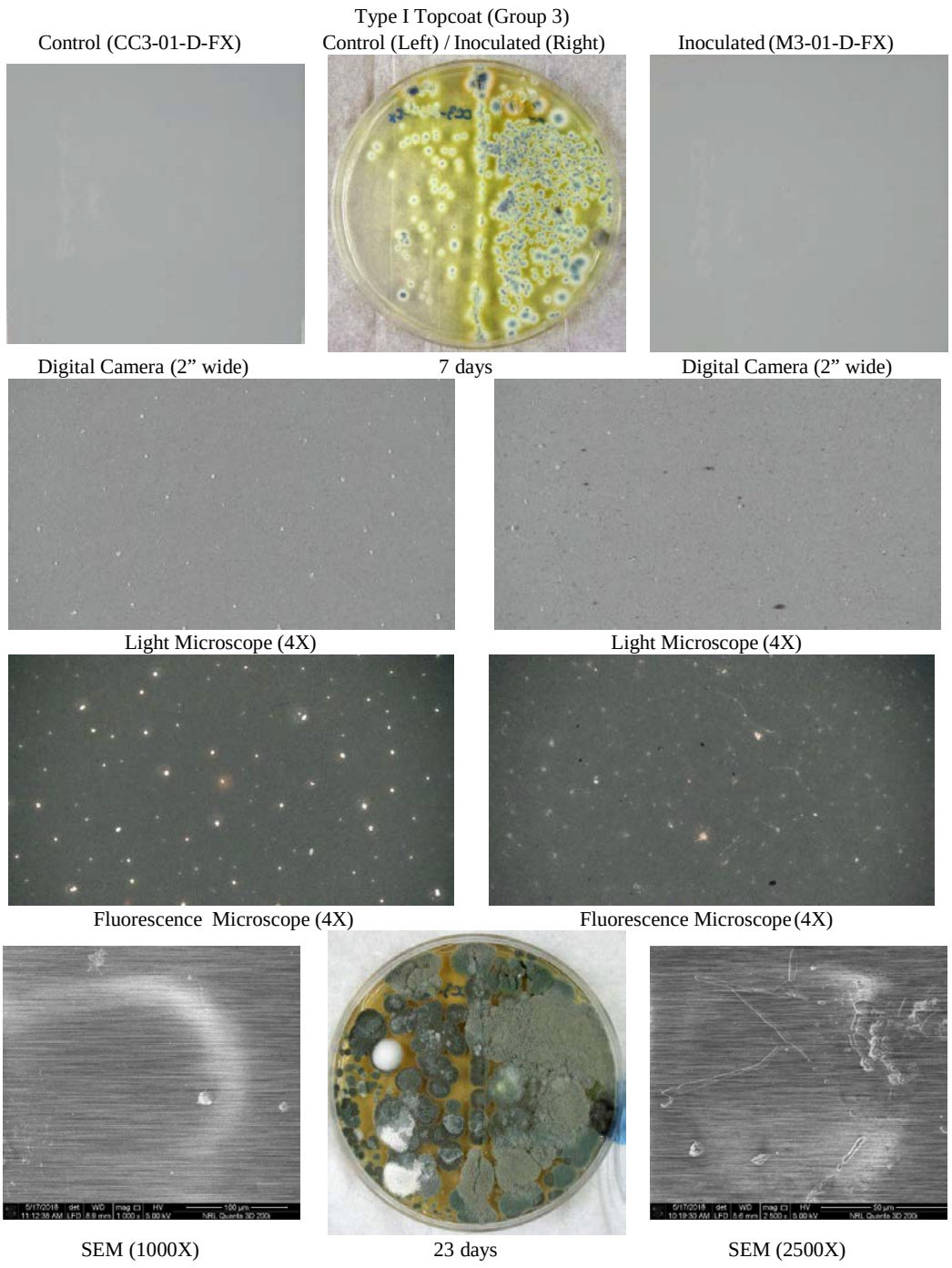

Figure 6. (Group 3): Metal coupons covered with Type I topcoat exposed to elevated heat and humidity for 86 days without fungi (control, left) and inoculated (right). Potato dextrose agar culture plates were inoculated with swabs taken from the coupons after 86-day exposure; left side of the plate was swabbed from the control coupon, while the right side was swabbed from the inoculated coupon. Culture plates are shown at 7 and 23 days after inoculation.

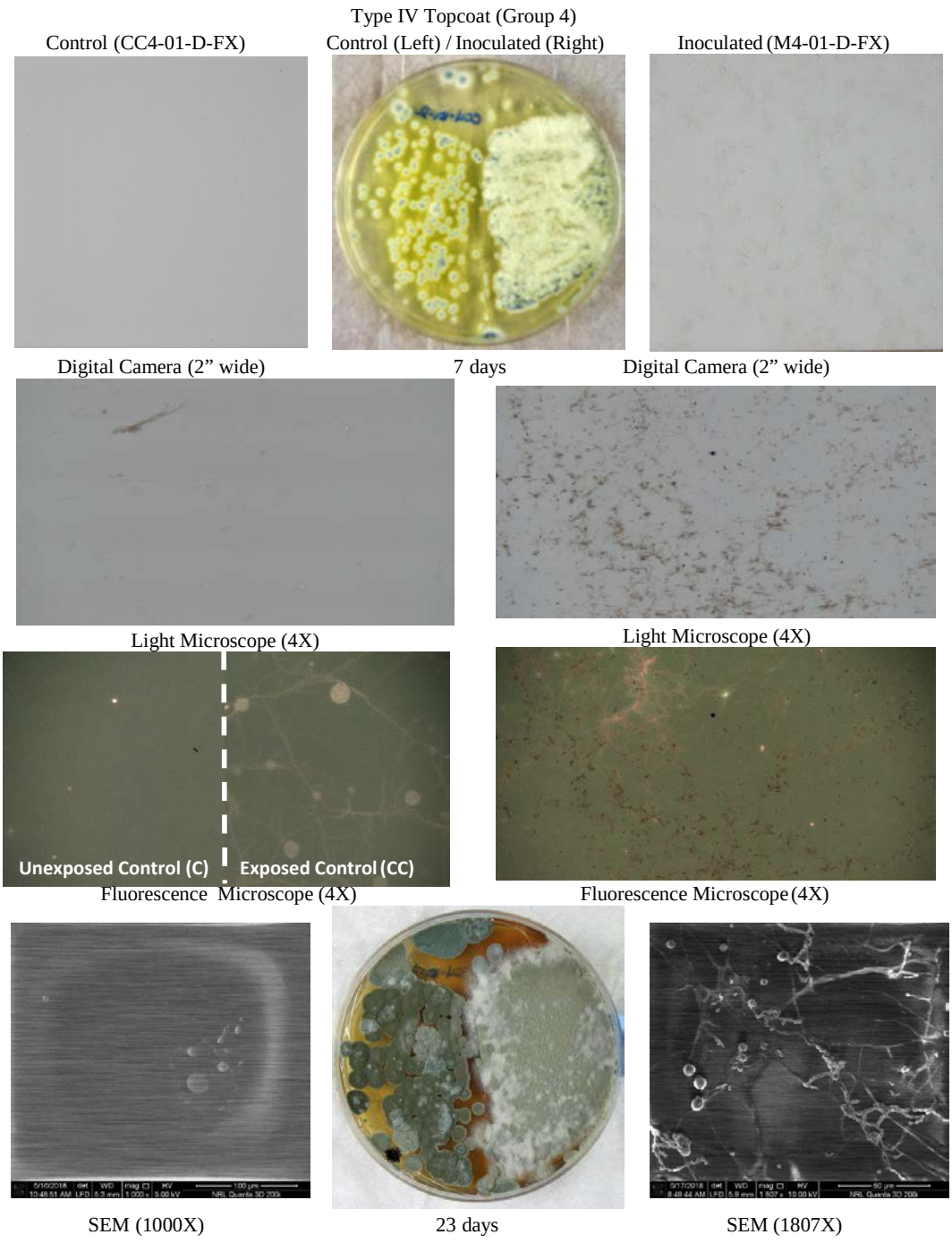

Figure 7. (Group 4): Metal coupons covered with Type IV topcoat exposed to elevated heat and humidity for 86 days without fungi (control, left) and inoculated (right). Potato dextrose agar culture plates were inoculated with swabs taken from the coupons after 86-day exposure; left side of the plate was swabbed from the control coupon, while the right side was swabbed from the inoculated coupon. Culture plates are shown at 7 and 23 days after inoculation.

Super Hydrophobic Coating: Type I (Group 7) vs. Type IV (Group 11)

A super-hydrophobic coating was applied to Type I and Type IV topcoats. Figure 8 shows the condition of the Type I topcoat with super-hydrophobic coating after 86 days with and without fungal inoculation. Both control and inoculated coupons caused the beading of water droplets on the coupon surface. Only a few isolated patches of fungal hyphae were observed on the inoculated coupon. No hyphae were observed on the control. In comparison, the Type IV topcoat with super-hydrophobic coating had visible fungal colonies seen as black dots in the light microscopy images in Figure 9. Water droplet beading was also observed. As evidenced in the culture plates, different species of fungi were proficient in growth after extraction from the Type I (Figure 8) and Type IV (Figure 9) topcoats with super-hydrophobic coating. Therefore, even with the same super-hydrophobic coating, the underlying topcoat effected fungal growth patterns. Comparing the topcoats with (Group 7 & 11) and without hydrophobic coating (Group 3 & 4), it can clearly be seen that the presence of a super-hydrophobic coating decreased the amount of fungal growth compared with bare topcoat coupons.

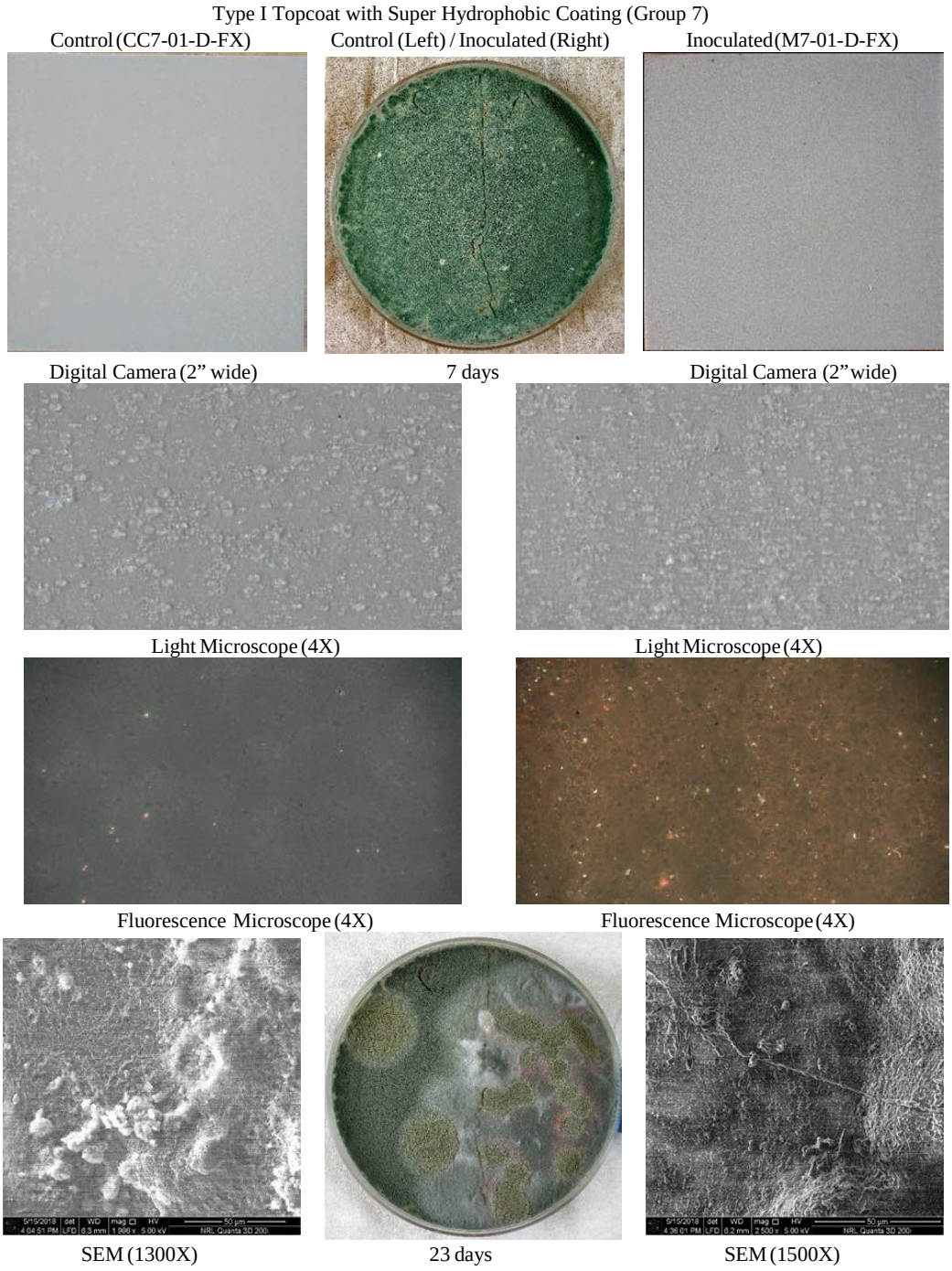

Figure 8. (Group 7): Metal coupons covered with super-hydrophobic coating over Type I topcoat exposed to elevated heat and humidity for 86 days without fungi (control, left) and inoculated (right). Potato dextrose agar culture plates were inoculated with swabs taken from the coupons after 86-day exposure; left side of the plate was swabbed from the control coupon, while the right side was swabbed from the inoculated coupon. Culture plates are shown at 7 and 23 days after inoculation.

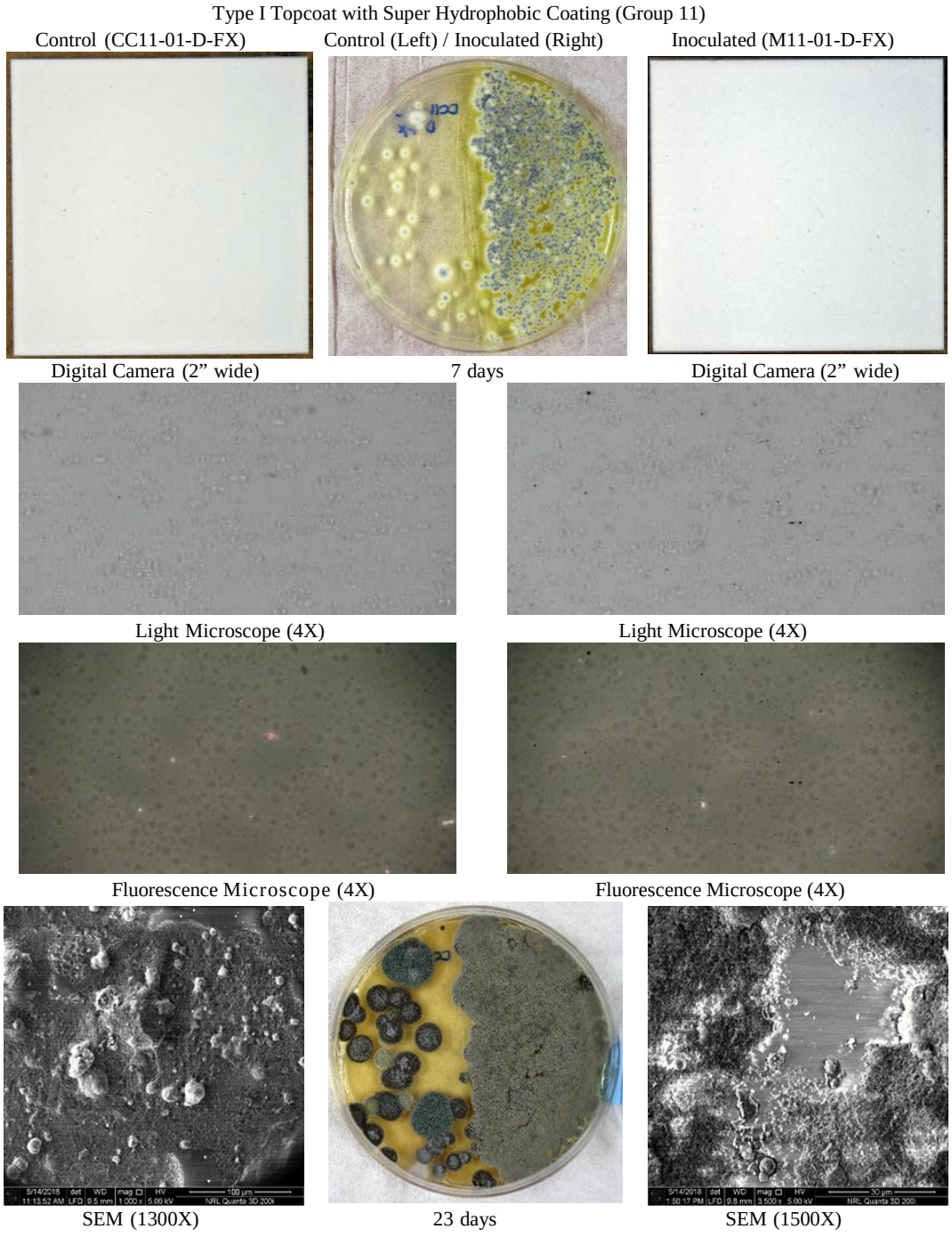

Figure 9. (Group 11): Metal coupons covered with super-hydrophobic coating over Type IV topcoat exposed to elevated heat and humidity for 86 days without fungi (control, left) and inoculated (right). Potato dextrose agar culture plates were inoculated with swabs taken from the coupons after 86-day exposure; left side of the plate was swabbed from the control coupon, while the right side was swabbed from the inoculated coupon. Culture plates are shown at 7 and 23 days after inoculation.

Hydraulic Fluid: Type I (Group 8) vs Type IV (Group 12)

Hydraulic fluid was applied to topcoat covered coupons to simulate conditions often observed in operational airframes. Figures 10 and 11 shows the results of hydraulic fluid covered Type I and Type IV topcoats, respectively. Hydraulic fluid coalesced into large puddles on Type I topcoats (Figure 10). Small patches of fungi were observed as black dots on the control samples (right side of digital camera image). The inoculated coupons exhibited substantially more visible growth. The puddles of hydraulic fluid were larger as compared to the controls, and they were ringed by black fungi. Light, fluorescence and electron microscopy showed extensive fungal hyphae in both control and inoculated exposures; however, the culture plates showed that the fungal species were different. The Type IV topcoat with hydraulic fluid also showed extensive fungal growth in both control and inoculated exposures (Figure 11). The control samples showed extensive hyphae growth with small patches of spores. In contrast, the inoculated exposure exhibited more spore conglomeration with hyphae growth. In comparison to Type I topcoat (Figure 10), the Type IV topcoat caused the hydraulic fluid to bead into smaller droplets. In addition, the culture plates for the Type IV topcoat showed more diverse fungal species for both the control and inoculated coupons. These results reinforce that hydraulic fluid provides an excellent environment for fungal growth.

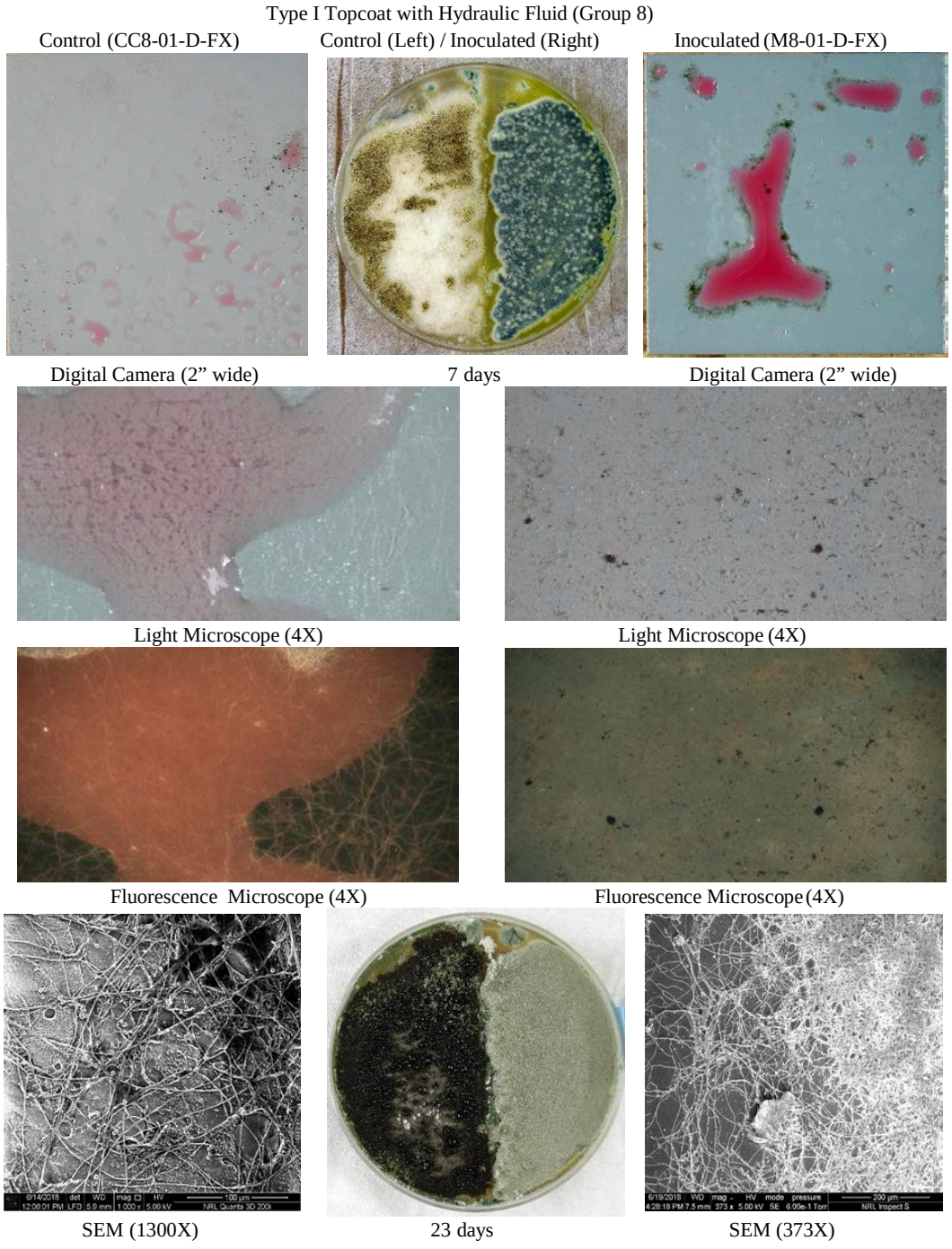

Figure 10. (Group 8): Type I topcoat coupons covered with hydraulic fluid and exposed to elevated heat and humidity for 86 days without fungi (control, left) and inoculated (right). Potato dextrose agar culture plates were inoculated with swabs taken from the coupons after 86-day exposure; left side of the plate was swabbed from the control coupon, while the right side was swabbed from the inoculated coupon. Culture plates are shown at 7 and 23 days afterinoculation.

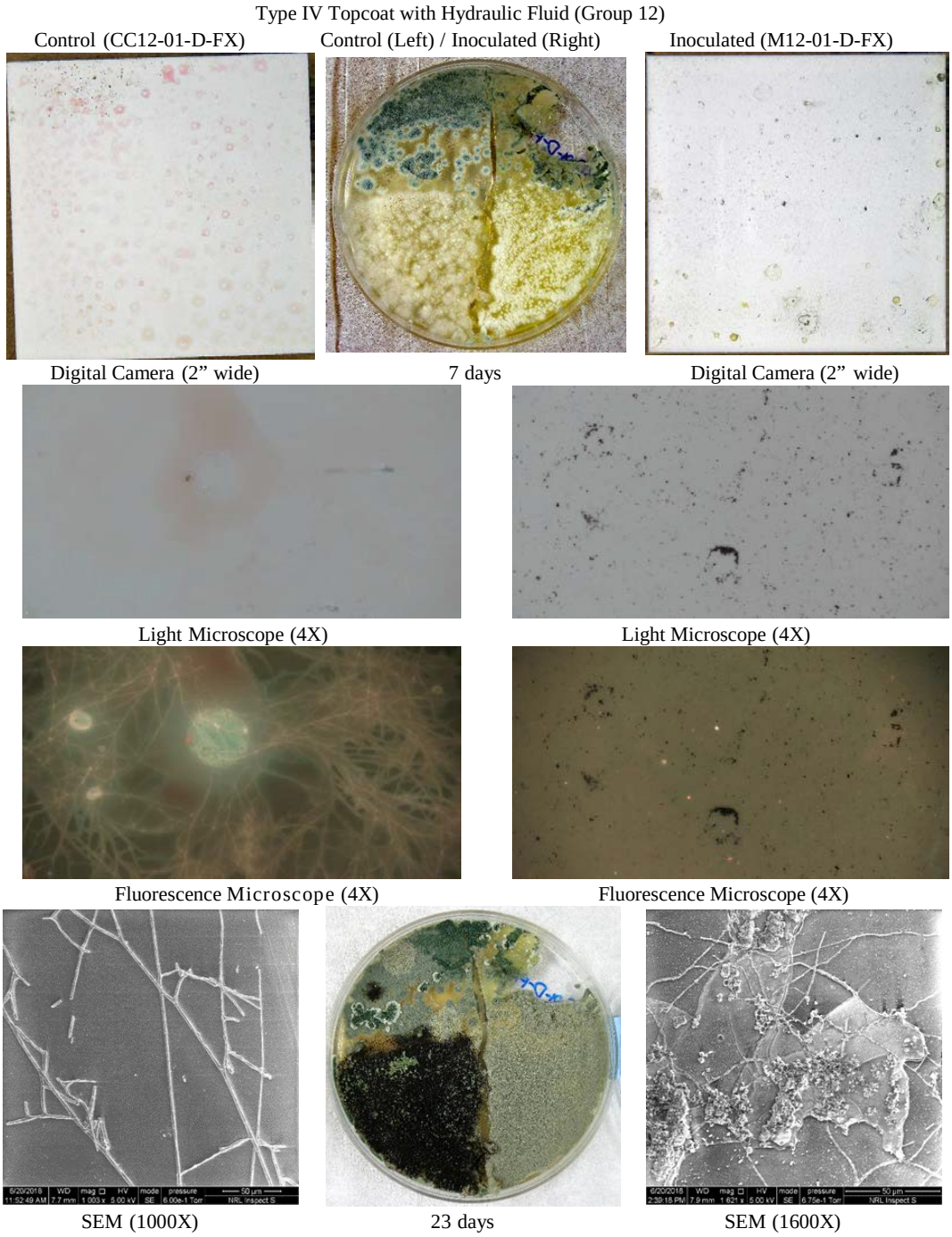

Figure 11. (Group 12): Type I topcoat coupons covered with hydraulic fluid and exposed to elevated heat and humidity for 86 days without fungi (control, left) and inoculated (right). Potato dextrose agar culture plates were inoculated with swabs taken from the coupons after 86-day exposure; left side of the plate was swabbed from the control coupon, while the right side was swabbed from the inoculated coupon. Culture plates are shown at 7 and 23 days afterinoculation.

CPC: With vs Without Omacide for Types I and IV Topcoats (Groups 5, 6, 9, 10)

CPC Cor-Ban 35 with and without Omacide was applied to Type I and Type IV topcoats prior to exposure. Figure 12 shows the Type I topcoat with CPC (Group 5) after exposure. In both control and inoculated exposures, fungal growth in the form of hyphae and spores were observed. However, the extent of fungal hyphae was much greater in the inoculated coupons as observed by fluorescence and electron microscopy. The fungal growth was also different species-wise between the two exposure types. The CPC was patchier in appearance in the control. Addition of Omacide to the CPC (Group 6) had a significant effect on fungal growth as shown in Figure 13. Hyphae growth was not observed in the control exposure and was limited in the inoculated exposure as seen by electron microscopy. The CPC with Omacide was patchy in both the control and inoculated conditions with the control CPC exhibiting larger holes. The culture plates for the inoculated conditions for the CPC without (Figure 13) and with Omacide (Figure 14) were very similar, in contrast to the control conditions which showed difference between CPC with and without Omacide. CPC addition to Type IV topcoat showed similar results to the Type I topcoat exposure. Figure 14 shows Type IV topcoat with CPC addition (Group 9). CPC was patchy in both control and inoculated conditions with extensive hyphae growth in both as well. More fungal spores were observed in the inoculated coupon. However, the culture plates showed that there were specie differences of the fungi between the conditions. As shown in Figure 15, addition of Omacide to the CPC on the Type IV topcoat (Group 10) significantly decreased visible hyphae growth. Also, the control exposure resulted in a patchier coating of CPC with significant holes in the film. Spores were still visible on top of the CPC with Omacide in the inoculated conditions. From these results, it can be deduced that CPC alone provides fungi a suitable growth environment. Addition of Omacide significantly decreases fungal hyphae growth in CPC but does not kill the spores. Therefore, we recommend that a fungicide should always be incorporated into a CPC to prevent fungal growth in the CPC during storage and after application to an airframe.

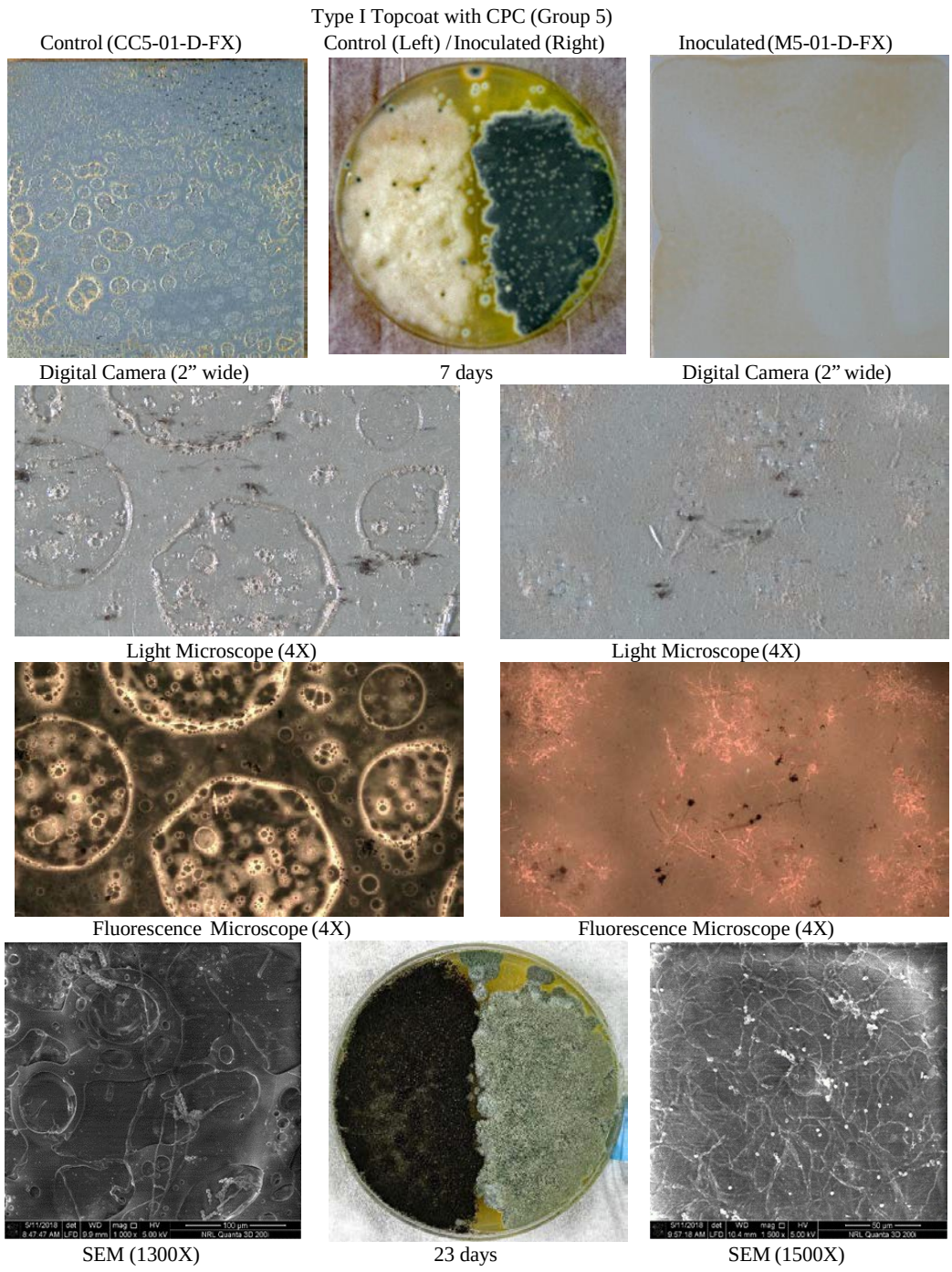

Figure 12. (Group 5): Type I topcoat coupons covered with Cor-Ban 35 corrosion preventive compound (CPC) and exposed to elevated heat and humidity for 86 days without fungi (control, left) and inoculated (right). Potato dextrose agar culture plates were inoculated with swabs taken from the coupons after 86-day exposure; left side of the plate was swabbed from the control coupon, while the right side was swabbed from the inoculated coupon. Culture plates are shown at 7 and 23 days after inoculation.

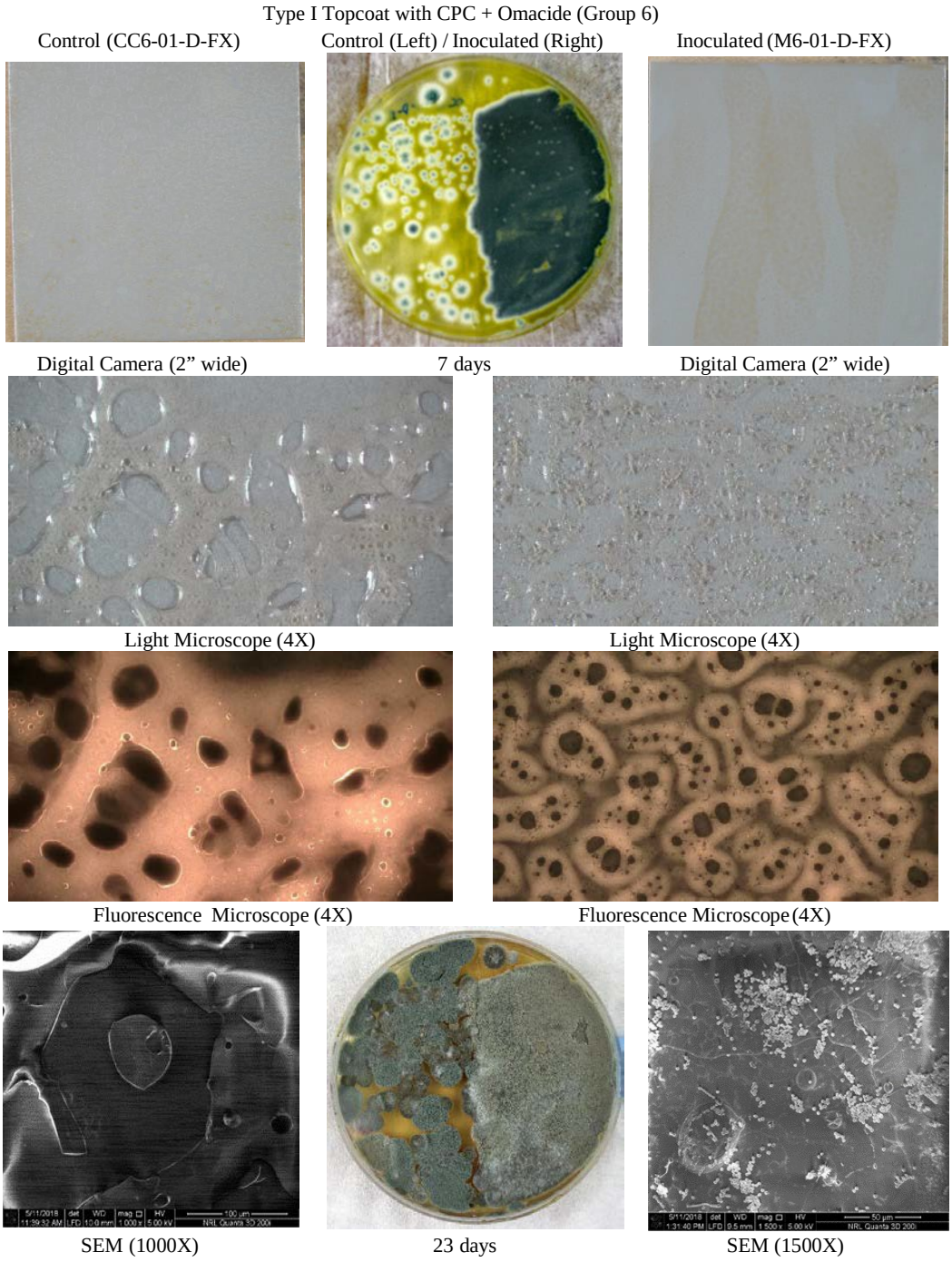

Figure 13. (Group 6): Type I topcoat coupons covered with Cor-Ban 35 corrosion preventive compound (CPC) with Omacide and exposed to elevated heat and humidity for 86 days without fungi (control, left) and inoculated (right). Potato dextrose agar culture plates were inoculated with swabs taken from the coupons after 86-day exposure; left side of the plate was swabbed from the control coupon, while the right side was swabbed from the inoculated coupon. Culture plates are shown at 7 and 23 days after inoculation.

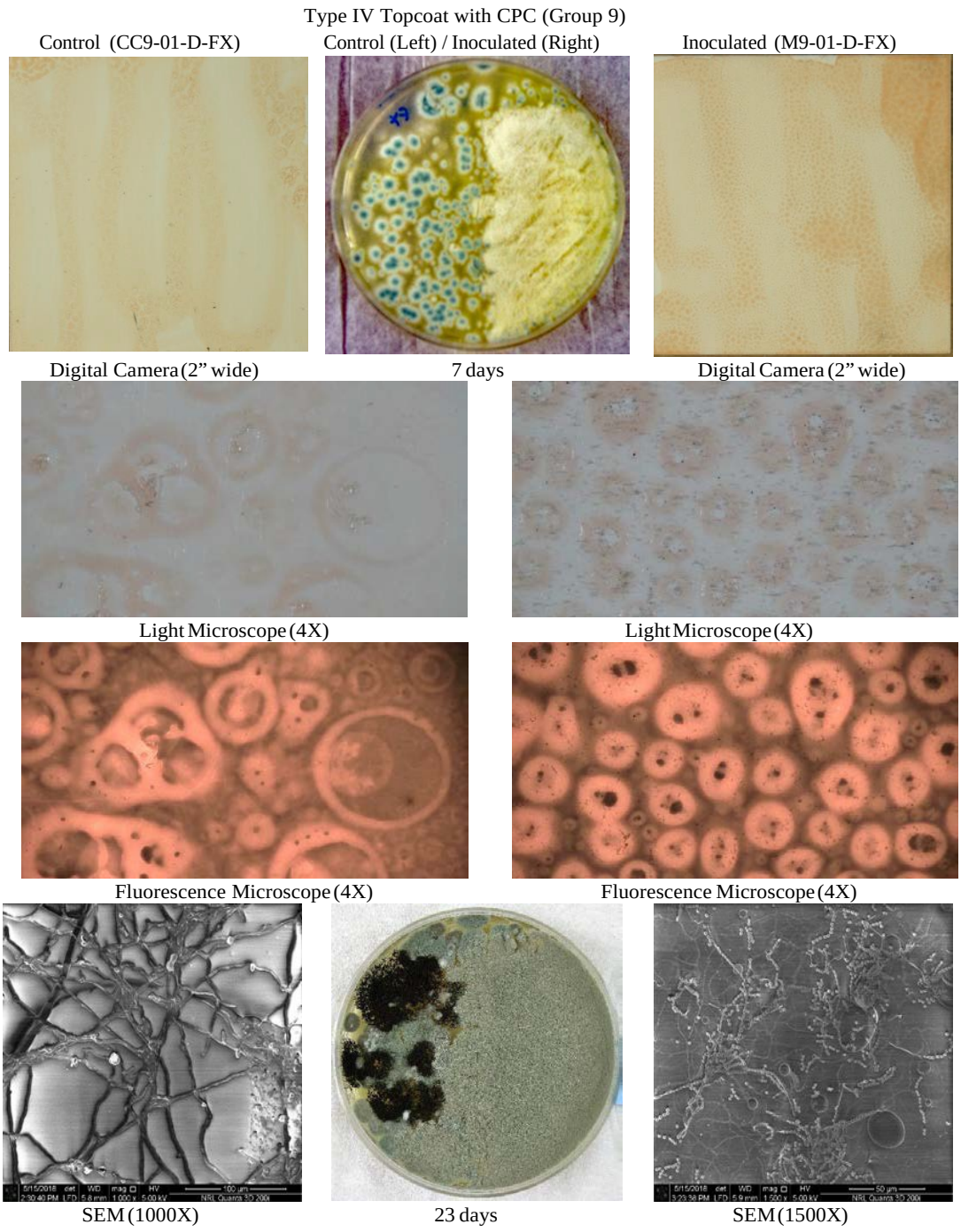

Figure 14. (Group 9) Type IV topcoat coupons covered with Cor-Ban 35 corrosion preventive compound (CPC) and exposed to elevated heat and humidity for 86 days without fungi (control, left) and inoculated (right). Potato dextrose agar culture plates were inoculated with swabs taken from the coupons after 86-day exposure; left side of the plate was swabbed from the control coupon, while the right side was swabbed from the inoculated coupon. Culture plates are shown at 7 and 23 days after inoculation.

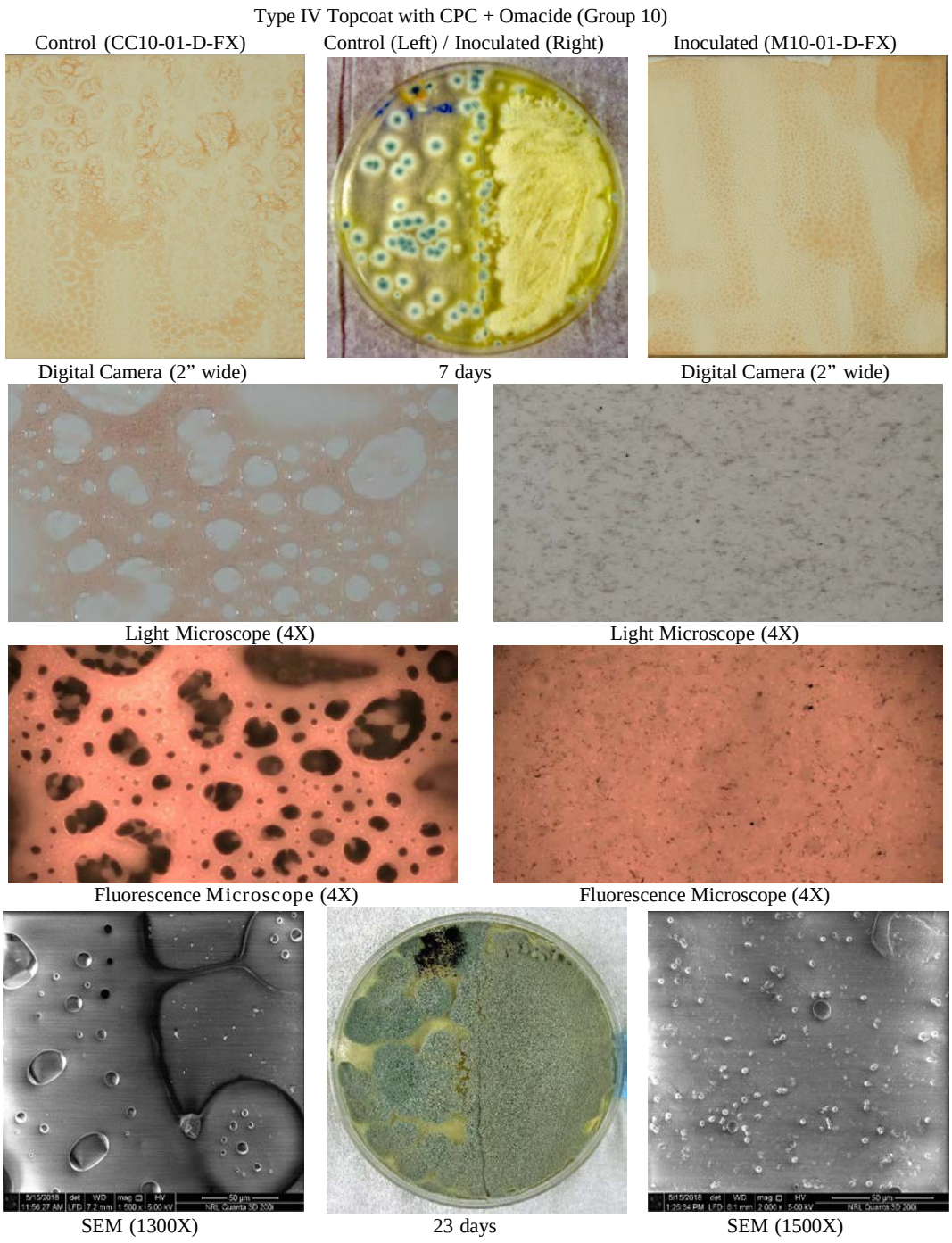

Figure 15. (Group 10) Type IV topcoat coupons covered with Cor-Ban 35 corrosion preventive compound (CPC) with Omacide and exposed to elevated heat and humidity for 86 days without fungi (control, left) and inoculated (right). Potato dextrose agar culture plates were inoculated with swabs taken from the coupons after 86-day exposure; left side of the plate was swabbed from the control coupon, while the right side was swabbed from the inoculated coupon. Culture plates are shown at 7 and 23 days after inoculation.

Cleaning Study

Topcoat Only

To examine coating degradation of the exposed coupons, removal of fungal biofilms and additives (e.g. CPC, hydraulic fluid) on the coupon surface was required. Cleaning protocols were evaluated for their abilities to remove fungal hyphae, spores and additives. As the first step, iso-propyl alcohol (IPA) was used to clean a Group 4 coupon (Type IV topcoat with no additives), after which fungal hyphae and spores were seen visually and at higher magnification via SEM (Fig. 16 top left). Visual inspection indicated the fungal biofilm had been removed. However, inspection at higher magnification revealed the hyphae and a few spores persisted (Fig. 16 top right). Serial applications of IPA, acetone (ACE), ethanol (EtOH) and methanol (MeOH) did not completely remove the fungal biofilm (Fig. 16 bottom left). Only after application of NavClean followed by a distilled water (dH_2O) rinse was the entire biofilm removed.

Primer Only

Primer-only (chromate primer (Group 1) (Figure 17) and non-chromate primer (Group 2) (Figure 18) post-exposure coupons having fungal biofilms were cleaned using the three separate cleaning methods: 1) IPA, 2) IPA>ACE>EtOH>MeOH and 3) NavClean> dH_2O. Separate areas were cleaned on each coupon using one of the cleaning methods. Regardless of cleaning method or primer type, fungal hyphae and spores were no longer visible at high magnification post-cleaning.

Topcoat with CPC

The effectiveness of the cleaning procedures was evaluated on coupons covered in CPC without Omacide with Type I (Group 5, Figure 19) and Type IV (Group 9, Figure 20) topcoats. Three separate areas on each coupon were chosen for cleaning with one of the cleaning methods. As shown in Figures 19 and 20, regardless of topcoat type, fungal spores persisted in the CPC. The Type I topcoat with CPC after cleaning with IPA was examined by atomic force microscopy (Figure 21). Prior to cleaning, segmented fungal hyphae can clearly be observed either on or within the CPC itself (left side images). Cross-sectional profiles of the hyphae (bottom images) show the hyphae protruded above the surface of the CPC. After cleaning (right side images), the hyphae were as shown by comparison of electron microscopy images (top). Atomic force microscopy images indicated trenches in the CPC where fungal hyphae were prior. These results indicate that fungi grow within the CPC but do not adhere to the topcoat itself. In comparison, fungal growth on bare topcoat produced a significantly more adherent fungal hyphae mat that required NavClean for complete removal.

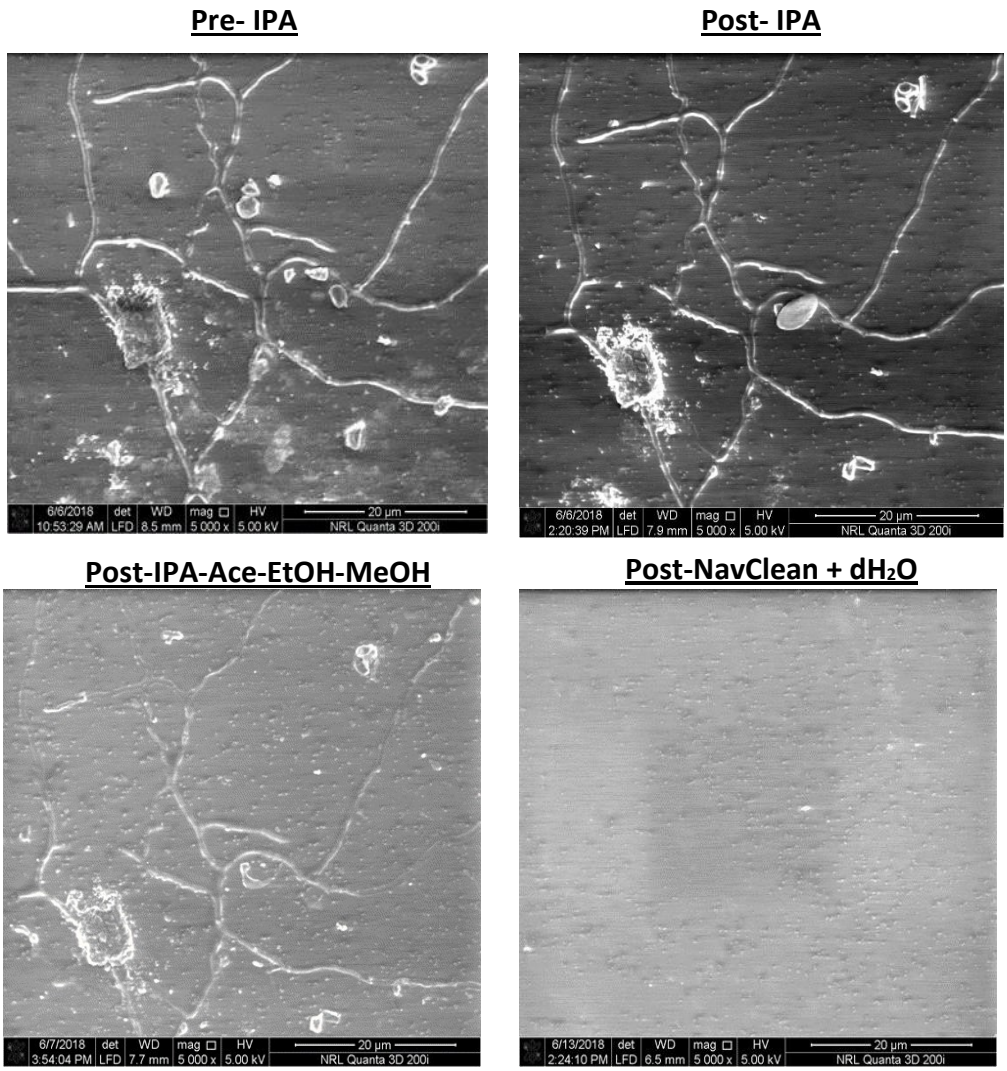

Figure 16. (Group 4): Serial surface cleaning of an isolated location on an inoculated Type IV topcoat using combinations of iso-propyl alcohol (IPA), acetone (Ace), ethanol (EtOH), methanol (MeOH) and NavClean with a distilled water (dH_2O) rinse.

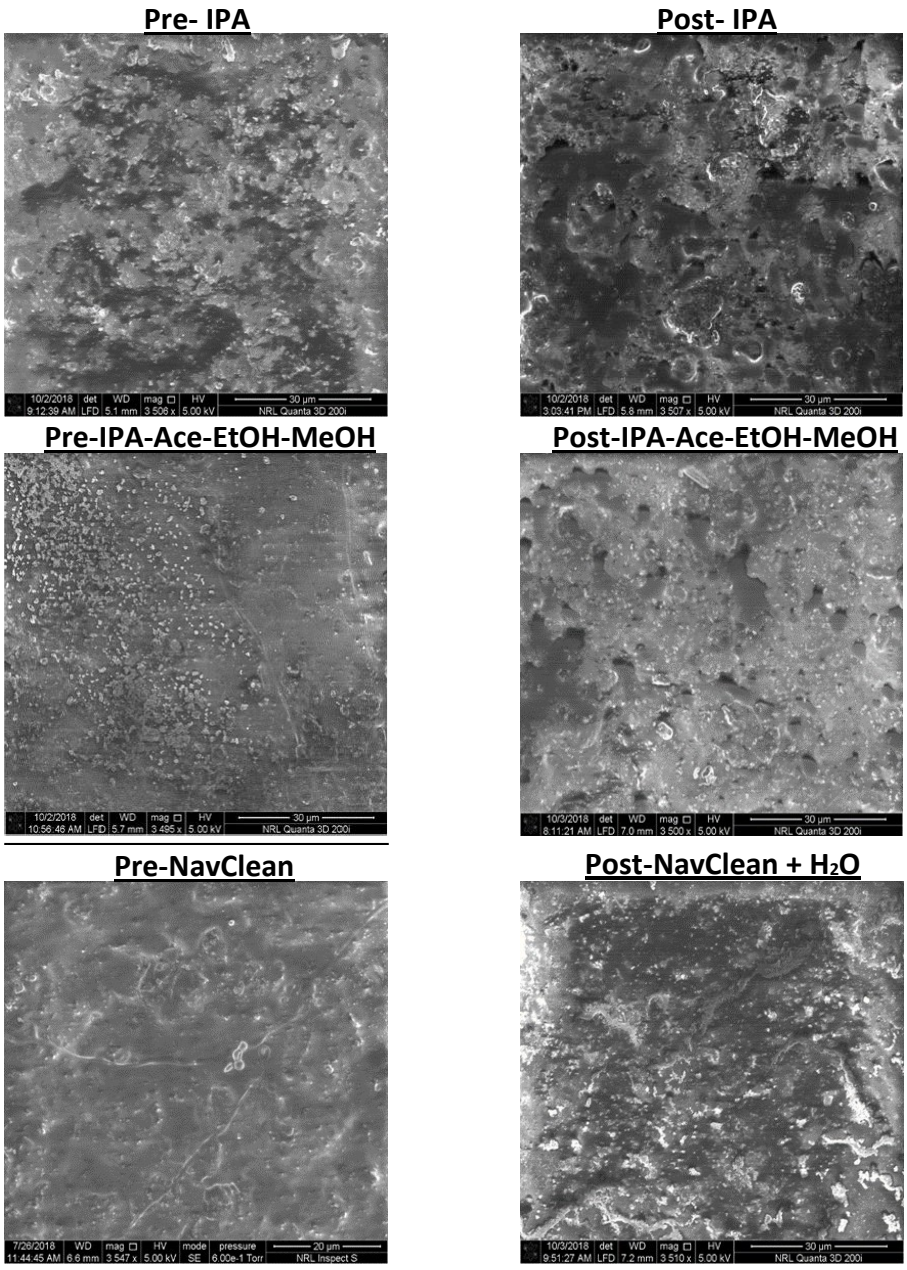

Figure 17. (Group 1): Surface conditions of inoculated chromate primer coupons pre- and post-surface cleaning of separate isolated locations using combinations of iso-propyl alcohol (IPA), acetone (Ace), ethanol (EtOH), methanol (MeOH) and NavClean with a distilled water (dH_2O) rinse.

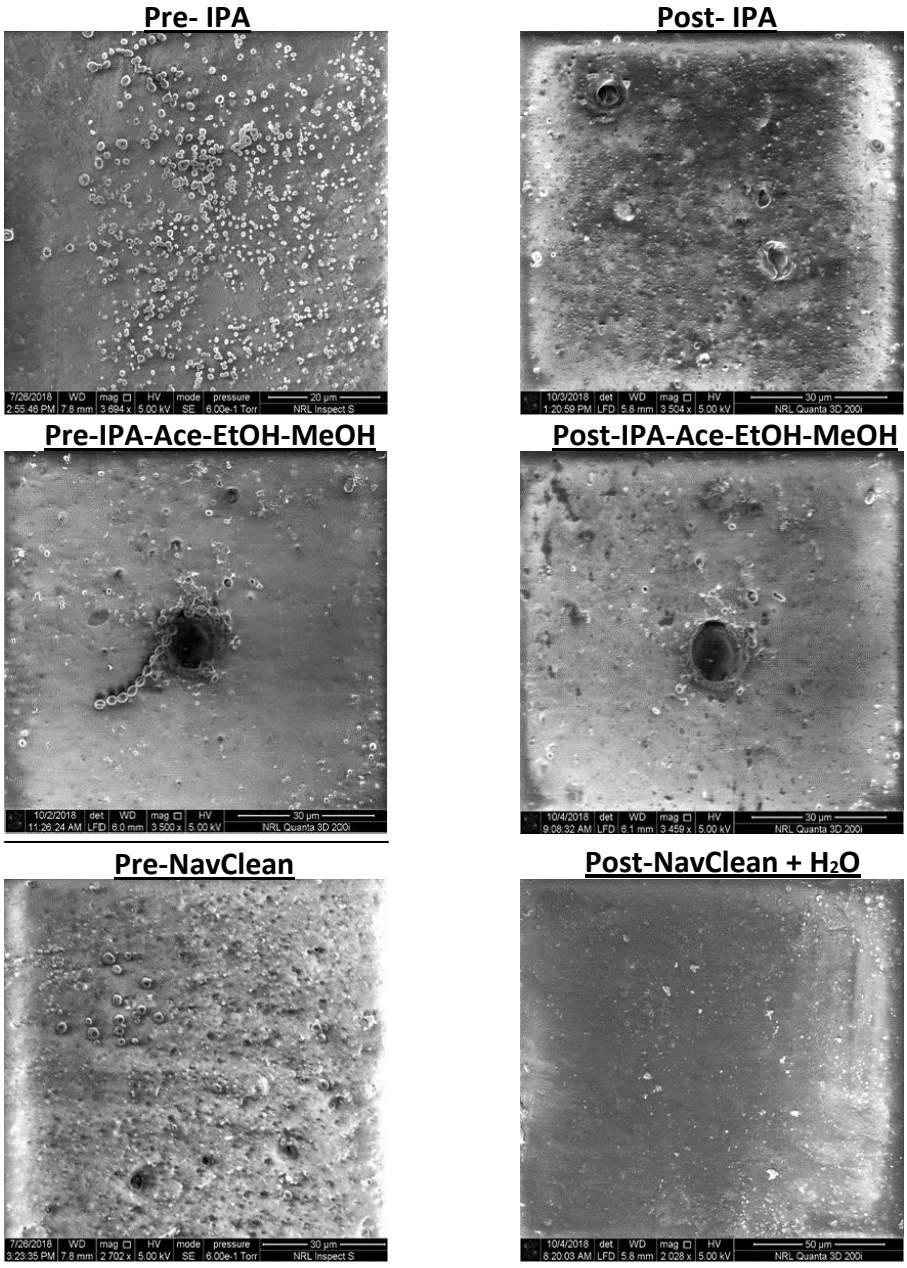

Figure 18. (Group 2): Surface conditions of inoculated chromate primer coupons pre- and post-surface cleaning of isolated locations using combinations of iso-propyl alcohol (IPA), acetone (Ace), ethanol (EtOH), methanol (MeOH) and NavClean with a distilled water (dH_2O) rinse.

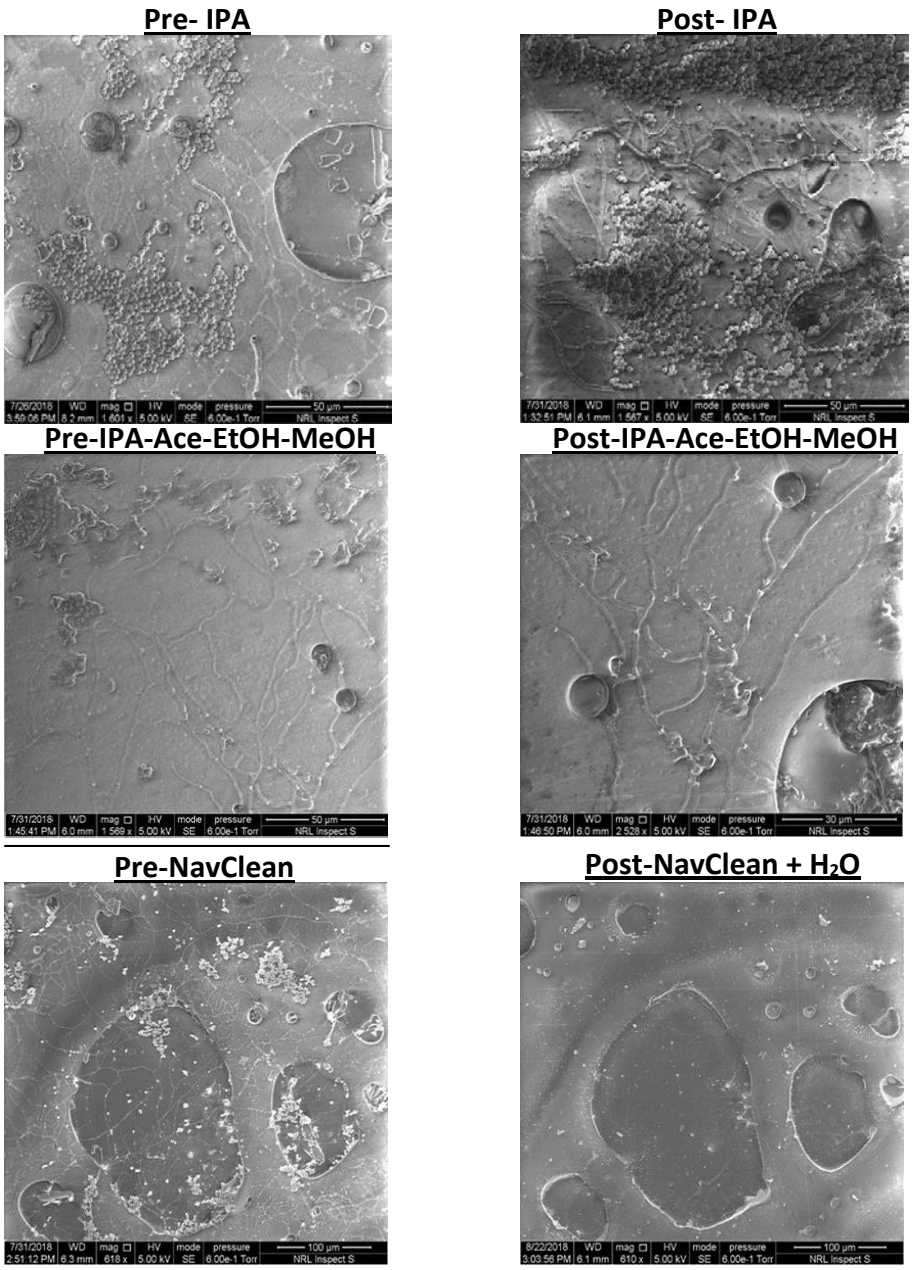

Figure 19. (Group 5): Surface conditions of inoculated Type I topcoat with corrosion preventative compound (CPC) pre- and post-surface cleaning of isolated locations using combinations of iso-propyl alcohol (IPA), acetone (Ace), ethanol (EtOH), methanol (MeOH) and NavClean with a distilled water (dH_2O) rinse.

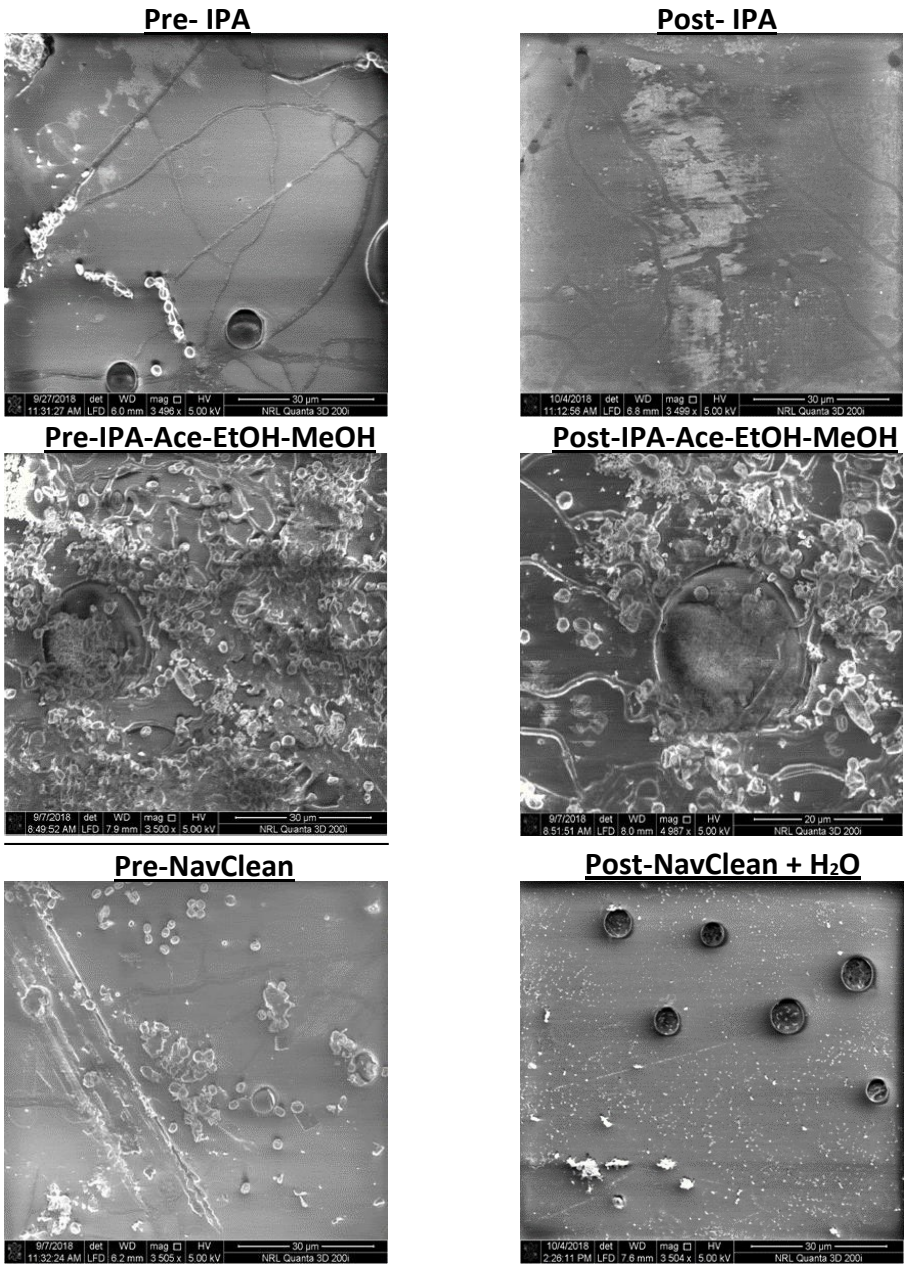

Figure 20. (Group 9): Surface conditions of inoculated Type IV topcoat with corrosion preventative compound (CPC) pre- and post-surface cleaning of isolated locations using combinations of iso-propyl alcohol (IPA), acetone (Ace), ethanol (EtOH), methanol (MeOH) and NavClean with a distilled water (dH_2O) rinse.

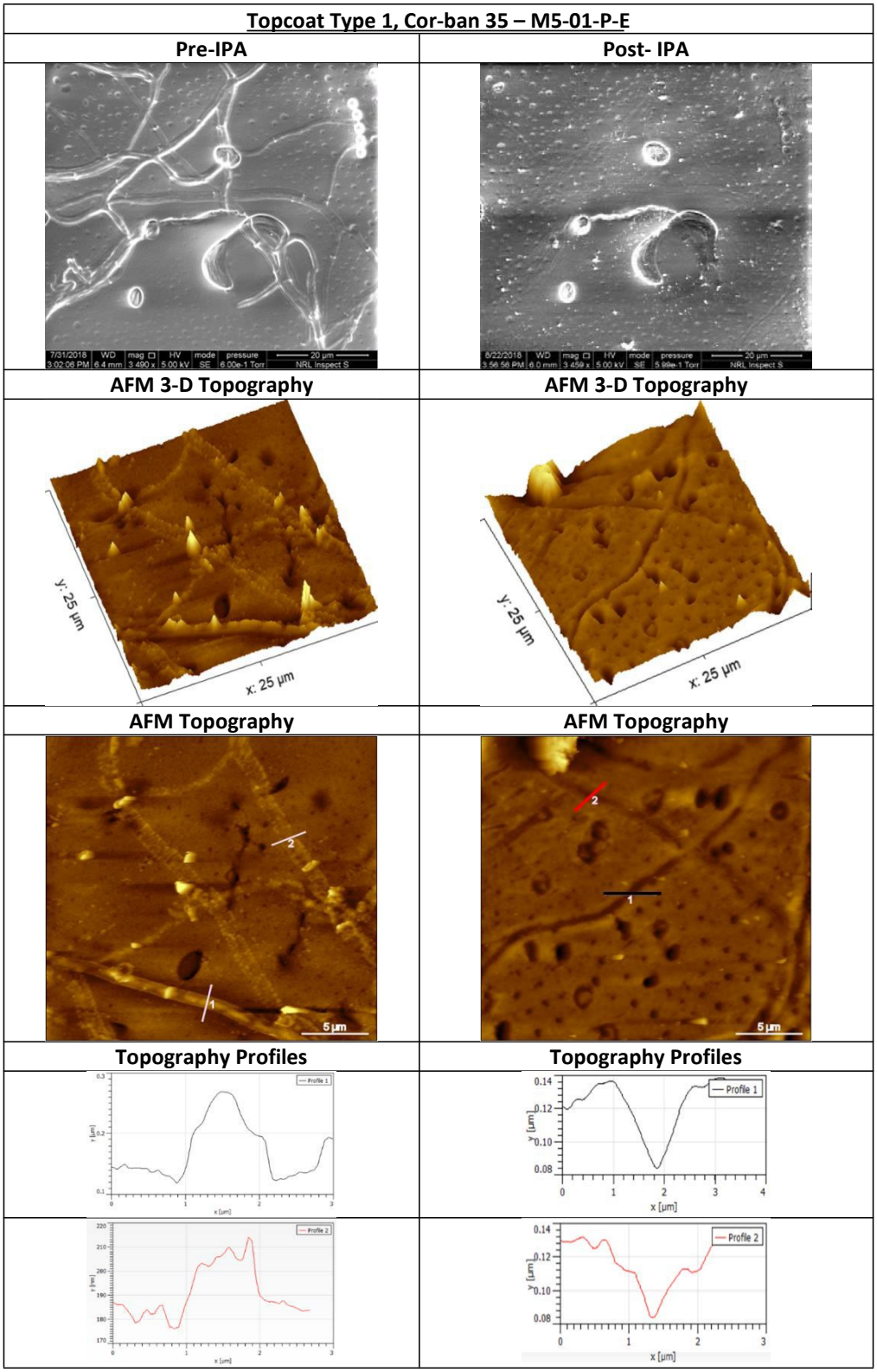

Figure 21. (Group 5): Electron microscopy (top) and atomic force microscopy images (middle) and profiles (bottom) of Type I topcoat with CPC and fungal inoculation pre- and post-cleaning with iso-propyl alcohol (IPA).

FTIR, GS-MS and GPC Observations and Results:

Fourier Transform Infrared (FTIR) Spectroscopy

For the epoxy-only samples, Groups 1 and 2, no changes were observed from the control. Other sample groups showed this trend as well with the unmodified coating exposures, Group 3 and 4, showing no changes, as seen in Figure 22. The other sample groups that showed no change were Group 8 and the hydrophobic Groups 7 and 11, and the microbial (M) exposure of 12 (M12). For all these samples it appears that no degradation occurs however; it may be that the spot size of the ATR crystal, 3 mm, is too large to see any minor changes in the coatings. Also of interest is that both Groups 7 and 11 had Never Wet™ applied to the coating and its spectrum was observed in all the samples implying that it may have limited degradation to the samples.

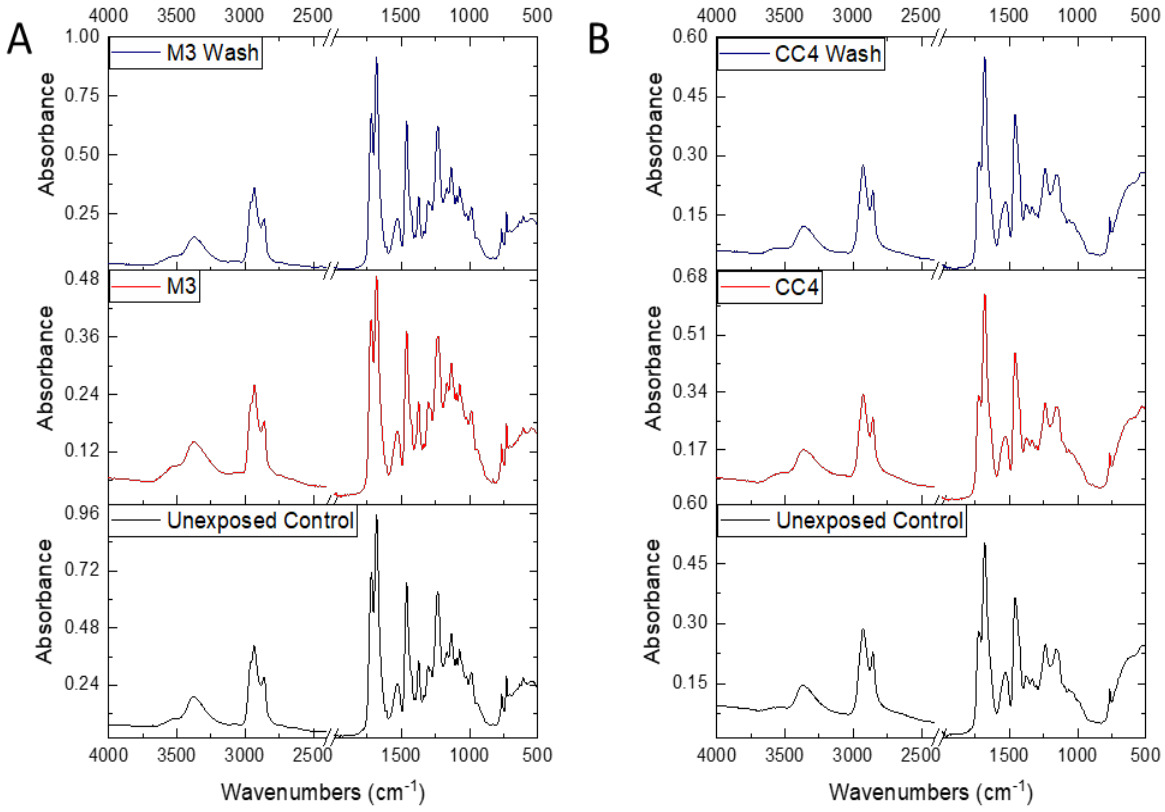

Figure 22. FTIR of A) Group 3 (Type I topcoat) control, microbial exposure and microbial exposure after was. FTIR of B) Group 4 (Type IV topcoat) control, climate controlled exposure and climate controlled exposure after wash as examples of samples with no changes observed in IR analysis.

The samples with observed changes fell into several different categories depending on exposure and group. The first category is where changes are seen on the exposed coating but after washing the original spectrum reappears. This occurs in the climate controlled (CC) of Group 5 and Group 12, and to a lesser degree in CC of Group 6. For CC 5 the exposed spectrum appears to be a combination of the applied Cor-Ban, the coating

and some water on the surface. Upon washing, the water and residual Cor- Ban are removed and the spectrum afterwards matches the unexposed. CC6 is similar to CC5 in that the exposed spectrum is a combination of the Cor-Ban and the unexposed coating; however, upon washing, the spectrum still appears as a combination. While still a spectral combination after washing, the spectrum more closely matches the unexposed coating. The CC12 analysis reveals that the exposed spectrum is a combination of the hydraulic fluid and the coating, and upon cleaning the hydraulic fluid is washed away to show the original spectrum.

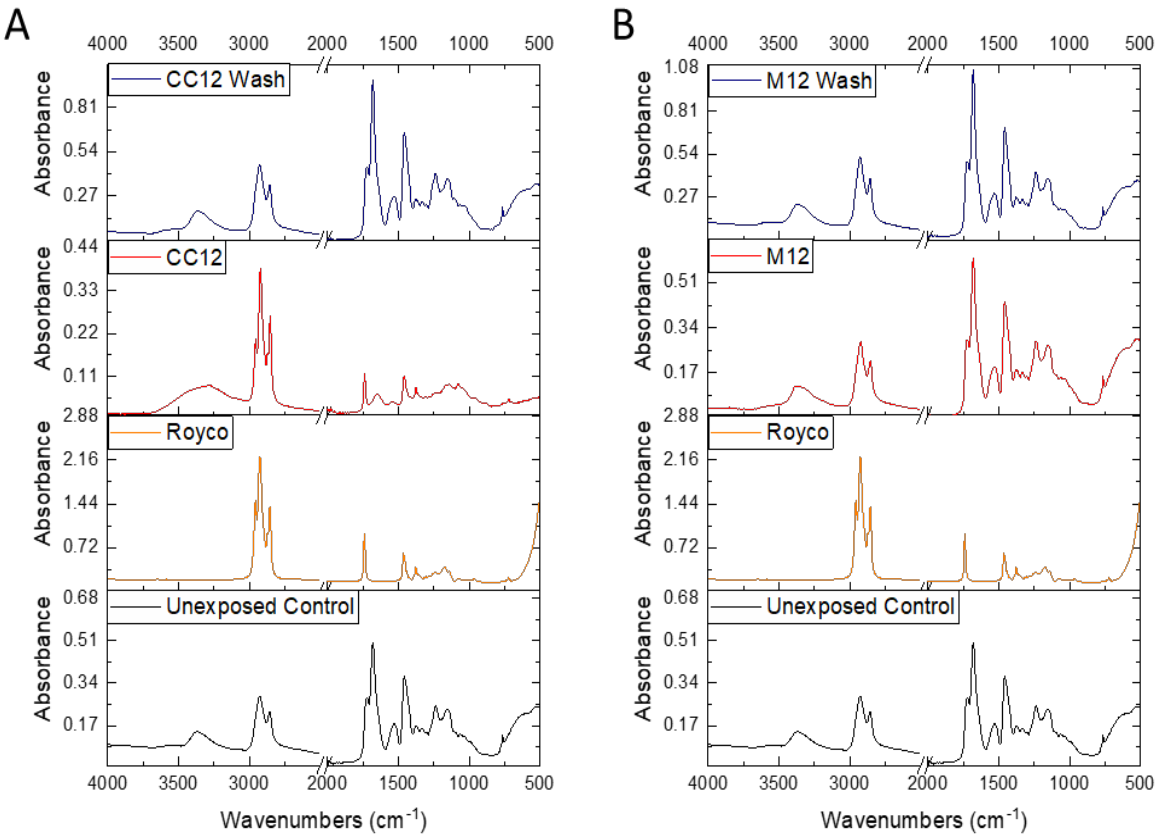

Figure 23. FTIR of A) CC12 exposure showing spectrum as a combination of hydraulic fluid and unexposed (C12) with a return to original after washed and B) M12 exposure showing all coating spectra matching unexposed.

These samples reveal that some of the applied fluids remain on the surface after exposure to environmental factors and can be removed through washing. By looking at Figure 23 it can be said that exposed CC12 showing hydraulic fluid while M12 does not provides evidence that the microbes are digesting the applied fluids. It is also possible that these fluids may provide the initial source of organic matter for the microbes to colonize on the coating. In the M5 and M6 exposed spectrum a combination of the coating and Cor-Ban is observed however this changes after the samples are washed. The samples showed the disappearance of peak at 1650 cm^{-1} which indicates loss of carbonyl from the polyurethane coating.

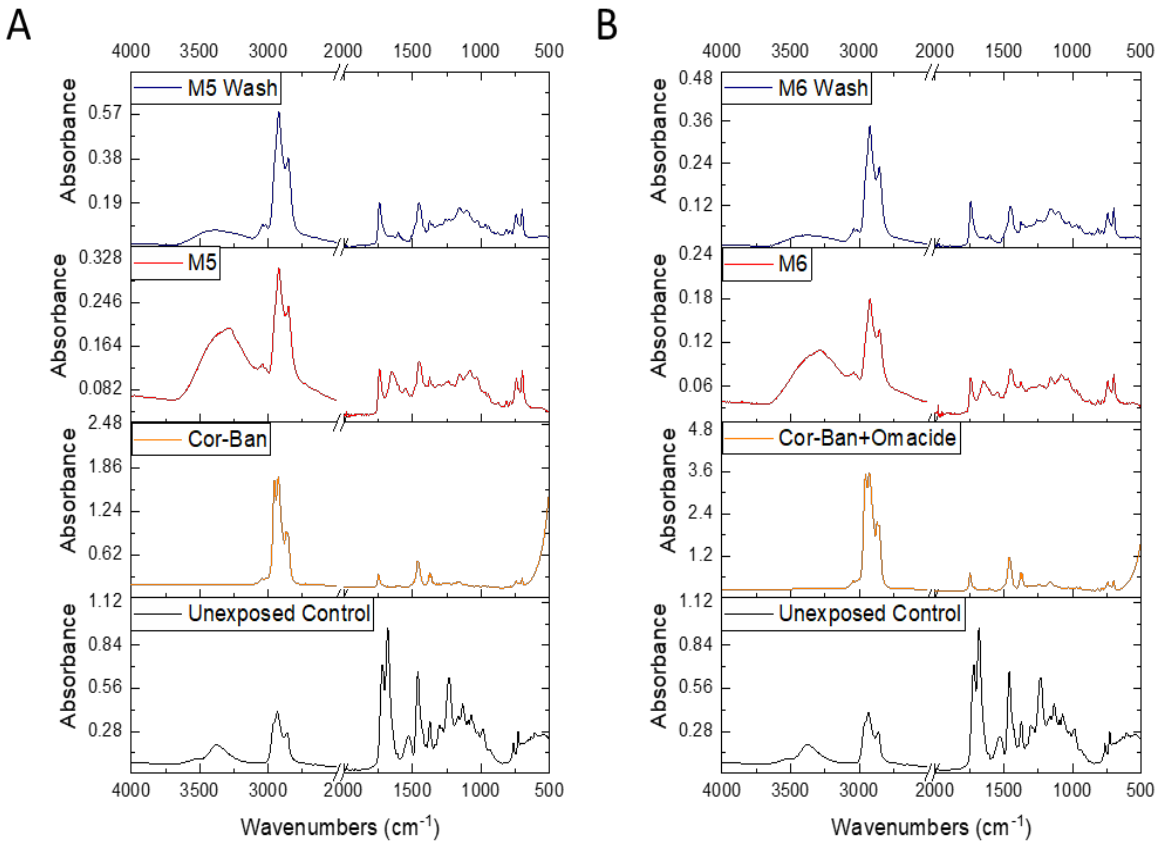

Figure 24. FTIR of A) M5 exposure showing spectrum as a combination of Cor-Ban and unexposed (C5) with a loss of peak at 1650 cm^{-1} after washed and B) M6 exposure showing same changes seen in M5.

The loss of carbonyl implies that the urethane or ester linkages are being degraded in the coating. Another indicator of this is the reduction of the peak at 1230 cm^{-1} in both the microbial exposed and then further reduction after washing. This peak represents the carbon-oxygen bond found in both urethane and ester linkages and loss of the signal also implies degradation. Some peaks that are representative of Cor-Ban, 1741, 948, 743 and 700 cm^{-1}, are still present after the NavClean wash showing that at least some remained in the coating for both M5 and M6. Very similar spectra were observed for the other sample groups with Cor-Ban, all of Groups 9 and 10. For these samples it appears that the Cor-Ban has remained and some degradation has occurred just like the spectra seen in Figure 24. The changes seen in samples M9 and M10 in particular closely matched samples M5 and M6, indicating that both had degradation occur and some of the Cor-Ban is still present. The main difference being in the CC samples of 5 and 6 compared to CC samples of 9 and 10 was a reduction in peaks matching the coating after the wash instead of an increase like was seen in CC5 and CC6. This implies that the CC9 and CC10 coating had further degradation than the CC5 and CC6 coatings. Other techniques may confirm this observation.

Overall most exposures had no change from the unexposed samples and no change after being washed. It should be mentioned that IPA was tried initially but no changes were observed in the spectra. The lack of changes seen in ATR-FTIR in addition to ESEM work that showed microbes are still on the surface after the IPA wash. NavClean was used as an alternative to remove microbial growth so that the coating could be examined directly. Only the samples with applied fluids showed changes after exposure, Groups 5, 6,

9, 10, and 12. These samples fell into two different categories based on how the spectra changed after being washed with NavClean. For the CC samples of 5, 6, and the M Group 12 exposures the spectra returned to the original unexposed spectra after cleaning implying no degradation. For the M samples of 5 and 6, and all of Group 9 and 10 the loss of additional peaks shows degradation on the surface of the samples.

Gas Chromatography / Mass Spectrometer (GC-MS) and Gel Permeation Chromatography (GPC) [aka Size Exclusion Chromatography (SEC)]

GPC analysis was done in order to detect any large molecular weight (MW) species that have been liberated from the coating due to weathering or microbial action. Samples of the unexposed were run as controls and no peaks were detected as seen in Figure 25A.

All exposed samples run on the GPC also had no peaks. While this was unfortunate it was not totally unexpected. The GPC instrument can only detect MWs in the range of 2,500 to 936,000 which limits the system to large species. The lack of detection implies that either no degradation took place or that the molecules generated by the degradation were smaller than 2,500. The latter case is entirely feasible and is why GCMS was utilized to detect any small molecules that may have been liberated during the exposures.

The GCMS analysis of unexposed samples all showed unreacted monomers, fillers and in some cases chemicals applied to surface of coatings. In addition, Cor-Ban, hydraulic fluid and Cor-Ban with Omacide were all run on GCMS in order to find out which molecule they contained so that those molecules can be accounted for in the other samples. The unexposed coatings and applied fluids provided a control which the climate controlled (CC) and the microbial (M) exposures could be compared against to determine degradation products. For example, if a peak in an exposed sample has the same retention time and mass spectrum as one from the unexposed coating it is not from degradation of the coating system. An example from this work was the groups that had Cor-ban applied (Groups 5, 6, 9, and 10) contained a set of peaks around 20 min retention time that was from Cor-ban and was not caused by weathering or microbial action. Similarly, the Omacide had a few peaks in the exposed samples. Another peak that was discounted was for diethyl phthalate because it is a common contaminant found in most samples. It was detected in all the exposed samples, however, it is a plasticizer and came from the plastic packaging used during shipping, not from any degradation.

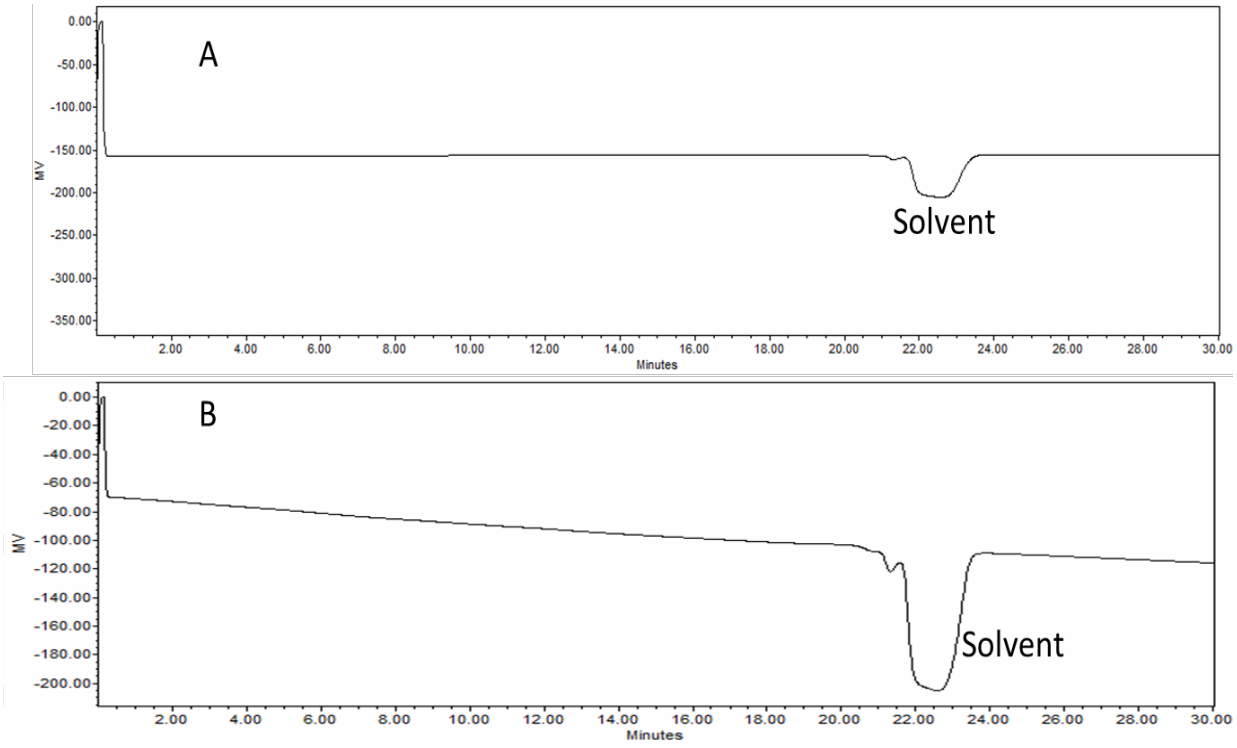

Figure 25. GPC traces of A) Group 2 control and B) Group 11 control with no peaks detected during the run.

Total Peak Area of Epoxy Samples

Molecules from the exposed samples were grouped by retention time, MW, and functional groups. The CC Group 1 (CC1) sample had 4 peaks from 17.1 to 18.5 minutes with MW of 149, 191, 135 and 229. These peaks were either ketones or alcohols most likely from the degradation of the epoxy, fillers or unreacted monomers. The M1 exposure had the same group of peaks from 17.1 to 18.5 minutes but also contained an additional amine peak possibly indicating further degradation. CC2 extraction also had peaks from 17 to 18.5 with MW 191, 149, and 135 that were from degradation similar to CC1. The M2 sample closely match the CC2 with all the same peaks, however, the areas were significantly lower than those observed in CC2. Noticing this difference, it was decided to take the total area of the peaks to get a representation of the amount of degradation of the sample, Table 4 below has the results for Groups 1 and 2. It is important to note that while the total peak area can be an indication of degradation it is only a measure of the amount of small molecules extracted from the coating and that these small molecules can be from environmental degradation or action as well as microbial.

Table 4. Total Peak Area of Epoxy Primer Samples

Samples	Total Peak Area
CC1	138,956
M1	150,291
CC2	250,556
M2	81,937

Using the total peak area, Table 4, it can be seen that CC1 has slightly less degradation than M1 which is likely due to the extra peak observed. For Group 2 exposures the lower peak intensities seen in M2 are easily seen in the much lower total peak area compared to the CC2 sample. This indicates that the CC2 had more degradation of extractable species then the M2 which could be due to several factors. The main factors could be that while the CC samples were climate controlled there still is the possibility for microbial growth or the microbes could be consuming leachable material. Other techniques, like SEM, showed that a higher degree of microbial growth had occurred suggesting lower leachable material detected was due to consumption by microbes. It is also important to note that while the total peak area can give us a measure of degradation it is not very precise due to the lack of any standards and lack of enough samples to get standard deviation. This is important to remember because small differences between the areas may be within the error and not statistically different.

Extracts from the topcoat samples overall had more variability than the epoxy samples. CC3 extract had only two large peaks at 15.4 and 23.5 minutes with MW of 214 and 340, respectively. Both of these peaks were esters fragments which makes sense since the topcoat is a polyurethane/polyester coating. While only a few peaks were present the total area of these peaks was about 7 million which was much higher than the epoxy samples, Table 4. The M3 sample had three small peaks from 14 to 15 minutes that were aromatic, benzene ring containing, compounds with MW of 162, 163, and 206. Also a group of several peaks in the 21 to 22.5 minutes range with MW of 206, 252, and 250. These peaks were aliphatic esters along with a nitrogen containing molecule. The aromatic compounds are most likely fillers; however, the other peaks appear to be from the coating either as leached material or degradation of the polymer. The total peak area for M3 was 960,000 which is significantly lower than CC3. This matches what was seen in Group 2 epoxy sample with the CC having higher areas than the M exposures. Continuing with the topcoat Type I samples CC5 had a small aliphatic nitrogen containing peak at 11.8 min, MW 171, along with many peaks from 20 to 22 minutes. These peaks were a mix of ester, amine and ketone/alcohol containing molecules with MW of 252, 281 and 266. The M5 sample looked very similar to the CC5 with only one additional peak in the 20 to 22 minutes range with a MW of 493. The total peak areas of the two samples can be seen in Table 5 and continue the trend of CC samples having much higher areas than M samples.

Table 5. Total Peak Area of Topcoat Type I Samples

Samples	Total Peak Area
CC3	7,113,260
M3	963,661
CC5	25,725,496
M5	2,402,089
CC6	11,874,936
M6	1,429,856
CC7	0
M7	408,088
CC8	19,603,788
M8	9,088,395

CC6 exposure also had a large group of peaks from 20 to 22.5 minutes with esters, amines and ketones however the MW for the molecules was different with 226, 343, and 438 detected. The similar retention time and functional groups for CC5 and CC6 reveal that the molecules detected are both from the same source material, either the topcoat or the Cor-ban. The different molecular weights are likely just different molecules or sections of the same molecule that have been degraded or from the microbial action resulting in different products. M6 sample matched CC6 with peaks in the 20 to 22.5 minutes range that had MW of 226 and 343 however no peak with MW 438 was detected. Once again the total peak area followed the trend seen in all samples. The addition of the Omacide 100 to the Cor-Ban application leaded to a lower total peak area for Group 6 samples compared to Group 5 which implies that the Omacide works to reduce microbial growth.

CC7 samples had no peaks that were any different than the control, indicating no degradation took place. The Group 7 coatings had Never Wet™ applied to the surface and this may have protected that coating from degradation. The M7 sample did have a small nitrogen containing peak at 24.4 minutes with a MW of 383 and a peak area of 408,000. This peak may be from some degradation on the surface however the area is less than half as high as any other topcoat type I exposure, Table 5, implying that if degradation took place it was slowed. The results for Group 7 appear to show that degradation was slowed or prevented by the application of Never Wet™. This should be confirmed by another method since it is possible that Never Wet™ is limiting the acetonitrile's ability to extract molecules from the coating.

The extract of CC8 had a small aliphatic nitrogen containing peak at 11.8 min, MW 171, along with a group of peaks in the 20.5 to 22.5 minutes range. These peaks were aliphatic esters and amide with MW of 281,

341, and 384. M8 matched exactly with only smaller peaks than those seen in CC8 which indicates that less degradation occurred or microbes consumed leachable material. Group 8 samples had hydraulic fluid applied to the surface and the only peak found corresponding to it was triphenyl phosphate at 23.8 minutes indicating that most of the hydraulic fluid had been degraded or consumed. The Group 8 samples had the highest total peak area when comparing all topcoat Type I CC samples to each other. This is also true for the M samples indicating that Group 8 had the highest amount of degraded material most likely due to the hydraulic fluid providing an easy source of organic material for the microbes to consume. The trend of the CC exposures having higher total peak area than the M exposures was consistent throughout the topcoat Type I testing with the exception of the samples with "Never Wet" applied. All the topcoat Type I samples that appear to have degradation had peaks in the 20.5 to 22.5 minute range and many had the same or similar MW and functional groups.

The sample set utilizing topcoat Type IV had many similarities to the topcoat Type I samples. CC4 extracts had a group of three peaks from 20 to 21 minutes that were esters and an amine with MW of 241, 343, and 428. The M4 sample matched CC4 exactly with only some variation in peak area, Table 6. An interesting thing to note is that the total peak area for CC4 was higher than M4 but not significantly so as has been seen for all other samples. The CC9 exposure had a small ester group at 11.9 minutes with a MW of 148 and a group of peaks from 20.5 minutes to 23.5 minutes. These peaks were aliphatic esters and amines with MWs of 252, 266, and 281. M9 also had a peak at 11.9 and a grouping of peaks centered around 22 minutes with lower peak areas. Also the peak with MW of 281 was not detected but a different peak with MW of 391 was detected, implying alternative sources for some of peaks seen. The Group 9 exposures returned to the trend of the CC exposure having a significantly higher total peak area when compared to the M exposures of the same group.

Table 6. Total Peak Area of Topcoat Type IV Samples

Samples	Total Peak Area
CC4	2,509,927
M4	2,118,755
CC9	4,572,910
M9	1,153,076
CC10	13,228,546
M10	995,252
CC11	612,216
M11	253,686
CC12	1,211,128
M12	279,249

The CC10 extract had the same peak at 11.9 with a MW of 148 as did the Group 9 samples but there were more peaks in the 20 to 23 minutes range with MWs of 238, 252, 266, 392 and 493. As with other samples these peak had ester and amine characteristics with the addition of an aromatic molecule. The M10 sample had the peak at 11.9 min and a smaller group of peaks in the 20 to 23 minute range. For M10 the peak in that range were esters and amines with MWs of 252, 266, and 392. The very similar products seen for all of Group 9 and 10 indicate that the degradation pathway of these samples was the same. The presence of a peak at approximately 11.9 for all the samples with Cor-ban, Groups 5, 6, 9, 10, but not any others indicates that the peak is a degradation product of the Cor-ban and not anything from the coating.

The extract for CC11 only had one peak not seen in the control at 22.6 minutes. The peak was an aromatic molecule with MW of 392. It is likely that the molecule is from a filler and not from the polymer backbone of the coating. M11 also only had one peak but it was located at 23.4 minutes and was an aliphatic nitrogen containing molecule with a MW of 354. The molecule detected in M11 could be either a degradation product or a filler, alternate analysis should help determine if any degradation took place on the coating. Like Group 7, Group 11 had "Never Wet" applied to the surface and this may have protected that coating from degradation. Both sample set that had "Never Wet" applied appear to have either no degradation or very limited degradation, warranting further investigation.

The CC12 exposure had only a pair of peaks at 24 and 24.2 minutes that were aliphatic esters with MWs of 384 and 325. Peaks in M12 matched CC12 exactly except for lower peak area. These samples had hydraulic fluid applied and just like in Group 8 the only trace of it was the triphenyl phosphate. It is possible that the microbes consumed the hydraulic fluid leaving behind the hard to consume fire retardant.

For all groups the CC samples had higher total peak areas than the M samples with the exception of Group 1 epoxy samples. The Group 1 epoxy samples contain chromate species that may explain the CC and M exposures being nearly the same through limiting environmental degradation. The higher peak area in the climate controlled samples may be due to the microbes consuming the organic fillers and pieces of coating, either degraded or unreacted, that leave from climate exposure resulting in lower total peak area for the microbial samples. ESEM analysis appears to support this with large amounts of microbes on the surface of the microbial and only a few seen on the climate controlled samples. Further analysis is needed to determine the exact cause of this trend. Overall an increase in peak area was seen in all exposed samples compared to controls except perhaps the ones where Never Wet™ was applied, Groups 7 and 11. While a few peaks were observed the significantly reduced number of peaks and lower total peak area provides evidence that either no or very limited degradation occurred in these samples. This provides a possible chemical that could increase the life of the coatings but further work is needed to confirm the lack of degradation and how long does the effect last. The presence of Omacide in both topcoat Types I and IV resulted in lower total peak area in the M samples compared to the Cor-Ban M samples which implies that the Omacide reduced microbial action. As with other observations confirmation with another technique would provide further support of the observed trend. Comparison of topcoat Type I and topcoat Type IV reveals that almost all of topcoat Type 1 samples had higher total peak areas which may indicate more leachable substances than topcoat Type IV. If confirmed the lower amount of leachable organics from topcoat Type IV means that it may be a better system for applications where fungal growth is a concern than topcoat Type I since the fungus spores use the leachable material to grow before attacking the polymer backbone of the coating.

Laser Scanning Microscopy (LSM)

LSM was conducted at NAWCAD PAX on six as-coated control Groups 1, 2, 3, 4, 7 and 11. Due to the analysis time required by the LSM to scan entire coupons, smaller regions were selected in a 3x3 grid pattern for detailed profilometry and then average and standard deviation of all roughness parameters were taken over these nine sites. Thus the standard deviation represents an "average standard deviation" of these nine sites. These same areas were scanned after the 84-day ideal growth condition exposures. These initial baseline control coupon profilometry data are presented in Table 7. These values represent the control baselines from which percentage changes were calculated after the post-microbial surface profilometry.

Overall it was observed that both topcoat types were very smooth with roughness values of S_a<0.5 µm and Sq<0.65 µm (Groups C3 and C4 in Table 7). Non-chromate primer had roughness S_a =2.46 µm (Group C2) and the chromate primer (Group C1) which was the roughest with S_a value 3.92 µm.

The RMS roughness values (S_q) were slightly higher than the respective S_a values for each coating system but followed the same relative trend. Again, these values represent nine-site averages. S_v parameters corresponding to the deepest valley were very similar for Type I and IV topcoats, being 7.1 and 7.9 um respectively, with almost identical standard deviations from site- to-site. At each site analyzed, three images are presented prior to the roughness values in each row – these images represent the Laser/Optical view of the region, the second represents the topographical profile

heights colorized for ease of interpretation, and an optical micrograph of the region scanned. The non-chromate and chromate primer S_v values were approximately 19 µm and 27 µm, respectively. Similarly, the deviation- from-planarity measured by S_{dr} values followed the increasing trend: MIL-PRF-85285 Type I (Group C3) S_{dr}=0.14, Type IV (S_{dr}=0.17), Group C2 non-chromate primer (S_{dr}=1.46) and Group C1 chromate primer (S_{dr}=13.3). These values indicate the relative increase in surface area as compared to a flat plane with the chromate primer clearly having the greatest roughness (with exception of the super-hydrophobic coatings which are designed to be rough-textured). The S_{dr} parameter is dimensionless since it's a ratio between area values. The hydrophobic coating was applied to Group 3 (M85285 Type I) topcoat forming Group 7, and applied to Group 4 (M85285 Type IV) topcoat forming Group 11. Since the Group 3 and Group 4 coatings were so similar in roughness values, the supplemental hydrophobic coating was assumed to be represented by the profilometry measurements with respect to comparing the two.

Table 7. Roughness Parameters of Unexposed Control Groups C1-4, 7 and 11.

Group		S_a	S_q	S_p	S_v	S_z	S_{dr}
		µm	µm	µm	µm	µm	---
C1	Avg	3.92	5.36	29.3	27.1	56.4	13.3
	σ	0.30	0.43	8.8	0.82	9.1	0.94
	Avg*	3.82	5.22	26.2	27.0	53.2	13.1
	σ*	0.12	0.15	1.1	0.81	1.52	0.78
C2	Avg	2.46	3.23	17.2	18.5	35.7	1.46
	σ	0.12	0.41	12.1	15.3	18.8	0.14
	Avg*	2.45	3.10	12.9	19.2	35.2	1.44
	σ*	0.12	0.16	1.2	16.1	16.8	0.14
C3	Avg	0.48	0.64	5.82	7.1	12.9	0.14
	σ	0.10	0.17	5.4	8.2	7.9	0.066
	Avg*	0.47	0.60	4.5	7.6	12.1	0.14
	σ*	0.11	0.13	4.1	8.6	8.0	0.068
C4	Avg	0.39	0.51	6.3	7.9	14.2	0.17
	σ	0.01	0.05	7.5	8.2	8.7	0.01
C7	Avg	5.35	8.36	59.53	30.85	90.38	0.81
	σ	0.69	0.95	8.57	9.38	11.76	0.07
C11	Avg	5.85	8.72	60.53	33.02	93.55	2.96
	σ	0.43	0.64	3.76	12.55	11.89	0.84
* One site removed from nine-site average calculation due to anomalies such as a fiber adhered to surface in that region.							

For Group 7, S_a=5.35 µm and S_q=8.36 µm, while Group 11 was only slightly rougher with S_a=5.85 µm and S_q=8.72 µm. The S_{dr} values were only slightly different with Group 7 S_{dr} =0.81 while Group 11 was 2.96. As expected these supplemental coatings were fairly similar most likely reflecting natural differences in coating variation when sprayed out.

Presented below is a summary of the change in roughness parameters of coating system Groups 1, 2, 3 and 4 after microbiological exposure with results and statistical comparisons created from the raw LSM data files after importing into Microsoft Excel for data analysis (Table 8).

The equation used to calculate the percentage change in the arithmetic roughness after exposure to optimal growth conditions is listed in Equation 3. This same formula was applied for the other five roughness parameters results listed in Tables 8 and 9 and examined for trends. Similarly, site-to-site standard deviation variability was characterized using Equation 4.

$$\{\sum_{n=1}^{9} [(S_{a2(n)} - S_{a1(n)}) / (S_{a1(n)})]\} / 9$$

Where n is the site number; $S_{a1(n)}$ is the arithmetic roughness at site n prior to microbial exposures; and $S_{a2(n)}$ is the arithmetic roughness at site n after microbial exposures.

Eqn. 3. Arithmetic roughness parameter (S_a) percentage change after microbiological exposure to growth conditions (averaged over a nine-site grid pattern)

$$\{\sum_{n=1}^{9} [(\sigma_{2(n)} - \sigma_{1(n)}) / (\sigma_{1(n)})]\} / 9$$

Where n is the site number; σ1(n) is the standard deviation at site n prior to microbial exposures; and σ2(n) is the standard deviation at site n after microbial exposures.

Eqn. 4. Standard deviation (σ) percentage change after microbiological exposure to growth conditions (averaged over a nine-site grid pattern)

S_a and S_q, the arithmetic and root-mean-square roughness parameters respectively, changed by absolute value percentages ranging from only a couple percent (Groups 1, 3 and 4) to nearly 7% for Group 1. Group 1 the chromate primer roughness parameters decreased by about 6.5% (S_q was -6.6% indicating a slightly smoother surface) while the non-chromate primer showed a very slight 0.5% increase in roughness. The non-chromate primer exhibited the most consistent before/after S_a and S_q roughness values, and yet had the highest percentage change in deviation from planarity (increased 55%) of the two primers and even the two topcoats which doesn't seem internally consistent. Group 1 chromate primer exhibited a smoother surface after exposure and IPA wipe cleaning as designated by the negative S_{dr} value (-16.3%) indicating greater planarity (the only negative S_{dr} measured in these first four control coating groups) perhaps due to dissolution of chromate pigment particles at the surface and/or IPA wiping removal of high spots including these particulates. Roughness increased slightly more on type IV topcoat relative to a slightly smoother overall surface on Type I (loss of a few percent). All of these coupons at NAWCAD had been wiped using the same pre-saturated IPA wipe as described in Table 1.

Table 8. Differential Laser Profilometry Calculations and Analyses of Microbiologically Exposed Coating Systems M1-M4

Group		Delta Parameter Values (% Change)					
		S_a	**S_q**	S_p	**S_v**	S_z	S_{dr}
M1	*Avg	-6.28	-6.64	17.2	-6.47	5.10	-16.3
	σ	7.61	8.55	36.75	7.09	18.8	11.6
M2	*Avg	0.42	0.51	9.72	64.3	35.0	54.9
	σ	0.11	0.11	0.12	1.79	0.87	0.20
M3	Avg	-1.66	-4.91	14.6	398	45.9	29.9
	σ	19.4	21.4	97.3	713	67.9	46.2
M4	Avg	1.86	-0.19	59.8	207	49.0	5.50
	σ	4.28	9.50	135	480	152	5.82

* One site removed from nine-site average calculation due to extraneous anomaly such as a fiber adhered to surface in that region.

S_v parameters were expected to identify the deepest attack site since the parameter identifies the "deepest valley", however, some of the largest percentage changes observed at individual analysis sites (which were very high) were attributed to anomalous features, thus masking the subtle effects of microbial digestion at the three months' coupon exposure time. Detailed localized scans were attempted to eliminate these spikes in the data, potentially making the S_v parameter a more viable measurement.

Roughness values of the fluid contaminated coupons after the microbiological growth cycle are presented in Table 9. Pre-microbial control group data are included in the shaded rows for baseline comparisons. These specific coupons were not profiled prior to the microbial exposures so data are compared by assuming the control baseline data as being representative of the exposed coupons.

Hydraulic fluid contaminated coatings were determined to promote the most microbiological growth on the examined coating systems in this effort. Coating roughness values increased nearly four-fold for the Group 3 Type I topcoat (S_a =1.39 µm vs. 0.37 µm for control); Group 4 topcoat (Type IV) values approximately doubled (S_a =0.67 µm vs. 0.39 µm for control). Greater standard deviations were observed for the post-microbiological exposure as well. These profilometry data suggest micron-scale coating digestion could be occurring at a greater level on the Group 3 Type I polyurethane topcoat than the submicron scale increase in roughness on the Type IV (Group 4). Electron Microscopy had shown greater quantity of growth on the Group 4 coupons, so if the observed change in roughness correlates to microbial digestion then the microbes colonizing the Group 3 topcoat were more effective in digesting that coating chemistry. Group 7 and 11 hydrophobic coating surface profilometry was not priority due to the lack of growth observations in electron microscopy.

Table 9. Roughness Parameters of Coatings Exposed with Fluid Residues

Group		Inoculated-Exposed Roughness Parameter Values					
		S_a (µm)	S_q (µm)	S_p (µm)	S_v (µm)	S_z (µm)	S_{dr}
M5*	Avg.	2.51	3.15	34.3	16.0	50.3	0.37
	σ	0.69	0.78	24.0	4.00	26.2	0.09
M6*	Avg.	3.70	4.69	34.4	17.2	51.6	0.46
	σ	1.06	1.37	25.5	3.53	27.8	0.16
M8	Avg.	1.39	1.73	10.4	5.73	16.2	0.04
	σ	0.25	0.27	5.98	1.05	6.72	0.01
CC3	Avg.	0.37	0.50	5.32	6.7	12.0	0.30
	σ	0.09	0.14	5.31	8.4	8.1	0.07
M9*	Avg.	1.29	1.71	22.1	7.70	29.8	0.29
	σ	0.46	0.62	24.0	2.62	25.3	0.18
M10*	Avg.	0.68	0.88	10.5	4.04	14.5	0.09
	σ	0.23	0.28	9.88	1.67	10.4	0.04
M12	Avg.	0.67	0.84	9.72	3.66	13.4	0.04
	σ	0.55	0.61	8.84	1.21	8.84	0.00
CC4	Avg.	0.39	0.51	6.33	7.87	14.2	0.17
	σ	0.01	0.05	7.52	8.16	8.70	0.01

Note: "CC3" and "CC4" rows refer to Groups 3 and 4 baseline scans, respectively, on climate controlled untested coupons.

* These coupons were later determined to have a film of residual CPC.

The CPC-containing coupons did not provide meaningful data since they were later determined to have irregular films of residual CPC not removed by the cleaning process that affected the sensitive profilometer average roughness values. The LSM was not available to re-scan these coupons after a supplemental cleaning step to remove these residues.

Electrochemical Impedance Spectroscopy (EIS)

Initial control "as-painted" coupon scans were developed using EIS. It was observed that approximately two hours of brine immersion were required to obtain a stabilized OCP value for "As-coated" primer coated coupons. Initially a platinum mesh electrode with a planar configuration was used and results were not acceptable in that geometry. Configurations of electrodes and positioning were varied in an attempt to obtain improved results. After one week making several re-test attempts with platinum mesh while allowing the coated coupons to remain clamped to the glass cylinder containing the electrolyte, a graphite rod electrode was then used. Coupons were permitted to remain contact with the saltwater in a laboratory environment (e.g., remained clamped to the glass cylinders) for five months. EIS tests were run after approximately two weeks, two months and 4.5 months, and the cylinders were drained after five months. Coating impedance is defined in Eqn. 5:

$$\text{Impedance } Z(\omega)=E(\omega)/I(\omega)$$

Where the function $E(\omega)$ is the potential and $I(\omega)$ is the current function.

Eqn. 5. Coating Impedance

Results for the Group 1 and 2 epoxy primers are presented in Fig. 26(a, b). The Group 1 chromated primer showed decreasing impedance values during extended saltwater immersion up to 4.5 months (Fig. 26(a)) while the Group 2 non-chromated primer exhibited much more stable results with no statistical difference between 2 weeks to 4.5 months where values of $3x10^5$ were observed at the peak of each curve (Fig. 26(b)). Incompletely resolve arcs shown in any figures in this section occur in EIS spectra when R·C values are large (where R=resistance and C=capacitance for the coating) making coating properties difficult to accurately measure.

The Group 3 topcoat and Group 4 topcoat also showed differences in the control as-painted coupons with approximately a two order of magnitude difference in maximum impedance values. After two months of immersion Group 3 topcoat had an impedance value of ~$5x10^8$while after two months of immersion, the value of $2x10^8$ was observed on a fully resolved arc (Fig. 26(c)). In contrast, the Group 4 topcoat exhibited very consistent EIS output plots with impedance values estimated to be over $1x10^{10}$ (Fig. 26(d)).

Electrochemical Impedance – Control Specimens

- Primer, C1 (chromate)
  - 2 weeks to 4.5 months immersion, 3.5% NaCl solution

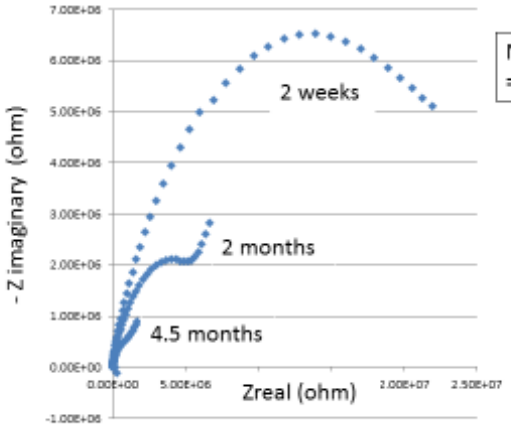

A

Electrochemical Impedance

- Primer, C2 (non-chromate)
  - 2 weeks to 4.5 months immersion, 3.5% NaCl solution

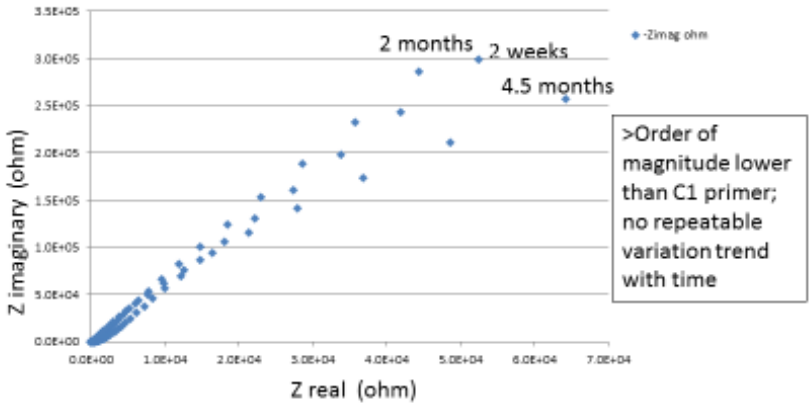

B

C

Electrochemical Impedance

- Topcoat, C3 (gray polyurethane)
  - 2 weeks to 2 months immersion, 3.5% NaCl solution

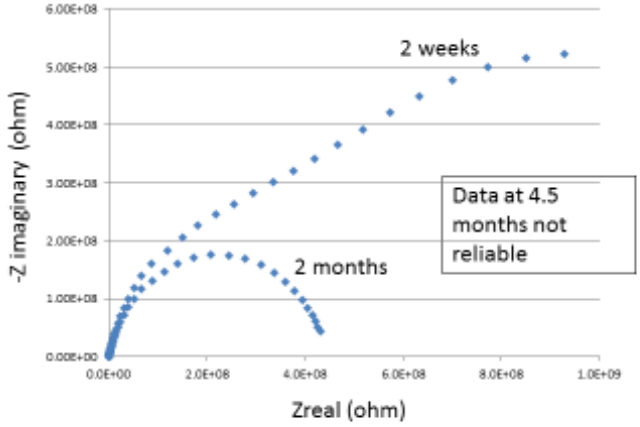

D

Electrochemical Impedance

- Topcoat, C4
  - 2 weeks to 2 months immersion, 3.5% NaCl solution

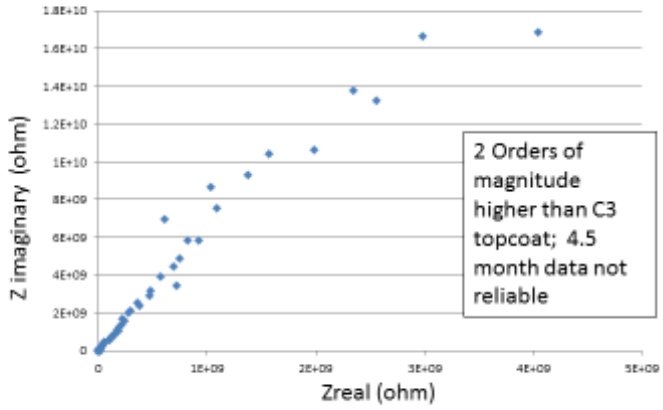

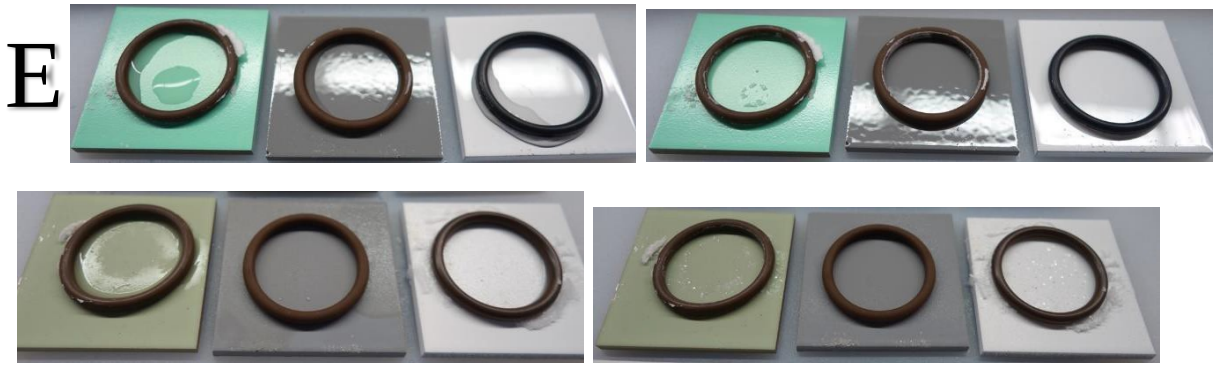

Figure 26. EIS spectra for primer coatings up to 4.5 month immersion in 3.5% sodium chloride solution: (A) Group 1 M85582 chromate primer; (B) Group 2 M85582 non-chromate primer, (C) Group 3 M85285 Type I polyurethane; (D) Group 4 M85285 Type IV polyurethane. (E) Surface conditions after test cell was drained of salt solution after ~5 month immersion in 3.5% salt water: Coupon Groups C2, C3 and C4 upon draining (top, left side) and after 6 hours (top, right side); Coupon Groups C1, C7 and C11 - upon draining (bottom, left side) and after 6 hours (bottom, right side).

Surface Energy/Tension

After five months of immersion in 3.5% sodium chloride solutions, the coating specimens were disassembled by pouring out solution and removing the clamped glass cylinder. The coupons were allowed to dry, leaving the O-ring in place on the coupon. Observations were made during drying with respect to surface tension of the coatings interacting with water droplets/residuals (Fig. 26(e)). The salt solution drained fairly completely from the high gloss top-coated coupons from Groups C3 and C4; C3 had the highest reflectance surface while C4 was second highest. The non-chromate primer C2 also drained almost completely except for a droplet of water which remained on the surface. The matte finish of the chromate primer coupon C1 with average roughness S_a=3.92 µm exhibited a hydrophilic character and was drying fastest in the center while liquid adhered to the coating adjacent to the O-ring periphery. After about six (6) hours the following observations were made: there was a ring of salt crystals around the interior of the O-ring periphery of coupon C1 due to its more hydrophilic character. After drying, salt crystals formed on the non-chromate primer coupon around the periphery of the droplet described earlier (Fig. 26(e)). The non-chromate primer average roughness had been measured at S_a=2.46 µm. Topcoat coupons C3 and C4 were glossy and devoid of noticeable residues. Hydrophobic coated coupon C7 had no visually apparent residues other than what appears to be the hydrophobic coating. The hydrophobic coating surfaces of coupon C11 appeared quite rough due to a layer of salt residue; this test cylinder had leaked water under the O-ring during storage/testing and may have crystallized this salt layer on the hydrophobic coating.

Scanning Kelvin Probe (SKP)

SKP analysis was used to determine any changes that may be occurring in the contact potential difference (CPD) across a coating due to fungal growth and other factors. Samples of the same coating type were examined together in the same scan so that results can be more directly comparable. For Groups 1, 2, 3, 4, 7, and 11; three different panels were scanned at once. In a single scan, each of the three panels was the same coating type but with different exposure conditions. The non-inoculated control (C) panels were coated than scanned. The microbiologically (M) inoculated panels were coated, then inoculated with mold spores and incubated. The climate control panels (CC) were coated, not inoculated, and then incubated. The arrangement for this is shown in Figure 27. Panels were placed

side by side, then scanned using optical surface profilometry, then using the SKP.

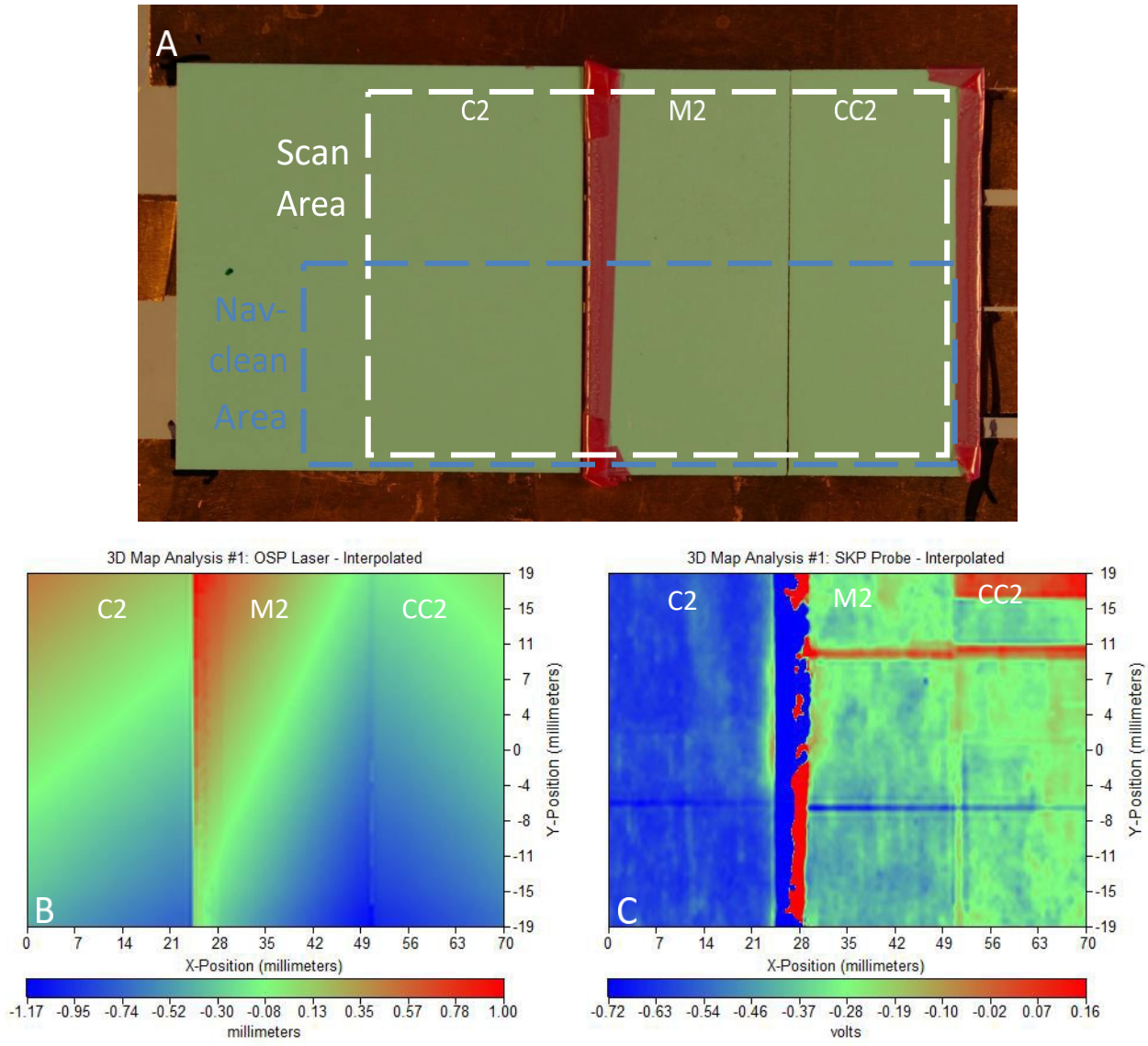

Figure 27. Samples from left to right: C2, M2, CC2 with top half as received, bottom half cleaned with Navclean. A) Optical image B) Optical surface profilometry map, adjusted to remove gaps between panels C) SKP area map.

For the OSP scan, gaps between the panels were measured, often a few millimeters deep. While accurate to the topography of the sample, this can cause problems when in Kelvin mode with height tracking where the probe touches the surface. For this reason, points in these gaps were changed to better match the height measured at the top of the panels, and data taken in these regions were not included in calculations. The adjusted, rather than the original height is shown in Figure 27B. Additionally, part of the scan area at the left of the M panel is covered by tape (see Figure 27A) and was not included in the resulting calculations. Horizontal lines can be seen in Figure 27C, specifically in the CC panel. These lines are due to the probe touching the surface, often at gaps between the panels and should not be considered features of interest. The bottom half of each of the panels were cleaned with Navclean, before the entire surface area of each panel was rinsed with deionized water.

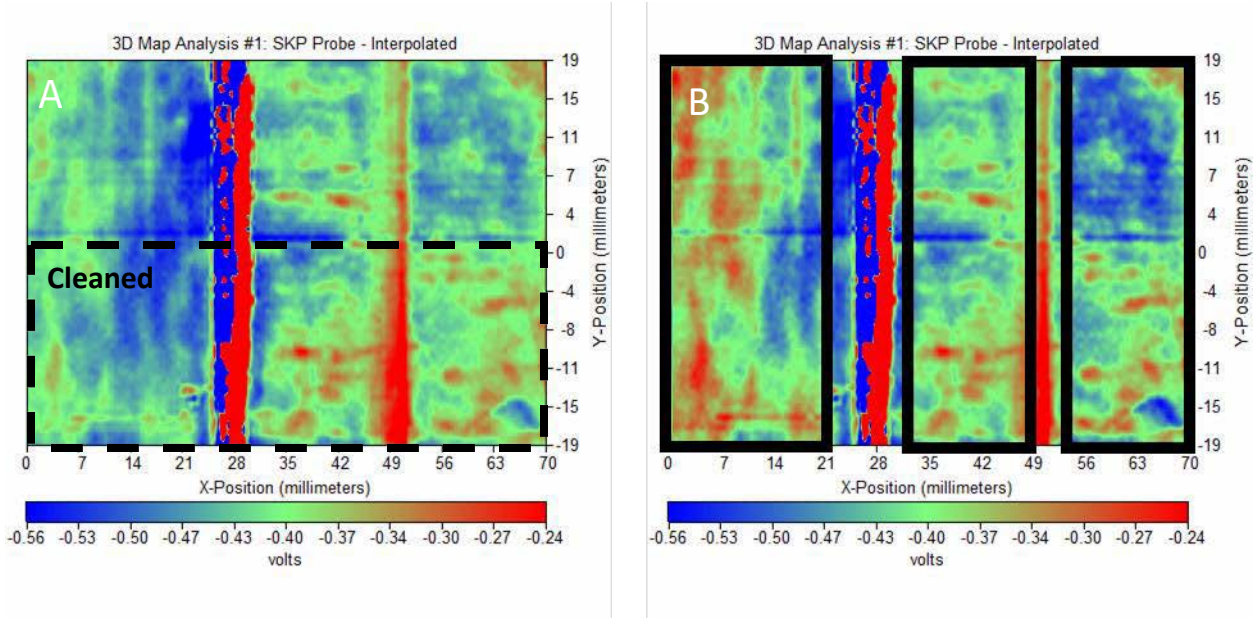

Figure 28. CPD map of Group 1 samples. Panels arranged from left to right C1, M1, and CC1. A) Full scan with color scale set to overall scan maximum scale B) Same scan data as A but with each black boxed panel section individually set to color scale maximum for just that boxed section

Table 10. Group 1 Average CPD (S.D.) in mV

	C1	M1	CC1
Uncleaned	-449 (42)	-423 (33)	-431 (37)
Cleaned	-442 (37)	-401 (43)	-385 (33)

Scan images and average CPD values for Group 1 are shown in Figure 28 and Table 10 respectively. Figure 28 A and B show the same data but scaled differently. In 28A, the image is scaled to the overall maximum scale across the areas of interest on all three panels, so that comparisons can be made between the separate panels, while 28B has each boxed area of interest set to its own maximum color scale, so that greater contrast within each panel is shown. The average and standard deviation values shown in Table 10 are calculated from the areas in each panel shown in the black box. These areas of each panel were chosen because they are far away from the edges of each panel that any edge distortions are minimized. For each of these black boxes, the uncleaned area average was taken across the width of the black box from the 2 mm point to the top of the scan. The cleaned area average was taken across the width of the panel from the -2 mm point to the bottom of the scan. The 4 mm gap left in the middle of the box was not included in any calculations, as the boundary of the cleaning process was not exact. The same areas were used to calculate average and standard deviation for the following 3 panel data in this section, except where noted. For the Group 1 samples, there is only a very small difference in the three different exposure conditions compared to the standard deviation. While the cleaned area of each panel did show an increase in CPD compared to its uncleaned control, this difference is also small compared to the standard deviations. Based on this data, there is little change shown in the Group 1 coating from either the different exposure conditions or cleaning with Navclean.

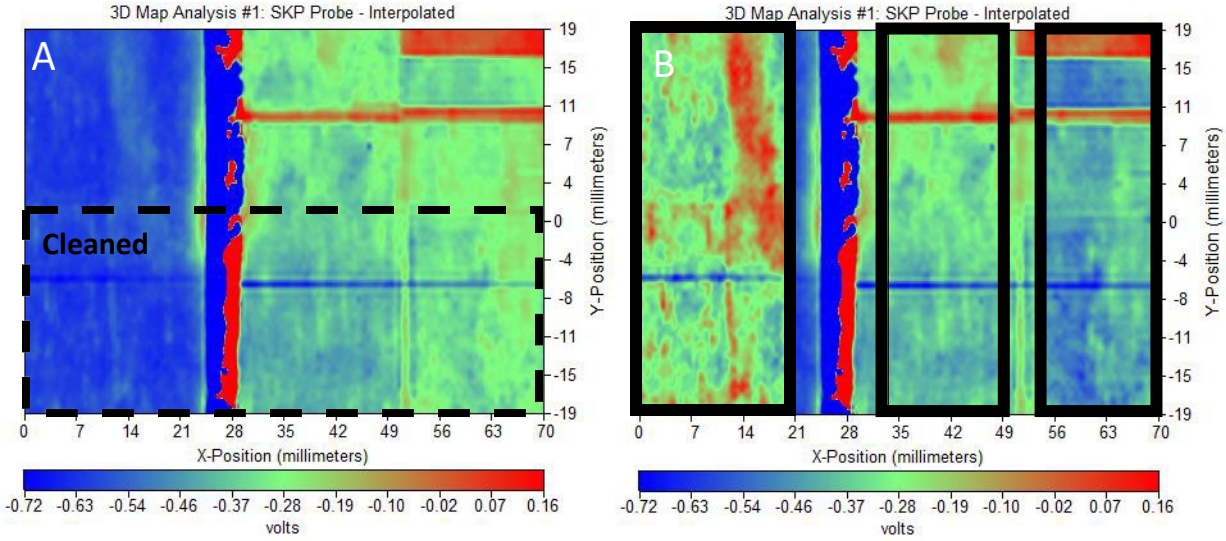

Figure 29 CPD map of Group 2 samples. Panels arranged from left to right C2, M2, CC2 A) Full scan with color scale set to overall scan maximum scale B) Same scan data as A but with each black boxed panel section individually set to color scale maximum for just that boxed section

Table 11. Group 2 Average CPD (S.D.) in mV

	C2	M2	CC2
Uncleaned	-593 (34)	-314 (49)	-289 (44)
Cleaned	-600 (28)	-407 (28)	-308 (41)

Figure 29 and Table 11 show the map and average values for CPD for the Group 2 samples. The mold and climate controlled panels showed horizontal areas of high and low CPD indicating a probe touch and not an inherent feature in the sample. These values of high and low work function were not included in calculations. It can still be seen that the average CPD for the M and CC panels are similar, while different from the non-inoculated unexposed panel. Additionally, in comparing the cleaned and uncleaned portions of the mold exposed panel, a difference can be seen of almost 100 mV, indicating that the cleaning process is affecting the CPD for the mold exposed panel.

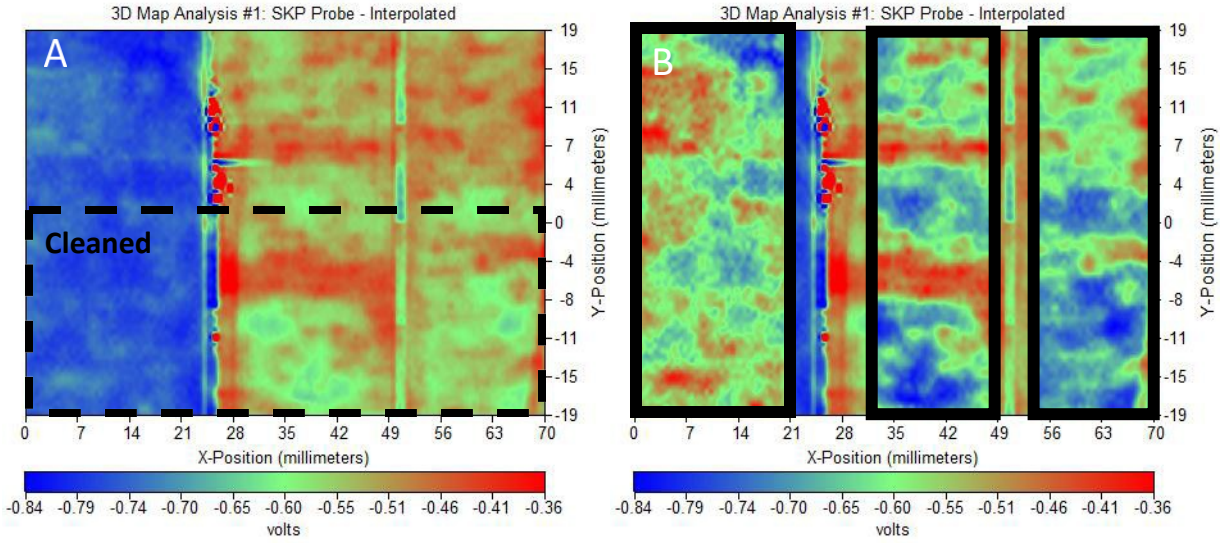

Figure 30. CPD map of Group 3 samples. Panels arranged from left to right C3, M3, CC3 A) Full scan with color scale set to overall scan maximum scale B) Same scan data as A but with each black boxed panel section individually set to color scale maximum for just that boxed section

Table 12. Group 3 Average CPD (S.D.) in mV

	C3	**M3**	**CC3**
Uncleaned	-756 (27)	-522 (39)	-497 (39)
Cleaned	-776 (18)	-559 (60)	-562 (45)

Figure 30 and Table 12 show the CPD map and averages for the Group 3 panels. Similar to the Group 2 panels, the non-inoculated panels exhibit different CPD values from the mold and climate control panels, whereas the difference in CPD values between the latter two treatments are not as large. The cleaning procedure shows little difference in the average values of the CPD on the uncleaned panel, but for both the mold and climate control panels there is an observable difference in CPD between the cleaned and uncleaned sections. This may indicate that the cleaning process is affecting the CPD for this coating type.

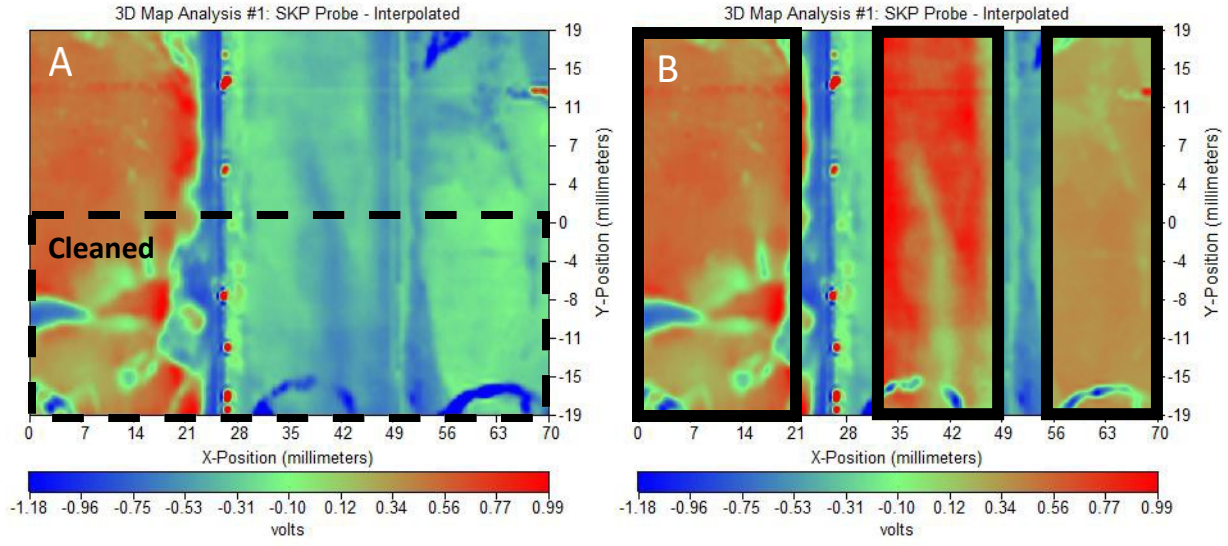

Figure 31. CPD map of Group 4 samples. Panels arranged from left to right C4, M4, and CC4. A) Full scan with color scale set to overall scan maximum scale B) Same scan data as A but with each black boxed panel section individually set to color scale maximum for just that boxed section

Table 13. Group 4 Average CPD (S.D.) in mV

	C4	**M4**	**CC4**
Uncleaned	465 (168)	-346 (61)	-376 (188)
Cleaned	212 (355)	-461 (152)	-329 (321)

Figure 31 and Table 13 show the map and average values for CPD for coating type 4. Due to the coating properties and experimental parameter optimization process, charging of the surface occurred and caused difficulties in making CPD measurements. When the surface charges, this changes the measured CPD and obscures the data showing the inherent properties of the surface. The experimental parameter optimization was done over the non-inoculated panel, possibly causing it to charge more than the others. Because of this, the large CPD difference seen between the non-inoculated panel and the other two panels may not accurately represent how the panels compare to each other in a discharged state. When looking at the effect of cleaning, there are large quantitative differences between the cleaned and uncleaned portions. However, many of the averaged areas are non-uniform, with areas of very high and low work function, as can be seen especially in the dark blue sections at the bottom of all three panels. These areas were included in the calculations for average and standard deviation because there was no apparent reason why these regions were different or why CPD values measured in this area would not accurately represent the coating. These regions of very negative CPD surrounded by more moderate CPD do not appear to be caused by cleaning. Further work in this area could allow for better determination of experimental parameters and procedures to get more accurate and meaningful results when scanning a panel with this coating type which is prone to surface charging.

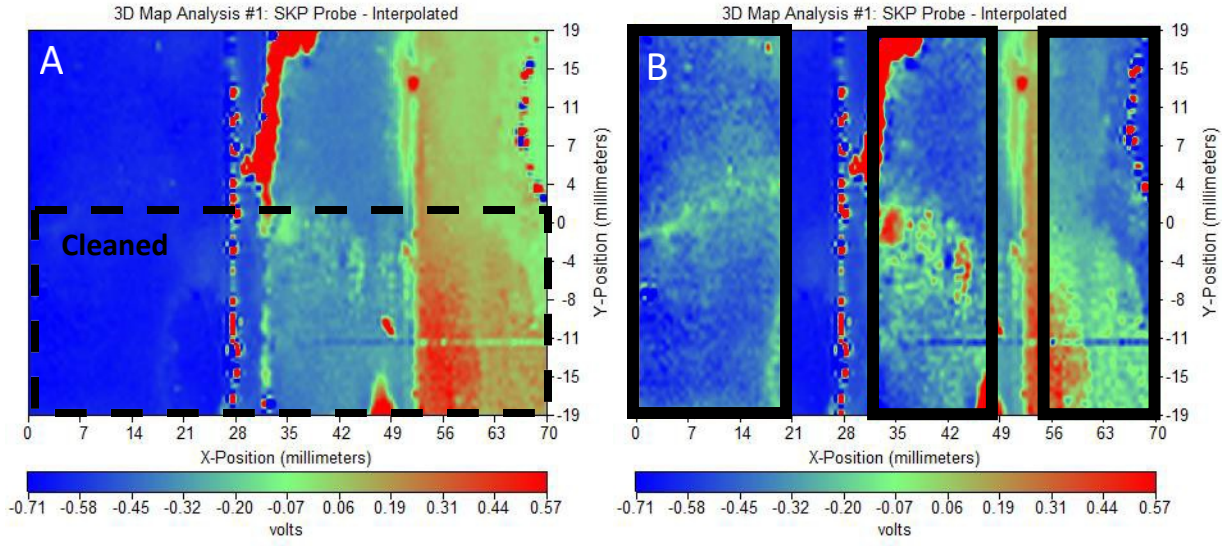

Figure 32. CPD map of Group 7 samples. Panels arranged from left to right C7, M7, CC7 A) Full scan with color scale set to overall scan maximum scale B) Same scan data as A but with each black boxed panel section individually set to color scale maximum for just that boxed section

Table 14. Group 7 Average CPD (S.D.) in mV

	C7	**M7**	**CC7**
Uncleaned	-639 (28)	-379 (24)	60 (31)
Cleaned	-645 (31)	-342 (135)	191 (123)

Figure 32 and Table 14 show the CPD map and average values for the Group 7 samples. In the top left corner of the M panel, as well as the top right section of the CC panel, the hydrophobic coating was peeling off, leading to areas of very high and low CPD that do not reflect the panel average. These areas were not included in calculations. There is a significant CPD difference from each panel to the next. In the non-inoculated and mold samples, the cleaned and uncleaned portions have similar average CPD values compared to the standard deviations, but in the climate control sample, the CPD is much higher in the cleaned section than the uncleaned. In the cleaned region in the CC panel, large CPD differences are seen within that region, and the differences are not a sharp contrast between top and bottom as would be expected if the cause was cleaning. It is not known whether those differences were there before exposure or cleaning, and future work in the area would involve measuring CPD before exposure, before cleaning, and after cleaning to determine the cause of these CPD differences.

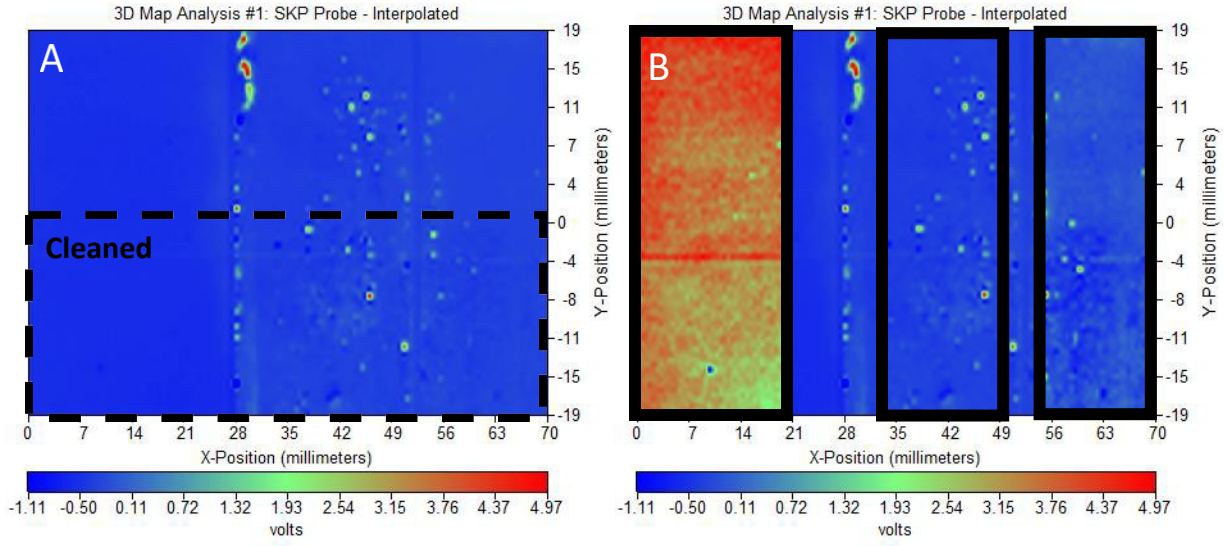

Figure 33. CPD map of Group 11 samples. Panels arranged from left to right C11, M11, and CC11. A) Full scan with color scale set to overall scan maximum scale. B) Same scan data as A but with each black boxed panel section individually set to color scale maximum for just that boxed section

Table 15. Group 11 Average CPD (S.D.) in mV

	C11	**M11**	**CC11**
Uncleaned	-532 (22)	-379 (72)	-295 (55)
Cleaned	-571 (24)	-336 (125)	-319 (80)

Figure 33 and Table 15 show the scan and average values for the Group 11 coating. While the unexposed coating shows a fairly homogenous surface with a low standard deviation, the spots of high CPD appear on the exposed scans, causing a high standard deviation. In the M and CC panels, there were spots, which appeared to line up with the spots seen on the SKP scan, where the hydrophobic coating was missing, leaving the shinier coating underneath exposed. While these spots changed the average work function for their areas, the baseline coated sections of each panel appeared to be very similar across the three different panels, indicating that aside from the removed outer coating, the exposure and cleaning had little effect on the coating in terms of CPD values.

For coatings 5, 6, 8, 9, 10, and 12, only two panels of each type were received: M and CC as shown in Figure 34.

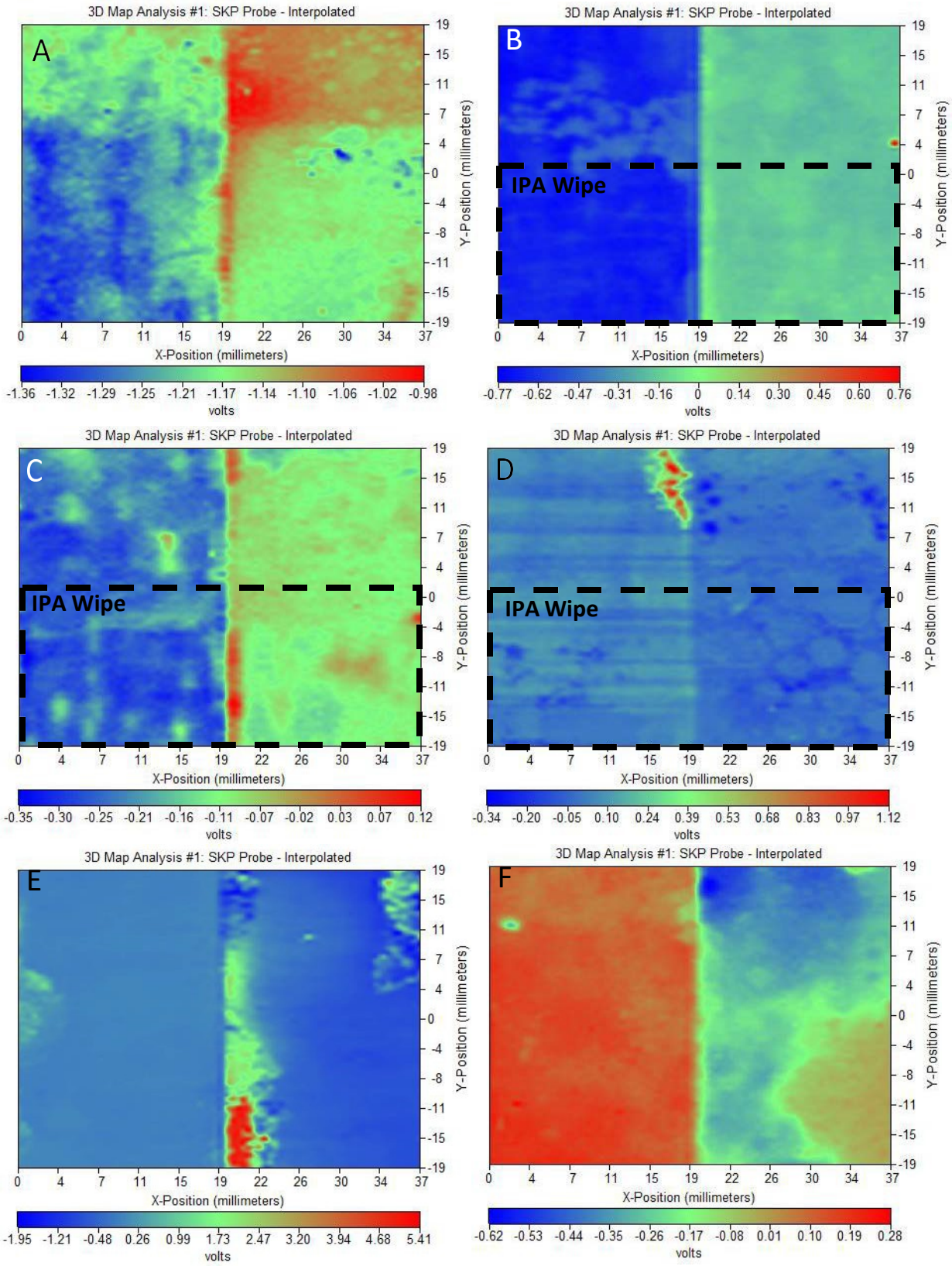

Figure 34. Two-panel SKP scans of Groups 5 (A), 6 (B), 8 (C), 9 (D), 10 (E), 12 (F). The fungal inoculated M panel on the left, climate control CC panel on the right. IPA wipe as indicated.

For Groups 5, 6, and 8 (Figure 34A, B, C) the M panel showed a much lower CPD than the CC panel. For Group 12 (Figure 34F) the M panel showed a much higher CPD, while the remaining coatings showed little difference between the two exposure conditions. Many of the samples were partially wiped with isopropyl alcohol to remove the mold, and these IPA wiped areas are indicated in the figures. This cleaning procedure showed little effect both visually and qualitatively in the SKP scans.

Preliminary work was done to scan a panel before and after cleaning with Navclean on a mold inoculated coating 4 sample. The panel examined in this test is a different panel from that shown previously in the 3 panel side-by-side comparison for that coating type. However, the same difficulties with surface charging were observed. The scan images are shown in Figure 35.

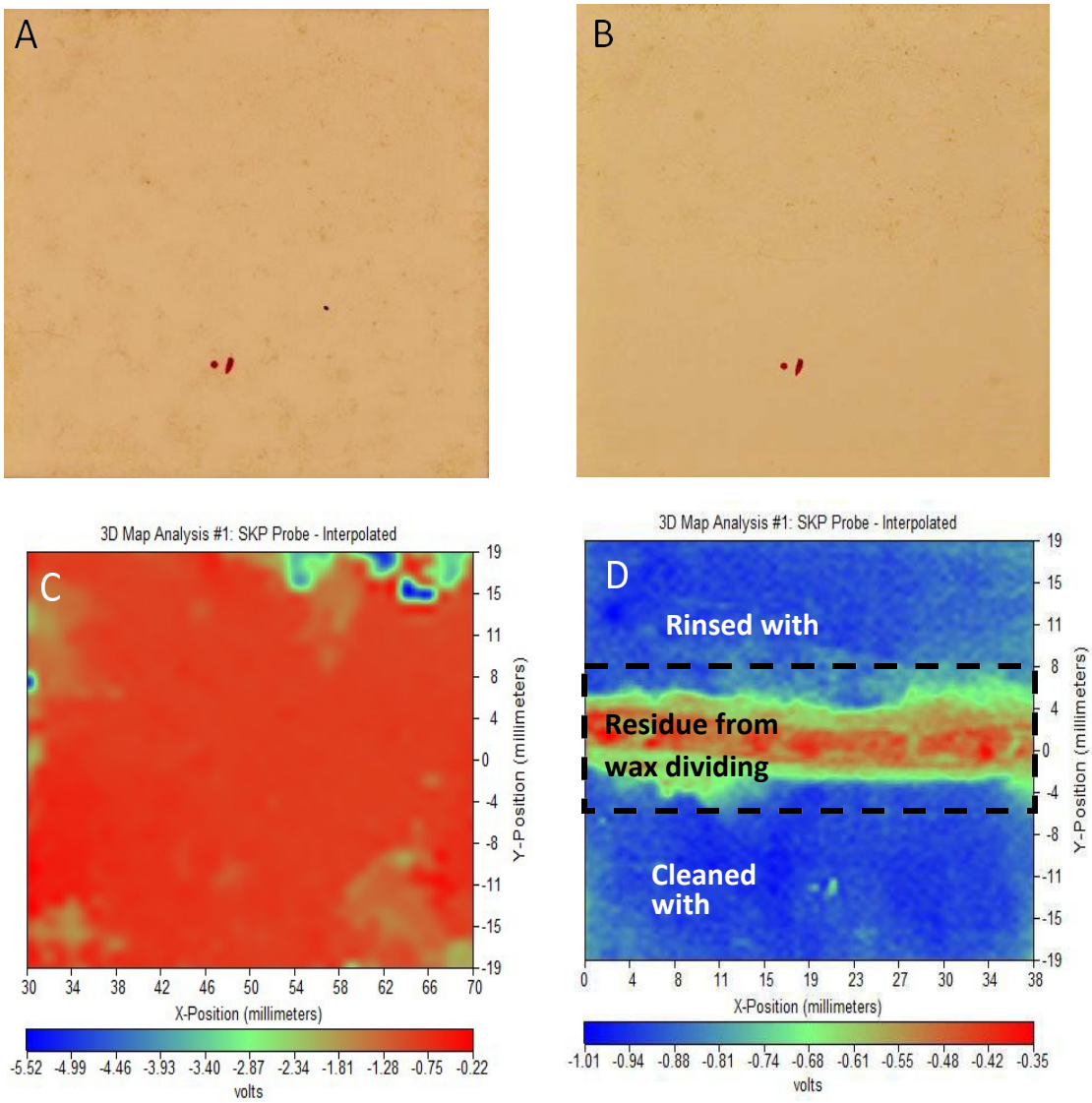

Figure 35. Mold exposed panel with coating type 4, different panel than shown in Figure 32 but with same exposure conditions A) Optical Image before cleaning, with red sharpie marker points. B) Optical Image after bottom half cleaned with NavClean, top half rinsed with water, with red sharpie marker points C) SKP scan before cleaning, without marked points D) SKP scan after cleaning, with marked points and wax residue dividing line across center.

The panel was scanned in its "as received" state, then scanned after the bottom half was cleaned with Navclean then rinsed with water, and the top only rinsed with water. Comparing Figures 35A and B, the

Navclean effectively removed the fungi from the cleaned areas. When comparing the SKP scan images (Figures 35C and D) changes to the CPD were seen on both the top and bottom of the panel from the initial to the final scan, but the cleaned and uncleaned sections did not appear different from each other. Further work in this area would require a better control of the non-cleaned side, as well as further work into the effect of rinsing a coated and exposed panel with just water.

In addition to large area scans using the 500 um diameter probe tip, preliminary work was done to examine the localized effects of fungi clusters using the 150 um diameter probe tip. This smaller probe tip is better able to resolve small details, such as fungi clusters that were approximately 2 mm in width, as shown in Figure 36.

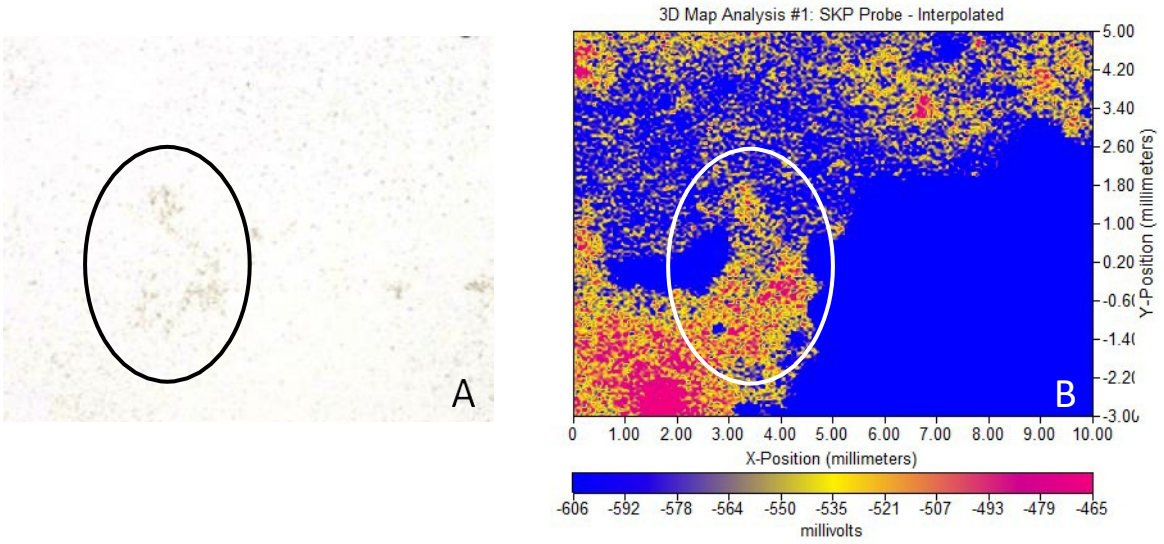

Figure 36. Mold cluster on M 4 fungi exposed panel, same panel as shown in Figure 35 A) Optical image B) SKP scan image.

While the SKP scan shows large areas of high and low CPD that do not correspond with anything seen in the optical image, there is a match of the triangular feature shown in each. There are many factors, of which only some are optically visible, which can affect the CPD, and this correlation shows that the fungal growth can change the CPD.

Conclusions

- ATR-FTIR detected a reduction in the Amide I and Amide II peaks on the CPC containing coupons after the microbial growth cycle. This was initially attributed to polyurethane linkage breakdown, however, it was noted that a thin film of CPC obscured the Type I and Type IV topcoat signals to some extent which led to uncertainty about the extent of polyurethane chain decreases.

- In this effort, non-inoculated control coupons showed more diverse growths of fungal hyphae than expected as compared to the coupons inoculated with the prepared solution (5 species) despite the inoculated coupons having the same baseline environmental surface contamination as all the other coupons.

    - We recommend that, in future effort, more detailed fungi identification be planned to include identifying which species are most prevalent propagating on each coating type and how geographic factors affect which species are active in DoD systems.

- GC-MS quantified extractable molecule content with/without fungi on Type I and Type IV Navy/USMC topcoats

    - Fungal growth consumed extractable molecules.

    - Non-inoculated extractable content was greater than the inoculated content.

    - The larger magnitude of fungal growth on Type IV topcoat consumed more extractable material from the coating as compared to the Type I topcoat with less fungal growth.

- LSM results revealed that after the 84-day microbial exposures:

    - Group 1 chromate primer had the most notable lowering of roughness parameters (smoother surface) after IPA cleaning, indicating either dissolution of chromate pigments or physical removal of high points of the matte finish coating.

    - The Group 2 non-chromate primer roughness parameters S_a and S_q changed the least of all coatings.

    - The Group 4 topcoat was slightly rougher by ~1.9% while the Group 3 topcoat was smoother by ~1.7%

    - The six roughness parameters analyzed in this effort were diluted in their ability to detect local pitting type coating attack associated with the fibrous pattern of mycelia growth and propagation and also because we used a multi-site sampling pattern of analysis on control coupons due to instrument availability issues.

- SKP differentiated both qualitatively and quantitatively among the fungal-inoculated coupons, control coupons, and climate controlled coupon conditions.

- Differences in average CPD values seen between non-exposed and climate control samples, indicating the microbial incubation conditions affect the surface.
- The SKP technique provides a qualitative assessment to identify areas of localized high and low CPD which indicates localized changes in the coating.
- SKP is able to detect localized microbial growth.

- The hydrophobic coating Rust-o-leum NeverWet appeared to experience limited or no coating degradation based on the microscopic observations in this project, and did not show any meaningful fungal attachment of propagation. Overcoating of fungi-prone surfaces with hydrophobic coatings such as included here may limit long term polyurethane degradation.

- With respect to fungal growth conditions:
  - Hydraulic fluid provided the most conducive environment for fungal growth.
  - CPC alone provides nutrients for fungal propagation and tended to protect the polyurethane coating beneath.
    - Addition of a fungistat inhibits hyphae propagation but does not kill spores.
  - Presence of chromate in the Group 1 primer did not significantly alter fungal growth compared to non-chromate primer; the observed species acclimated to chromate will need to be positively identified in the subsequent effort.
  - MIL-PRF-85285 Type IV topcoat supported significantly more fungal growth than Type I.

- Coating surface cleaning methods:
  - IPA wiping removed the fungal spores but not the hyphae on polyurethanes (actively growing microbiological films), however, IPA wipes did effectively clean the Groups 1 and 2 epoxy primers.
  - Sequential wiping with acetone, ethanol then methanol also could not remove physically attached hyphae from polyurethanes.
  - NavClean completely removed fungal spores and hyphae growth but was inadequate to remove CPC residues.

- EIS identified several interesting phenomena:
  - The observed two orders of magnitude increase in impedance values for the MIL-PRF-85285 Type IV, Class H extended weathering (also known as advanced performing) topcoat over the Type I, Class H topcoat was a surprising result and may warrant additional study.
  - It was also noteworthy that the EIS characteristics of the chromated primer changed significantly over 4.5 months of immersion in 3.5% salt water solution while the non-chromated primer remained substantially the same.

- The hydrophobic character of the Group C2 non-chromate primer was retained after five (5) months full immersion in the salt solution, easily shedding water and avoiding salt crystal formation more readily than the chromated Group C1 primer. Retention of water correlates to time-of-wetness being studied in relation to corrosion rates of accelerated corrosion tests (current SERDP/ESTCP projects). Both topcoats C3 and C4 polyurethanes retained a very hydrophobic character as well as high apparent gloss values.

- GPC Analysis of extracts from all samples showed no peaks, indicating that molecular weights in the range of 2,500 to 936,000 were not detected for the 84-day exposure conditions and contaminant film configurations in this SEED. GPC is expected to provide more data if sufficiently large molecular degradation products are formed.

- Extending test duration may increase the coating degradation permitting more fidelity in the analyses; including other analytical equipment now available will enable more sensitive surface analyses.

- These laboratory studies complemented ongoing Navy/USMC field testing of coatings which includes microbiological degradation.

    - The extended weatherability MIL-PRF-85285 Type IV, Class H (high-solids) topcoat was observed to support more tenacious fungal growth than the Type I polyurethane coating which may provide justification for applying Type I, Class H where fungal growth is anticipated to be a concern.

Mold/Mildew Growth Mitigation Considerations

Growth and Proliferation Mitigation Methods for USN/USMC Aircraft

The results of this project contributed to several noteworthy observations and conclusions regarding mold and mildew (fungal) growth and propagation for DoD assets. In a controlled laboratory environment, two of the operational fluids analyzed in this project were metabolized by different species contributing to microbial propagation – these included the Royco 782 hydraulic fluid (MIL-PRF-83282) and corrosion preventive Cor-Ban 35 (MIL-PRF-85054) without added fungistat (Omacide 100) [note that other hydraulic fluid specifications would need to be studied in a subsequent effort]. The Omacide 100 fungistat studied in this effort was shown to eliminate or at least greatly inhibit the propagation of fungal/mold activity when incorporated into the Cor- Ban 35 coating (at 0.5% w/w). MIL-PRF-85054 products are typically recognized as having higher durability in the maritime operational environment than thinner grades of CPC which are often used and therefore may offer longer lasting resistance to fungal species propagation when formulated with an added fungistat. As of this writing one MIL-PRF-81309 CPC product does contain a microbial inhibitor. Navy field studies were begun during this SEED effort to evaluate effectiveness of MIL-PRF-85054 CPC with and without fungistat since, based on SEED results, elimination or at least a substantial reduction in propagation was documented in these laboratory analyses. With funding from the Naval Aviation Enterprise, at least one Navy aircraft has been coated with Cor-Ban 35 inhibited and non-inhibited controls for long term assessment. The aircraft is stationed at Naval Air Station Whidbey Island, WA, where year-round moist conditions foster fungi growth.

- Other CPC chemistries used across the DoD Fleet for interior growth-prone compartments may be considered for inclusion of a fungistat within the formulation. As a fungistat by definition does not kill fungal spores but rather controls proliferation, localized cleaning methods applied to growth-prone areas of aircraft should be chosen such that they are very effective in removing the spores and neutralizing any remaining fungal hyphae to halt propagation. Microscopic presence/adherence of fungal activity remained after most of the chemical cleaning procedures compared in this study (i.e., the readily available isopropyl alcohol, plus acetone, ethanol, and methanol solvents (chosen for experimental purposes).

- Corrosion preventative compound Cor-Ban 35 (MIL-PRF-85054) is expected to remain intact longer for corrosion protection of surfaces compared to some other types of CPCs which are less resistant to water/saltwater and therefore may be a better choice for delivering fungistat chemicals and supplemental corrosion protection where they are needed on military platforms and within equipment.

The extended weatherability MIL-PRF-85285 Type IV, Class H (high-solids) topcoat was observed to support more tenacious fungal growth than the Type I polyurethane coating which may provide justification for applying Type I, Class H where fungal growth is anticipated to be a concern. Our results will be provided to rotary aircraft programs for appropriate action. Likewise, the observation that chromate primers are also capable of retaining viable fungi spores provides an additional rationale why non-chromate primers could be viable alternatives for long term protection of DoD assets. Field studies would be required to validate these laboratory results which documented notable differences in the influence of primer and topcoat selection and effectiveness in Navy and Marine Corp aircraft interior compartments prone to fungi growth and propagation.

Changes have been proposed to the NAVAIR 01-1A-509 manual, part of a Joint Service maintenance publication, regarding the usage and comparative effectiveness of isopropyl alcohol and NavClean. This work also has implications on the Army controlled section, where references to phosphate solutions and associated chemical agent resistant (CARC) coating damage could be improved by incorporating products

and information from this project. One additional method in the joint service manuals for removal of fungal contaminated paint systems is to scuff abrade the area (i.e. Scotch-Brite® type pads) removing a layer of primer/paint which can scratch protective plating on adjacent fastener systems and decreases overall corrosion protection of the aircraft structure by thinning these coatings. Avoidance of mechanical methods which liberate hex chrome dust is possible through more effective chemical means.

SEED Project Implications for Continued Research and Applications

The follow-on proposal for an expanded scope effort will include the following focus areas based on the detailed analyses performed in the exploratory phase:

Extended Exposure Time Considerations

The results from this work shows that MIL-STD-810F Method 508.5 does not adequately provide enough exposure time (84 days) to observe significant degradation of the coatings examined. In addition, the standard only stipulates end-point measurements with no time series degradation process(es) examined. The follow-up work to this SEED project will increase the exposure time from 84 days to at least 6 months. Also, more samples will be added to the matrix so that examination after intermediate exposure times can be achieved. These results will provide transient information regarding damage rates as opposed to cumulative end-point damage assessment. Longer exposures will also be compared with the currently deployed field samples that will have be exposed for up to 2 years. Another aspect for consideration is the complete fungal consumption of additive carbon sources (i.e. hydraulic fluid, CPC) over longer exposure periods. A fully developed biofilm, having consumed the additive, may turn its metabolistic efforts on the underlying organic coating and cause significant degradation.

Improved Control Experiment Implications

All coated coupons showed presence of fungi irrespective of intentional fungal inoculation; for example, control coupons had associated fungi on their surfaces. To distinguish abiotic degradation due to heat and humidity from fungal degradation, more rigorous control procedures will be required. Specifically, all samples (control and inoculated) will need to be sterilized prior to exposure. The sterilization method may include UV radiation, autoclaving, and/or a chemical treatment such as NavClean. The criteria for sterilization will include complete removal of biological material and the least damage to the coupon. In addition, fungi may be associated with the additive carbon sources themselves. Microbiological examination of these additives will be performed.

Cleaning Procedure Regrowth Studies

A knowledge gap identified is how long a cleaned surface remains free of significant fungal growth. Samples with fully developed biofilms will be cleaned with an appropriate method and the regrowth patterns will be observed. These results will provide guidance in cleaning intervals required to prevent microbial degradation.

Microbial Growth Quantification

The hypothesis of the work is that microbial growth is quantitatively linked to coating degradation. Numerous analytical methods were used in the current work to determine coating degradation including: AFM, FTIR, GCMS, SKP, EIS, SEM and LSM. However, the matching quantification of microbial growth was not performed. MIL-STD-810F details a qualitative method for fungal growth via observation. A tractable protocol needs to be developed for microbial growth determination. For the follow-on work, numerous techniques will be employed to perform fungal quantification. Prospective techniques will include measurement of fungal cell wall constituents (e.g., ergo sterol and glucosamine), DNA fluorescent staining, molecular DNA/RNA methods and respiration studies. In addition, the current work showed that SKMP may provide a method for high resolution quantification of fungal coverage.

Future SKP Technique Development

Due to the very sensitive nature of the SKP, it can be difficult to determine which variations in the CPD of a surface are due to which cause. Any variations or features seen by SKP can be due to surface preparation, coating degradation, surface adsorption, and a variety of other factors. For this reason, to isolate the effects of mold growth and cleaning procedure, several areas of future work are recommended. First, being able to scan the same surface at multiple steps in the process would allow for a change in the surface to be attributed to a more exact process and cause. Scanning the same surface after coating, after inoculation, after incubation, and then after cleaning could show which of these steps is causing the behavior of the coating to change, and help to isolate the effects of the mold growth and cleaning. Additionally, the surface of interest (coated, with potential mold growth) is a complex system. Using a simpler system, such as a gold coated glass slide, could allow for better understanding of each individual component's effect on the CPD. With a greater understanding of how mold growth and cleaning affect a simple substrate, a greater understanding can be achieved regarding the coated substrates and other substrates of interest.

Analytical Test Sequencing for Higher Inter-correlations

Based on the results and observations in this project, overall results will benefit from improved sequential cascading of analytical procedures in the follow-on project. Test coupons of a wider variety of coating systems (i.e. including a different non-chromate primer that NAVAIR recently approved for U.S. Navy aircraft) would be exposed to the maximum feasible duration of optimal microbial growth conditions (6+ months), with initial detailed ESEM characterization and mapping coordinates of highly affected areas. Then coupons would be sent for other analyses such as SKP, AFM, LSM, FTIR and GCMS. Cleaning procedures would be carefully applied to a subset of coupons to remove growths leaving the coating surface microscopically clean for chemical analyses. Such analytical sequencing would better link species observed with degradation quantified by other methods on the coupons.

The six LSP roughness parameters analyzed in this effort were somewhat diluted in their ability to detect local pitting type coating attack associated with the fibrous pattern of mycelia growth and propagation. Due to analytical equipment time and other priorities during this SEED project, full coupon scans were not possible for all before and after coated coupons at nanometer-scale resolution. After lessons learned in this project, more information may be gleaned by targeted profiling as explained in the report and utilizing capabilities at more than one participating laboratory to spread out the equipment availability issues we encountered.

Chemical Cleaning Procedures for Removal and Sanitation of Coating Surfaces

Proposed research would apply other Fleet relevant chemical solutions in addition to NavClean including MIL-PRF-85570 aircraft cleaner used in bulk (10% solution) or pre-saturated wipes, NavSolve replacement for MIL-PRF-680 solvent, and one other commercial solution that is now available to clean microbially-contaminated surfaces. Another method listed in the joint service manuals regarding cleaning of highly contaminated fungal growths is to scuff abrade the area removing a thin layer of primer/paint (i.e. Scotch-Brite™ type pads) which scratches protective plating on adjacent fastener systems decreases overall protection of the vehicle structure by thinning primers (~0.001 inch) liberating toxic chromate dust where Class C primers are used, and thinning topcoat layers where they are present. Determining an alternative method would reduce exposure to toxic dust and improve coating lifetime. The task would be to clean by appropriate combinations of the above methods and microscopically analyze its' effectiveness, then replace the coupons in the growth chamber to quantify differences in microbial resurgence. This would contribute to the body of knowledge regarding longer term effectivity of the various mitigation methods. These laboratory studies would complement the ongoing Navy/USMC field testing which presently only includes Cor-Ban 35 with and without fungistat.

Other common CPC specifications should be studied for differences in persistence and effectiveness on DoD assets. There may be other effective fungistat besides Omacide 100 which would be considered for future efforts as well. All the analytical techniques discussed in this proposal will be used to determine the effectiveness of fungistats and cleaning procedures. So the least invasive methods of preventing recurrence of growths could be better understood, documented and communicated.

EIS Observations

The observed two orders of magnitude increase in impedance values for the MIL-PRF-85285 Type IV "extended weathering" or "advanced performing" topcoat over the standard Type I Navy polyurethane topcoat was a surprising result and may warrant additional study. Also, the time dependent changes in the chromate primer impedance values results compared to the stability of the non-chromate primer is not understood.

The hydrophobic character of the Group C2 non-chromate primer was greater than the matte finish Group C1 chromated primer as shown by its' faster water shedding properties and minimization of salt crystals/residue after five (5) months full immersion in the salt solution. This observation may correlate to another advantage as compared to legacy chromate primers in Navy field applications minimizing time-of-wetness during drying minimizes corrosion rates as being documented in ongoing SERDP-ESTCP projected focused on accelerated corrosion test improvements. Both topcoat Groups C3 and C4 polyurethanes retained a very hydrophobic character as well as high apparent gloss values.

Super hydrophobic Formulated Supplemental Coatings

The supplemental hydrophobic coating evaluated in this study (Rust-Oleum Never Wet™) showed promise to resist microbial attachment and proliferation. There are other products being evaluated by the Navy and inclusion of the ones most likely to be fielded would make logistical implementation of the super-hydrophobic coating into the Navy/USMC supply system more streamlined. Therefore, validating the laboratory and field performance of hydrophobic coatings is recommended.

Other Aviation Materials

Aircraft use many different types of materials so subsequent projects would include coatings that could affect pilot health such as interior heating and air conditioning coatings some of which are chromate and some non-chromate, personal gear, avionics materials, and others depending on conversations with other entities.

Literature Cited

Baikie ID, Smith PJS, Porterfield DM, Estrup PJ. 1999. Multitip scanning bio-Kelvin probe. Review of Scientific Instruments. 70:1842-1850.

Bare SR, Somarjai GA. 2002. In: RA Myers, editor. Encyclopedia of Physical Science and Technology. New York: Academic Press. p. 401-403.

Bergveld P, Hendrikse J, Olthuis W. 1998. Theory and application of the material work function for chemical sensors based on the field effect principle. Measurement Science and Technology. 9:1801-1808.

Grunmeier G, Juttner K, Stratmann M. 2000. In: M Schutze, Cahn RW, Haasen P, Kramer EJ, editors. Materials Science and Technology. Weinheim: Wiley-VCH. p. 340-352.

Hansen DC, Hansen KM, Ferrell TL, Thundat T. 2003. Discerning biomolecular interactions using Kelvin probe technology. Langmuir. 19:7514-7520.

Janata J, Josowicz M. 1997. Nernstian and non-nernstian potentiometry. Solid State Ionics. 94:209-215.

Lavoie DM, Little BJ, Ray RI, Hart KR, Wagner PA. 1997. Microfungal degradation of polyurethane paint and corrosion of aluminum alloy in military helicopters. CORROSION / 97, Houston, TX: NACE International.

Lee JS, Ray RI, Little BJ, Abbott WH, Lorch DP, Stropki JT, Hoth PH. 2012a. Potential biocidal properties of Cr+6 in coatings. CORROSION / 2012, Houston, TX: NACE International.

Lee JS, Ray RI, Little BJ, Stropki JT. 2012b. Fate of Cr+6 from a coating in an electrolyte with microorganisms. Journal of the Electrochemical Society. 159:C530-C538.

Ray RI, Little BJ, Arafat ES. 2010. A Laboratory Evaluation of Corrosion Preventive Compounds and Mildew Inhibitors in the Presence of Fungi. Stennis Space Center, MS. (NRL/MR/7330--10-9273).

Appendix A: Test Matrix of Organic Coatings and Contaminant Films

Sample Group #	Base Organic Coating System	Primer	MIL SPEC	Top Coat	MIL SPEC	Additional Feedstock Material
1	Chromate Primer	Deft 44-GN-007	MIL-PRF-85582	none	N/A	none
2	Non-Chromate Primer	Deft 44-GN-098	MIL-PRF-85582	none	N/A	none
3	Chromate Primer + Top Coat Type 1	Deft 44-GN-007	MIL-PRF-85582	Deft 03-GY-444	MIL-PRF-85285 Ty. I, Cl. H	none
4	Chromate Primer + Top Coat Type 4	Deft 44-GN-007	MIL-PRF-85582	PPG CA9800/CA9800Z	MIL-PRF-85285 Ty. IV , Cl. H	none
5	Chromate Primer + Top Coat Type 1	Deft 44-GN-007	MIL-PRF-85582	Deft 03-GY-444	MIL-PRF-85285 Ty. I, Cl. H	Cor-Ban 35 CPC
6	Chromate Primer + Top Coat Type 1	Deft 44-GN-007	MIL-PRF-85582	Deft 03-GY-444	MIL-PRF-85285 Ty. I, Cl. H	Cor-Ban 35 CPC w/0.5% Omacide
7	Chromate Primer + Top Coat Type 1	Deft 44-GN-007	MIL-PRF-85582	Deft 03-GY-444	MIL-PRF-85285 Ty. I, Cl. H	Rust-Oleum NeverWet
8	Chromate Primer + Top Coat Type 1	Deft 44-GN-007	MIL-PRF-85582	Deft 03-GY-444	MIL-PRF-85285 Ty. I, Cl. H	Royco 782 Hydraulic Fluid
9	Chromate Primer + Top Coat Type 4	Deft 44-GN-007	MIL-PRF-85582	PPG CA9800/CA9800Z	MIL-PRF-85285 Ty. IV , Cl. H	Cor-Ban 35
10	Chromate Primer + Top Coat Type 4	Deft 44-GN-007	MIL-PRF-85582	PPG CA9800/CA9800Z	MIL-PRF-85285 Ty. IV , Cl. H	Cor-Ban w/0.5% Omacide
11	Chromate Primer + Top Coat Type 4	Deft 44-GN-007	MIL-PRF-85582	PPG CA9800/CA9800Z	MIL-PRF-85285 Ty. IV , Cl. H	Rust-Oleum NeverWet
12	Chromate Primer + Top Coat Type 4	Deft 44-GN-007	MIL-PRF-85582	PPG CA9800/CA9800Z	MIL-PRF-85285 Ty. IV , Cl. H	Royco 782 Hydraulic Fluid

All Coupons were 7075-T6 aluminum panels pretreated with Bonderite-CR 1200S RTU (Ready-to-use) Aero, MIL-DTL-81706B, Type I, Class 1A.